The Use of Non-Contact Ultra-Widefield Imaging Devices in Infants

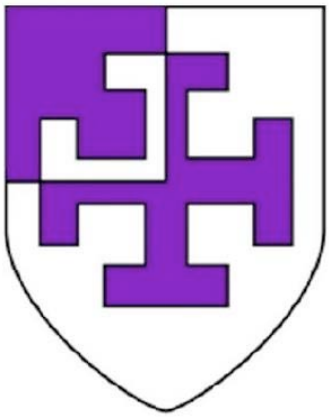

Timothy H. M. Fung MBChB

St Cross College

University of Oxford

A thesis submitted as requirement for the degree of Master of Research in

Clinical Neurosciences

Trinity Term 2015

Supervisor 1: Mr Chetan Kantibhai Patel

Supervisor 2: Dr Neil Bowles

Acknowledgements

I would like to express my sincere gratitude to my supervisors Chetan K Patel and Neil Bowles for their support and guidance in helping me complete this thesis. Mr Patel has been a wonderful and inspiring mentor throughout this degree. Dr Bowles has been a huge source of encouragement and provided much valued support.

I would like to thank my colleagues, friends, and most of all my family for their patience and support throughout this degree.

Abstract

The Use of Non-Contact Ultra-Widefield Imaging Devices in Infants

Timothy HM Fung, St Cross College

Master of Research in Clinical Neurosciences, Trinity Term 2015

The ability to image the peripheral retina is important for the diagnosis and management of infants with proliferative retinopathies. With the current retinal imaging techniques available for infants, peripheral sweeps and montage techniques are necessary when information about the retinal periphery is required. These techniques are labour intensive, require highly skilled photographers, and do not permit the simultaneous capture of the posterior pole and the retinal periphery in a single image. A recent technological advance has been the development of non-contact ultra-widefield retinal imaging devices, which can capture simultaneously the posterior pole and the retinal periphery in a single image. Image acquisition with these imaging modalities in the infant patient population has not been well studied. This thesis aimed to evaluate non-contact ultra-widefield retinal imaging in infants with retinal diseases.

A retrospective review of all infants who had non-contact ultra-widefield retinal imaging at the Oxford Eye Hospital with the Optos Panoramic 200MA and/or the Heidelberg Spectralis between July 2012 and July 2014 was conducted. An analysis of all retinal images was performed for each ultra-widefield imaging device to determine the quality of each retinal image acquired. Adequate quality images were used for analysis of captured peripheral retinal features and artefacts.

A total of 82 infants (range, 33 weeks postnatal age to 6 months old) diagnosed with retinopathy of prematurity, incontinentia pigmenti, or familial exudative

vitreoretinopathy had non-contact ultra-widefield retinal imaging. Eleven infants who underwent general anaesthesia had intravenous fundus fluorescein angiography (FFA) with the Heidelberg Spectralis in the operating room. Seventy-one infants were imaged with the Optos Panoramic 200MA in the outpatient setting. Of the 71 infants imaged with the Optos Panoramic 200MA, 42 infants had pseudocolour fundus imaging and 29 infants had FFA. Of the 29 infants who had FFA with the Optos Panoramic 200MA, 23 infants had sodium fluorescein administered intravenously and 6 infants had sodium fluorescein administered orally. A total of 2389 adequate quality ultra-widefield retinal images were analysed for peripheral retinal features and artefacts. A range of peripheral retinal features was adequately captured with both ultra-widefield imaging devices. Artefacts that decreased the field of view were present in images acquired from both ultra-widefield imaging devices.

The Optos Panoramic 200MA and the Heidelberg Spectralis were both capable of acquiring clinically useful, high resolution, ultra-widefield retinal images in infants with a range of retinal diseases.

List of Figures

Figure 1.1	Gross anatomy of the human eye	**19**
Figure 1.2	Electron micrograph of the retina demonstrating the layered arrangement	**24**
Figure 1.3	Fundus photograph of the left eye highlighting the en face aspect of the retina	**26**
Figure 1.4	Stage 1 ROP	**30**
Figure 1.5	Stage 2 ROP	**31**
Figure 1.6	Stage 3 ROP	**32**
Figure 1.7	Stage 4 and Stage 5 ROP	**33**
Figure 1.8	Aggressive posterior ROP	**34**
Figure 1.9	Zone border and clock hours used to describe the location and extent of ROP	**35**
Figure 1.10	Plus disease	**36**
Figure 1.11	Retinal pathologies in incontinentia pigmenti	**39**
Figure 1.12	Retinal pathologies in familial exudative vitreoretinopathy	**40**
Figure 1.13	Binocular indirect ophthalmoscopy of an infant	**41**
Figure 1.14	Phases of a normal fundus fluorescein angiogram	**45**
Figure 1.15	Normal fundus fluorescein angiogram of the macula	**46**
Figure 1.16	Examples of hyperfluorescent abnormalities seen in fundus fluorescein angiography	**48**
Figure 1.17	Examples of hypofluorescent abnormalities seen in fundus fluorescein angiography	**49**

Figure 1.18	Venous phase image of a fluorescein angiogram of the right eye of an infant with severe ROP	**51**
Figure 1.19	Late phase images of a fluorescein angiogram of the left eye of an infant with IP	**53**
Figure 1.20	Late phase image of a fluorescein angiogram of the right eye of an infant with FEVR	**54**
Figure 1.21	Traditional fundus photograph of the left eye of an infant, centered on the optic disc, illustrating the standard 30-degree field of view	**56**
Figure 1.22	Imaging the retina of an infant in 1969 using a vertically mounted Zeiss fundus camera	**57**
Figure 1.23	Retinal image from the digital binocular indirect ophthalmoscope	**58**
Figure 1.24	NIDEK fundus camera	**59**
Figure 1.25	Pictor digital fundus camera	**60**
Figure 1.26	The RetCam Digital Imaging System	**63**
Figure 1.27	An example of a RetCam colour fundus image	**64**
Figure 1.28	An example of a RetCam fluorescein angiographic image	**65**
Figure 1.29	The Optos Panoramic 200MA	**70**
Figure 1.30	Optics of the Optos Panoramic 200MA	**71**
Figure 1.31	An example of an Optos ultra-widefield pseudocolour fundus image	**72**
Figure 1.32	An example of an ultra-widefield fundus image from only the red laser light of the Optos Panoramic 200MA	**73**

Figure 1.33	An example of an ultra-widefield fundus image from only the green laser light of the Optos Panoramic 200MA	**74**
Figure 1.34	An example of an ultra-widefield fundus fluorescein angiographic image acquired with the Optos Panoramic 200MA	**75**
Figure 1.35	The "flying baby" position for Optos ultra-widefield retinal imaging in infants	**82**
Figure 1.36	Cheek rest reference point of the Optos Panoramic 200MA for retinal imaging in infants	**83**
Figure 1.37	Method for examining an infant at the slit lamp	**84**
Figure 1.38	Alignment of the infant's eye with the Optos imaging system	**86**
Figure 1.39	An example of an Optos ultra-widefield pseudocolour fundus image acquired in an infant	**87**
Figure 1.40	An example of an Optos ultra-widefield fundus fluorescein angiographic image acquired in an infant	**90**
Figure 1.41	Heidelberg Spectralis imaging system	**92**
Figure 1.42	Heidelberg Spectralis scanning laser camera head and touch panel	**93**
Figure 1.43	Multi-modal range of images of the retina that can be captured with the Heidelberg Spectralis imaging system	**95**
Figure 1.44	Imaging lenses available with the Heidelberg Spectralis	**97**
Figure 1.45	The use of the Heidelberg Spectralis scanning laser camera head as a mobile hand held device to image supine infants	**99**

Figure 1.46	Modified Heidelberg Spectralis for retinal imaging in infants	**102**
Figure 1.47	Multi-positional bracket of the modified Heidelberg Spectralis imaging system	**103**
Figure 1.48	Movement wheels of the custom made arm of the modified Heidelberg Spectralis imaging system	**104**
Figure 1.49	Position of the filter wheel of the Heidelberg Spectralis scanning laser camera head for fluorescein angiography	**105**
Figure 1.50	Imaging of an infant with the Heidelberg Spectralis ultra-widefield imaging lens	**108**
Figure 1.51	Correct working distance of the Heidelberg Spectralis imaging lens with an infants eye	**109**
Figure 1.52	An example of a Heidelberg Spectralis ultra-widefield fundus fluorescein angiographic image acquired in an infant	**110**
Figure 2.1	An example of an adequate quality Optos pseudocolour fundus image	**115**
Figure 2.2	Examples of inadequate quality Optos pseudocolour fundus images	**116**
Figure 2.3	Examples of peripheral retinal features captured with Optos ultra-widefield pseudocolour fundus imaging in infants with retinal diseases	**121**
Figure 2.4	Examples of image artefacts from Optos ultra-widefield pseudocolour fundus imaging in infants with retinal diseases	**123**

Figure 3.1	An example of an adequate quality Optos ultra-widefield fundus fluorescein angiographic image	**129**
Figure 3.2	Examples of inadequate quality Optos ultra-widefield fundus fluorescein angiographic images	**130**
Figure 3.3	An example of peripheral retinal features captured with an Optos ultra-widefield intravenous fundus fluorescein angiographic image in an infant with retinopathy of prematurity	**137**
Figure 3.4	Examples of peripheral retinal features captured with Optos ultra-widefield oral fundus fluorescein angiography in infants with retinal diseases	**138**
Figure 3.5	Examples of artefacts arising from Optos ultra-widefield fundus fluorescein angiography of infants with retinal diseases	**140**
Figure 4.1	An example of an adequate quality Heidelberg Spectralis ultra-widefield fundus fluorescein angiographic image	**148**
Figure 4.2	Examples of inadequate quality Heidelberg Spectralis ultra-widefield fundus fluorescein angiographic images	**149**
Figure 4.3	Examples of peripheral retinal features captured with Heidelberg Spectralis ultra-widefield fundus fluorescein angiography in infants with retinal diseases	**153**
Figure 4.4	An example of an image artefact obtained with the Heidelberg Spectralis ultra-widefield imaging lens	**154**

List of Tables

Table 2.1	Characteristics of 3 term infants who had pseudocolour fundus imaging with the Optos Panoramic 200MA	**118**
Table 2.2	Characteristics of 39 premature infants with ROP who had pseudocolour fundus imaging with the Optos Panoramic 200MA	**119**
Table 2.3	Artefacts from Optos ultra-widefield pseudocolour fundus images acquired in infants with retinal diseases	**122**
Table 3.1	Characteristics of 3 term infants who had non-contact ultra-widefield FFA with the Optos Panoramic 200MA	**132**
Table 3.2	Characteristics of 26 premature infants with ROP who had non-contact ultra-widefield FFA with the Optos Panoramic 200MA	**133**
Table 3.3	Fluorescein angiographic phases captured in infants who had non-contact ultra-widefield IV FFA with the Optos Panoramic 200MA	**135**
Table 3.4	Artefacts from Optos ultra-widefield fundus fluorescein angiographic images acquired in infants with retinal diseases	**139**
Table 4.1	Characteristics of 3 term infants who had non-contact ultra-widefield FFA with the Heidelberg Spectralis	**150**
Table 4.2	Characteristics of 8 premature infants with ROP who had non-contact ultra-widefield FFA with the Heidelberg Spectralis	**151**

Abbreviations

APROP	Aggressive posterior retinopathy of prematurity
ART	Automatic real time
BIO	Binocular indirect ophthalmoscope
BW	Birth weight
CPAP	Continuous positive airway pressure
cSLO	Confocal scanning laser ophthalmoscopy
EUA	Examination under anaesthesia
FAZ	Foveal avascular zone
FEVR	Familial exudative vitreoretinopathy
FFA	Fundus fluorescein angiography
GA	Gestational age
ICG	Indocyanine green angiography
ICROP	International classification of ROP
IP	Incontinentia pigmenti
IR	Infrared
IV	Intravenous
NNU	Neonatal unit
OCT	Optical coherence tomography
OEH	Oxford eye hospital
PC	Personal computer
PNA	Postnatal age
RLF	Retrolental fibroplasia

ROP	Retinopathy of prematurity
RPE	Retinal pigment epithelium
SLO	Scanning laser ophthalmoscopy
UK	United Kingdom

Table of Contents

Acknowledgements **2**

Abstract **3**

List of Figures **5**

List of Tables **10**

Abbreviations **11**

Chapter 1 ..... **18**

Introduction **18**

1.1. The Human Eye 18

1.1.1. Gross Anatomy of the Eye 18

1.1.1.1. The Cornea 19

1.1.1.2. The Sclera 20

1.1.1.3. The Iris 20

1.1.1.4. The Ciliary Body 21

1.1.1.5. The Choroid 21

1.1.1.6. The Lens 21

1.1.1.7. The Vitreous 22

1.1.1.8. The Retina 22

1.1.1.9. The Retinal and Choroidal Circulation 26

1.2. Infant Retinal Diseases 28

1.2.1. Retinopathy of Prematurity 28

1.2.1.1. Classification and terminology 28

1.2.1.2. Screening....36
1.2.1.3. Treatment....37
1.2.2. Incontinentia Pigmenti....37
1.2.3. Familial Exudative Vitreoretinopathy....39
1.3. Diagnostic Approach to Infant Retinal Diseases....41
1.3.1. Techniques of Clinical Examination....41
1.3.2. Fundus Fluorescein Angiography....42
1.3.2.1. Properties of Sodium Fluorescein....42
1.3.2.2. Side effects and Complications of Fundus Fluorescein Angiography....43
1.3.2.3. Interpretation of a Fundus Fluorescein Angiogram....44
1.3.2.4. Role of Fundus Fluorescein Angiography in Retinopathy of Prematurity....49
1.3.2.5. Role of Fundus Fluorescein Angiography in Incontinentia Pigmenti....52
1.3.2.6. Role of Fundus Fluorescein Angiography in Familial Exudative Vitreoretinopathy....53
1.3.3. Retinal Imaging Techniques in Infants....55
1.3.3.1. Traditional Fundus Camera....55
1.3.3.2. Binocular Indirect Ophthalmoscopy Digital Photographic System....58
1.3.3.3. NIDEK Digital Fundus Camera....59
1.3.3.4. Pictor Digital Fundus Camera....59
1.3.3.5. RetCam Digital Fundus Camera....61
1.4. Ultra-Widefield Retinal Imaging....66
1.4.1. Confocal Scanning Laser Ophthalmoscopy....66
1.4.2. Optos Ultra-Widefield Retinal Imaging....67
1.4.2.1. Optos Ultra-Widefield Retinal Imaging in Infants....76

1.4.2.2. Optos Ultra-Widefield Pseudocolour Fundus Imaging Technique in Infants.....80

1.4.2.3. Optos Ultra-Widefield Fundus Fluorescein Angiography Technique in Infants.....88

1.4.3. Heidelberg Spectralis Ultra-Widefield Retinal Imaging.....91

1.4.3.1. Heidelberg Spectralis Ultra-Widefield Retinal Imaging in Infants 100

1.4.3.2. Heidelberg Spectralis Ultra-Widefield Fundus Fluorescein Angiography Technique in Infants.....105

1.5. Research Aims 111

1.6. Outline of Chapters 111

Chapter 2 112

Evaluation of Optos Ultra-Widefield Pseudocolour Fundus Imaging in Infants 112

2.1. Introduction.....112

2.2. Methods.....113

2.2.1. Infants.....113

2.2.2. Image analysis.....113

2.3. Results.....117

2.3.1. Infants.....117

2.3.2. Image analysis.....120

2.4. Discussion 124

Chapter 3 126

Evaluation of Optos Ultra-Widefield Fundus Fluorescein Angiography in Infants 126

3.1. Introduction 126

3.2. Methods 127

3.2.1. Infants 127

3.2.2. Image analysis 127

3.3. Results 131

3.3.1. Infants 131

3.3.2. Image analysis 134

3.4. Discussion 142

Chapter 4 145

Evaluation of Heidelberg Spectralis Ultra-Widefield Fundus Fluorescein Angiography in Infants 145

4.1. Introduction 145

4.2. Methods 146

4.2.1. Infants 146

4.2.2. Image analysis 146

4.3. Results 150

4.3.1. Infants 150

4.3.2. Image analysis 152

4.4. Discussion 155

Chapter 5 157

Summary and Future Work 157

5.1. Summary 157

5.2. Future Work 159

References **160**

Publications **172**

Presentations **174**

Chapter 1

Introduction

1.1. The Human Eye

1.1.1. Gross Anatomy of the Eye

The human eye (Figure 1.1) is oblate spheroid in shape and is composed of three concentric layers. The outermost layer consists of the clear cornea anteriorly and the opaque white sclera posteriorly. The outermost corneoscleral layer is composed of tough and protective tissues. The middle layer of the eye is the uvea, which consists of the iris, ciliary body, and choroid. The uvea is a highly vascularised structure and serves a nutritive and supportive function. The innermost layer of the eye is the retina. This photosensitive layer contains the photoreceptors and neural elements that initiate the processing of visual information.

The human eye contains three compartments: the anterior chamber, the posterior chamber, and the vitreous cavity. The anterior chamber, the space between the cornea and the iris, is filled with aqueous humour. It is about 3 mm deep with an average volume of 200 μL. The posterior chamber is the anatomical portion of the eye posterior to the iris and anterior to the lens and vitreous face. It is also filled with aqueous humour and has an average volume of 60 μL. The vitreous cavity makes up more than two thirds of the volume of the eye and contains the vitreous gel.

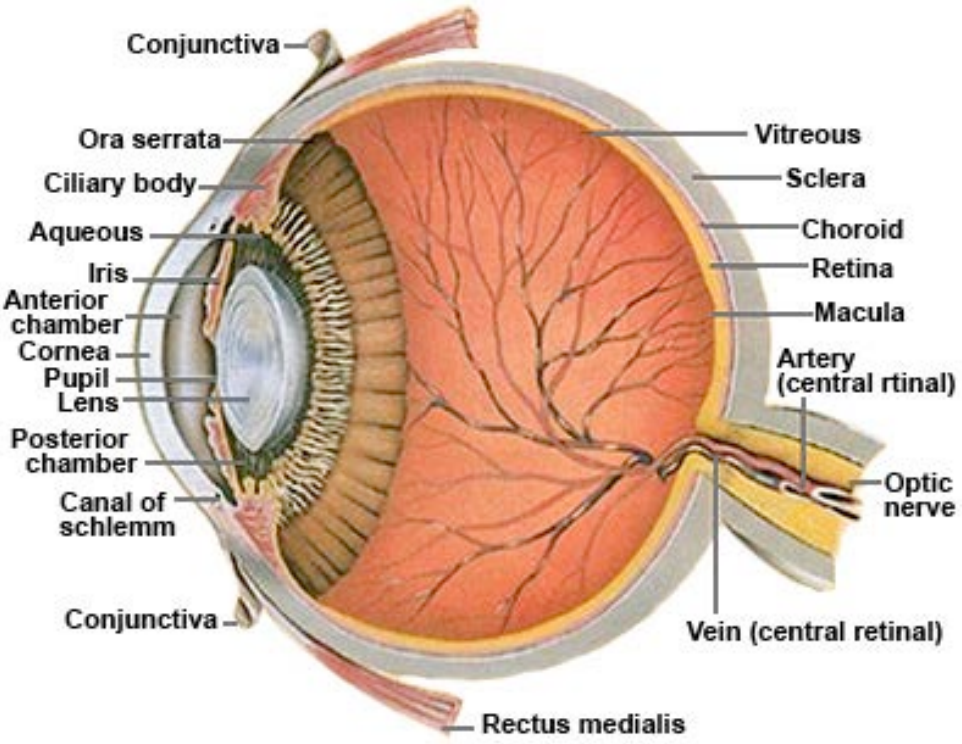

Figure 1.1: Gross anatomy of the human eye

1.1.1.1. The Cornea

The cornea is a transparent, avascular tissue that contributes approximately two thirds of the total dioptric power of a normal human eye. The shape of the cornea is prolate, being flatter in the periphery and steeper centrally, which creates an aspheric optical system. Histologically, the cornea is made up of five distinct layers. From anterior to posterior, these are as follows:

(1) The epithelium, which is composed of non-keratinised, non-secretory, stratified squamous epithelium, which is 4-6 cell layers thick.

(2) Bowman's membrane, which is a thin, avascular, superficial stromal layer consisting of randomly dispersed collagen fibrils.

(3) The stroma, which constitutes approximately 85% of the total corneal thickness in humans. It is composed of collagen-producing keratocytes, ground substance, and

regular layers of parallel collagen fibrils. The collagen fibrils are uniform in size and separation, and this regularity helps determine the transparency of the cornea.

(4) Descemet's membrane, which is the basement membrane of the corneal endothelium.

(5) The endothelium, which is made up of closely interdigitated cells arranged in a mosaic pattern of mostly hexagonal shapes. The active transport of ions by these cells leads to the transfer of water from the corneal stroma and the maintenance of stromal deturgescence and transparency.

1.1.1.2. The Sclera

The sclera is the white, opaque portion of the outer wall of the eye, covering the posterior four fifths of the eye's surface area. It is continuous anteriorly with the corneal stroma and posteriorly merges with the dura of the optic nerve sheath. The sclera is composed of collagen and elastic fibers embedded in a variety of proteoglycans. Histologically, the sclera is divided into three layers (from outermost inward): episclera, stroma, and lamina fusca. Its principal function is to protect the intraocular contents of the eye.

1.1.1.3. The Iris

The iris is the most anterior extension of the uveal tract. It separates the anterior segment of the eye into two compartments, the anterior chamber and the posterior chamber, and forms a circular aperture (pupil) that controls the amount of light transmitted into the eye. The iris is made up of blood vessels and eonnective tissue, in addition to the melanocytes and pigment cells that are responsible for its distinctive colour. The mobility of the iris allows the pupil to change size.

1.1.1.4. The Ciliary Body

The ciliary body, which is triangular in cross section, bridges the anterior and posterior segments. The apex of the ciliary body is directed posteriorly towards the ora serrata. The base of the ciliary body gives rise to the iris. The ciliary body has 2 principal functions: aqueous humour formation and lens accommodation. It also plays a role in the uveoscleral outflow of aqueous humour.

1.1.1.5. The Choroid

The choroid, the posterior portion of the uveal tract, nourishes the outer one third of the retina. It consists of 3 layers of blood vessels. The outer layer of vessels, known as the Haller layer, is relatively large. The vessels in this layer merge with smaller diameter vessels in a middle layer known as the Sattler layer. These vessels distribute the blood arriving from the short posterior ciliary arteries over the extent of the choroid. The inner layer of vessels, known as the choriocapillaris, is a rich network of fenestrated capillaries. Interspersed between the vessels of the choroid are loose connective tissue, melanocytes and fibroblasts.

1.1.1.6. The Lens

The lens is a transparent, biconvex structure whose functions are to maintain its own clarity, to refract light, and to provide accommodation. It lies posterior to the iris and anterior to the vitreous body. The lens is suspended in position by the zonules of Zinn, which consist of delicate yet strong fibers that support and attach it to the ciliary body. The lens is composed of the capsule, lens epithelium, cortex, and nucleus. The lens contributes approximately one third of the total dioptric power of a normal human eye.

1.1.1.7. The Vitreous

Occupying 80% of the volume of the eye, the vitreous is a clear matrix, composed of water, hyaluronic acid, and collagen. The vitreous body is composed of 2 main portions: the central, or core, vitreous and the cortical vitreous, the outer portion of the vitreous. The transparent vitreous humour is important to the metabolism of the intraocular tissues because it provides a route for metabolites used by the lens, ciliary body, and retina.

1.1.1.8. The Retina

The retina is the innermost layer of the eye. This layer is in the image plane of the eye's optical system and is responsible for converting relevant information from the image of the external environment into neural impulses that are transmitted to the brain for decoding and analysis. The retina consists of two layers: an inner neurosensory retina and an outer single layer of epithelium, the retinal pigment epithelium (RPE).

The neurosensory retina is a thin transparent layer of neural tissue, and in histological sections appears as eight distinct layers that include three layers of nerve cell bodies and two layers of cell synapses. The layered arrangement of the neurosensory retina is shown in Figure 1.2 [1]. The neurosensory retina is composed predominantly of neural cells, namely the rod and cone photoreceptors, bipolar cells, and ganglion cells. The activities of these neural cells are regulated by a number of supporting cells such as amacrine cells, horizontal cells, and muller cells. The collection of cells in the neurosensory retina is responsible for converting light stimuli into neural impulses. These impulses are then partially modulated and integrated locally before being transmitted to the brain via the ganglion cell axons in the optic nerve.

The RPE is the outer layer of the retina and has a number of physical, optical, metabolic and transport functions. It is composed of a continuous monolayer of hexagonal cells, which extends from the margins of the optic disc to the anterior margin of the neurosensory retina (ora serrata). Contiguous RPE cells are firmly attached by a series of lateral, intercellular junctional complexes. These not only provide structural stability but also play an important role in maintaining the outer blood-retina barrier.

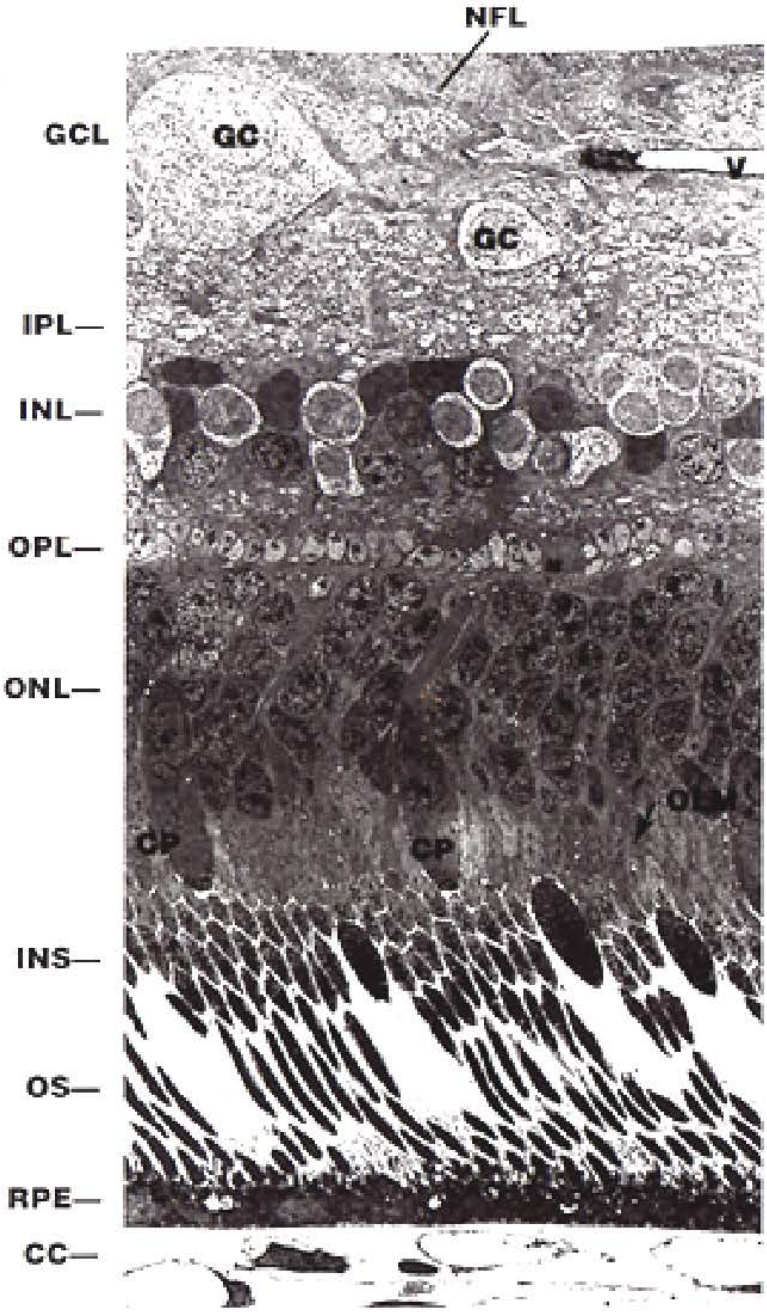

Figure 1.2: Electron micrograph of the retina demonstrating the layered arrangement (NFL: nerve fiber layer; GCL: ganglion cell layer; GC: ganglion cell; V: retinal vessel; IPL: inner plexiform layer; INL: inner nuclear layer; OPL: outer plexiform layer; ONL: outer nuclear layer; CP: cone pedicle; OLM: outer limiting membrane; INS: inner segments; OS: outer segments; RPE: retinal pigment epithelium; CC: choriocapillaris) (Forrester, Dick, Mcmenamin and Roberts, 2008, p45)

The *en face* aspect of the human retina can be defined into several regions with different topographical characteristics (Figure 1.3).

The posterior pole or central retina (anatomically, area centralis) is a 5-6 mm circular area of retina located between the superior and inferior temporal arteries. This region is cone dominated and is characterised histologically by the presence of more than one layer of ganglion cell bodies.

The macula lutea (anatomically, fovea) is a 1.5 mm diameter circular zone of retina in the posterior pole and is defined histologically as the area of the retina that has 2 or more layers of ganglion cells and contains xanthophyll pigment. It is the high concentration of this pigment, in conjunction with the increased density of RPE cells that causes the relative hypofluorescence of the macula seen on fluorescein angiography (see section 1.3.2.3). The macula lutea is located approximately 3 mm lateral to the optic disc.

The fovea centralis (anatomically, foveola) is a central 0.35 mm circular zone in the macula lutea, consisting of a depression surrounded by slightly thickened margins. This region consists exclusively of tightly packed cone photoreceptors.

The peripheral retina is the area of the retina that extends from the border of the posterior pole to the ora serrata anteriorly. It consists predominantly of rod photoreceptors and is characterised histologically by the presence of only one layer of ganglion cell bodies.

The optic disc (optic nerve head) is a circular structure that lies approximately 3 mm medial to the center of the fovea. It consists of ganglion cell axons and is devoid of photoreceptors. The central retinal vessels emerge at the center of the optic disc and radiate out to supply the retina. The retinal veins are usually seen to lie lateral to the retinal arteries. The optic disc is often used as a landmark to describe the retina as having supero- and inferotemporal and supero- and inferonasal quadrants.

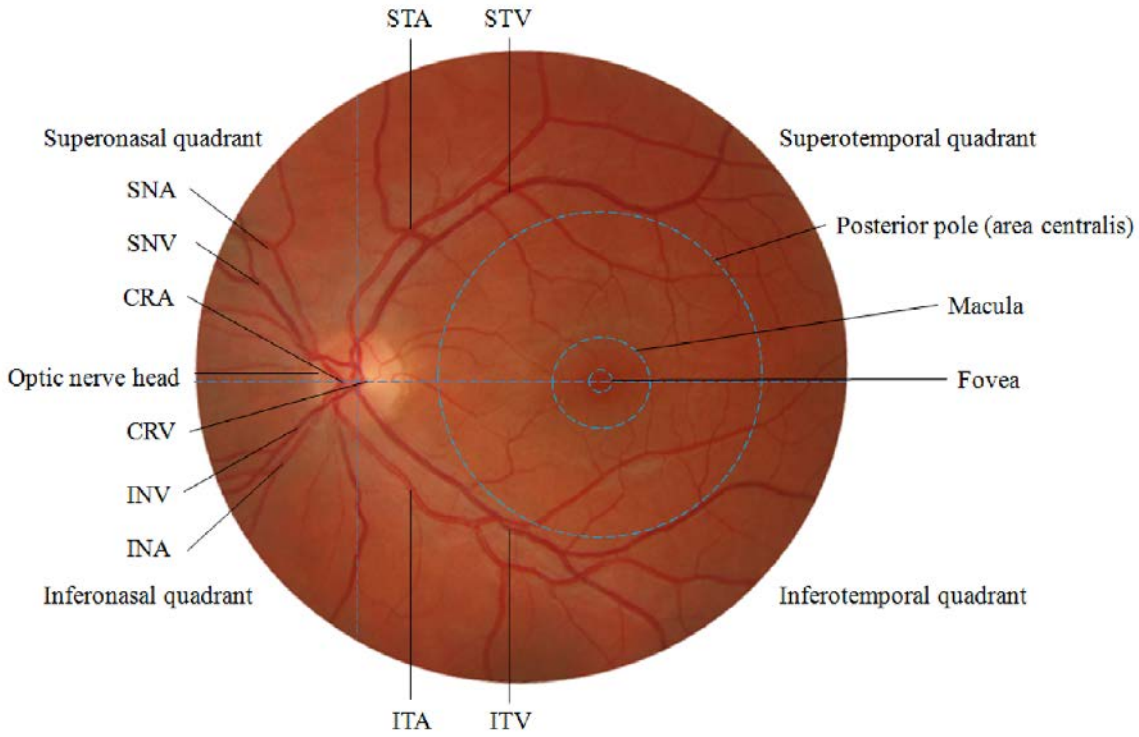

Figure 1.3: Fundus photograph of the left eye highlighting the en face aspect of the retina (CRV: central retinal vein; CRA: central retinal artery; STA: superotemporal artery; STV: superotemporal vein; SNA: superonasal artery; SNV: superonasal vein; INV: inferonasal vein; INA: inferonasal artery; ITA: inferotemporal artery; ITV: inferotemporal vein)

1.1.1.9. The Retinal and Choroidal Circulation

The retina has a dual blood supply to meet its high metabolic demands. Branches from the central retinal vessels supply the inner two-thirds of the retina, while the choroidal circulation supplies the outer one-third of the retina.

The central retinal artery, derived from the ophthalmic artery, arises from the center of the optic nerve and is in close association with the central retinal vein. The central retinal artery branches into superior and inferior branches, which subdivide into nasal and temporal arteries. The superior and inferior temporal arteries curve above and below the foveal region, with arteries passing over veins. Each of the four

major branches of the central retinal artery is a functional end artery that supplies a single quadrant of the retina between which there is no overlap.

There are two capillary networks in the retina. The inner capillary network is located at the level of the ganglion cell layer and the outer capillary network is located at the level of the inner nuclear layer. Retinal capillaries are more abundant in the posterior pole compared to the peripheral retina but are absent from the fovea itself. Retinal capillaries are characterised by circumferentially orientated endothelial cells joined by non-leaky tight junctions. These tight junctions form the inner blood-retinal barrier, which functions to prevent the intracellular movement of water-soluble molecules into the retina.

The central retinal vein and its tributaries follow the course of the central retinal artery and its branches and drain into either the superior ophthalmic vein or cavernous sinus directly.

The anterior and posterior ciliary arteries, which originate from the ophthalmic artery, are responsible for supplying the choroidal circulation. The posterior ciliary arteries divide into two long posterior ciliary arteries and numerous short posterior ciliary arteries. The short posterior ciliary arteries supply the posterior choriocapillaris. The branches of the long ciliary arteries and branches of the anterior ciliary arteries supply the anterior choriocapillaris.

A series of large vortex veins located at the equator of the globe drains blood from the choroid into the superior and inferior orbital veins in the orbit.

In approximately 30% of individuals [2], a small vessel, the cilioretinal artery, may be present near the optic nerve head and provide a small anastomotic connection between the choroidal and retinal circulations.

1.2. Infant Retinal Diseases

1.2.1. Retinopathy of Prematurity

Retinopathy of prematurity (ROP) is the current designation for what was previously called retrolental fibroplasia (RLF). It is a disorder that features abnormal proliferation of developing blood vessels at the junction of vascular and avascular retina. It is one of the few largely preventable causes of childhood vision impairment.

Normally, retinal vascular development begins during week 16 of gestation. Mesenchymal tissue containing spindle cells is the source of retinal vessels. The mesenchyme grows centrifugally from the optic disc, reaching the nasal ora serrata in the eight month of gestation and the temporal ora serrata up to 1 to 2 months later.

Premature birth (defined by the World Health Organisation as delivery of an infant before 37 completed weeks of gestation) is a risk factor for ROP, in which normal retinal vascular development is altered and abnormal neovascularisation may occur. The pathologic process may stop or reverse itself at any point, or the disease may eventually progress and lead to vitreoretinal traction and retinal detachment.

Premature infants weighing less than 1500 grams at birth are at risk for developing ROP, and the risk increases as gestational age and birth weight decrease.

1.2.1.1. Classification and terminology

The international classification of ROP (ICROP) published in 1984 and later revised in 2005 describes ROP by its severity or stage (Stages 1-5), location by zone (I-III), extent by clock hours, and by the presence of pre-plus and plus disease [3].

Prior to the development of ROP in the premature infant, vascularisation of the retina is incomplete or “immature”. There are five stages that describe the abnormal vascular response at the junction of the vascularised and avascularised retina. In stage

1 ROP, a thin and flat demarcation line separates the avascular retina anteriorly from the vascularised retina posteriorly (Figure 1.4). In stage 2 ROP, an elevated ridge of tissue that extends above the plane of the retina is seen arising in the region of the demarcation line (Figure 1.5). In Stage 3 ROP, extraretinal fibrovascular proliferation or neovascularisation extends from the ridge into the vitreous (Figure 1.6). In stage 4 ROP, the retina is partially detached (Figure 1.7A), whereas in stage 5, the retina is totally detached (Figure 1.7B). More recently, a rapidly progressing, severe form of ROP has been designated as aggressive posterior ROP (APROP). This type of ROP is characterised by its posterior location, and the prominence of plus disease out of proportion to its peripheral features (Figure 1.8) [4].

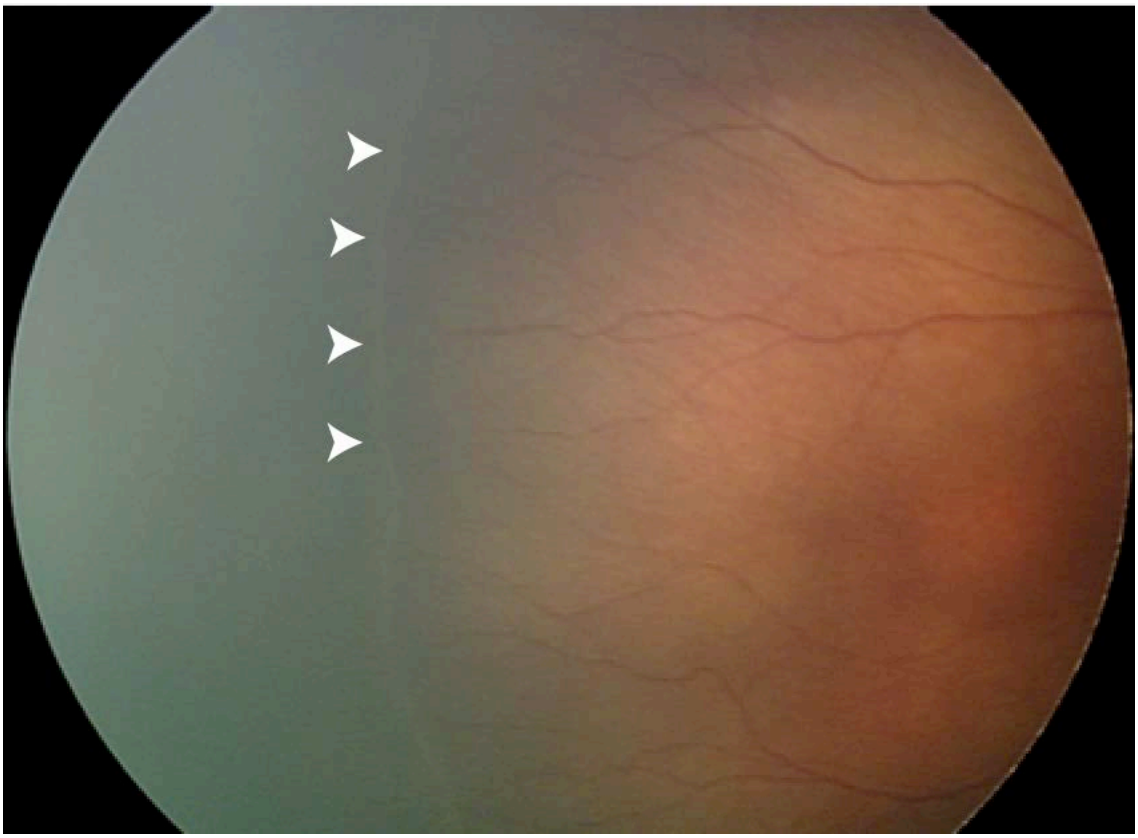

Figure 1.4: Stage 1 ROP

In stage 1 ROP a fine demarcation line (white arrowheads) is seen separating the posterior, vascularised retina from the anterior, avascular retina. It appears flat and white, and lies within the plane of the retina.

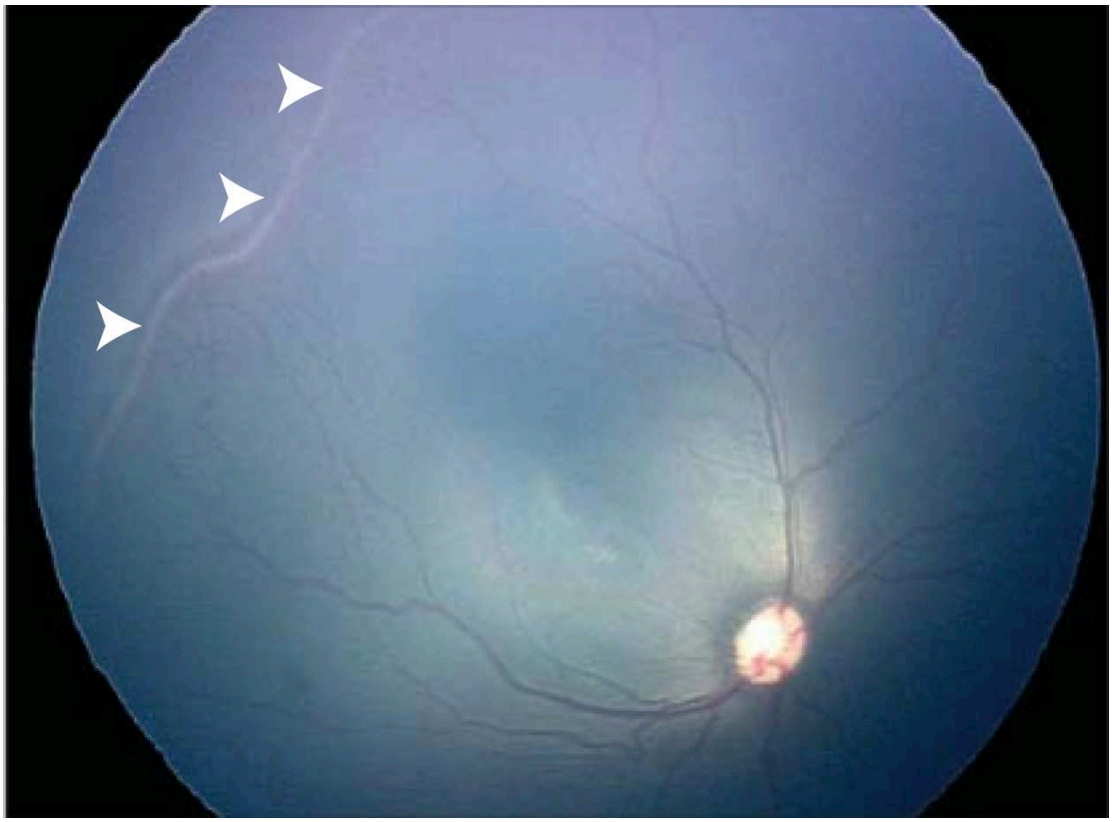

Figure 1.5: Stage 2 ROP

In stage 2 ROP, the demarcation line seen in stage 1 ROP has grown into a ridge (white arrowheads) with height and width, which extends centripetally within the globe (The international committee for the classification of retinopathy of prematurity, 2005, p993).

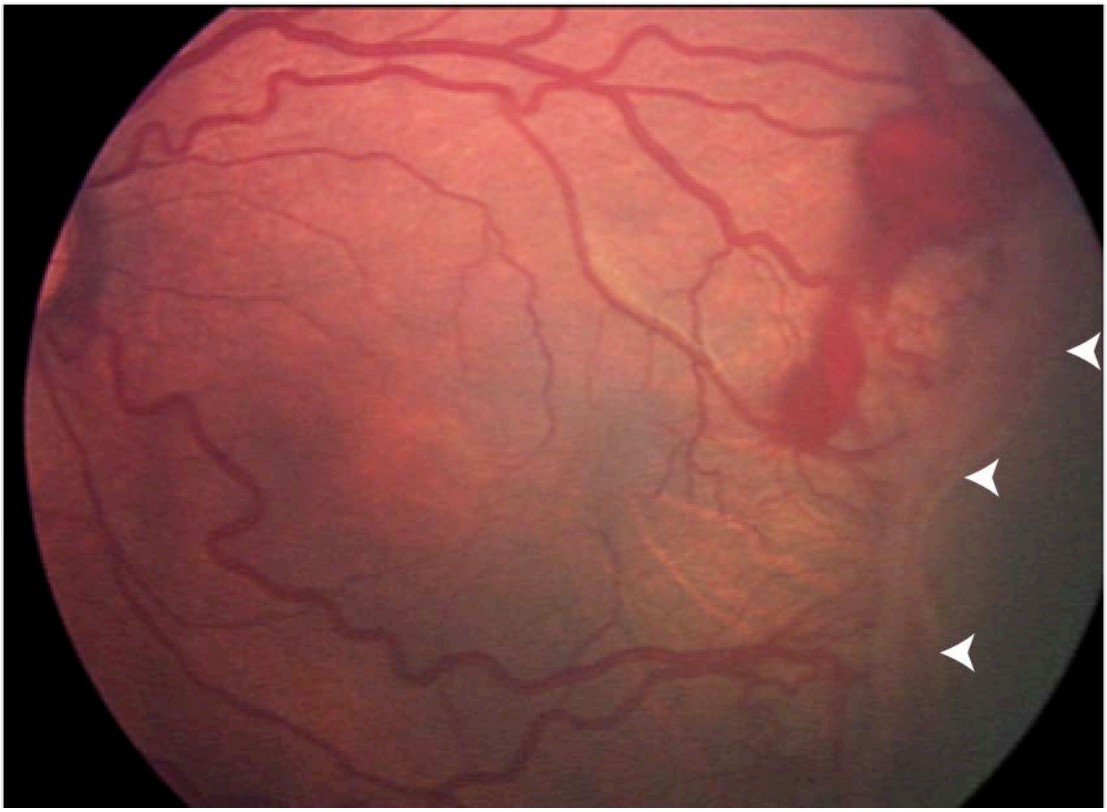

Figure 1.6: Stage 3 ROP

Stage 3 ROP is characterised by the addition of extraretinal, fibrovascular tissue (white arrowheads) proliferating from the former ridge seen in stage 2 ROP. This proliferating tissue is continuous with the posterior aspect of the ridge, causing a ragged appearance of the ridge as proliferation increases into the vitreous.

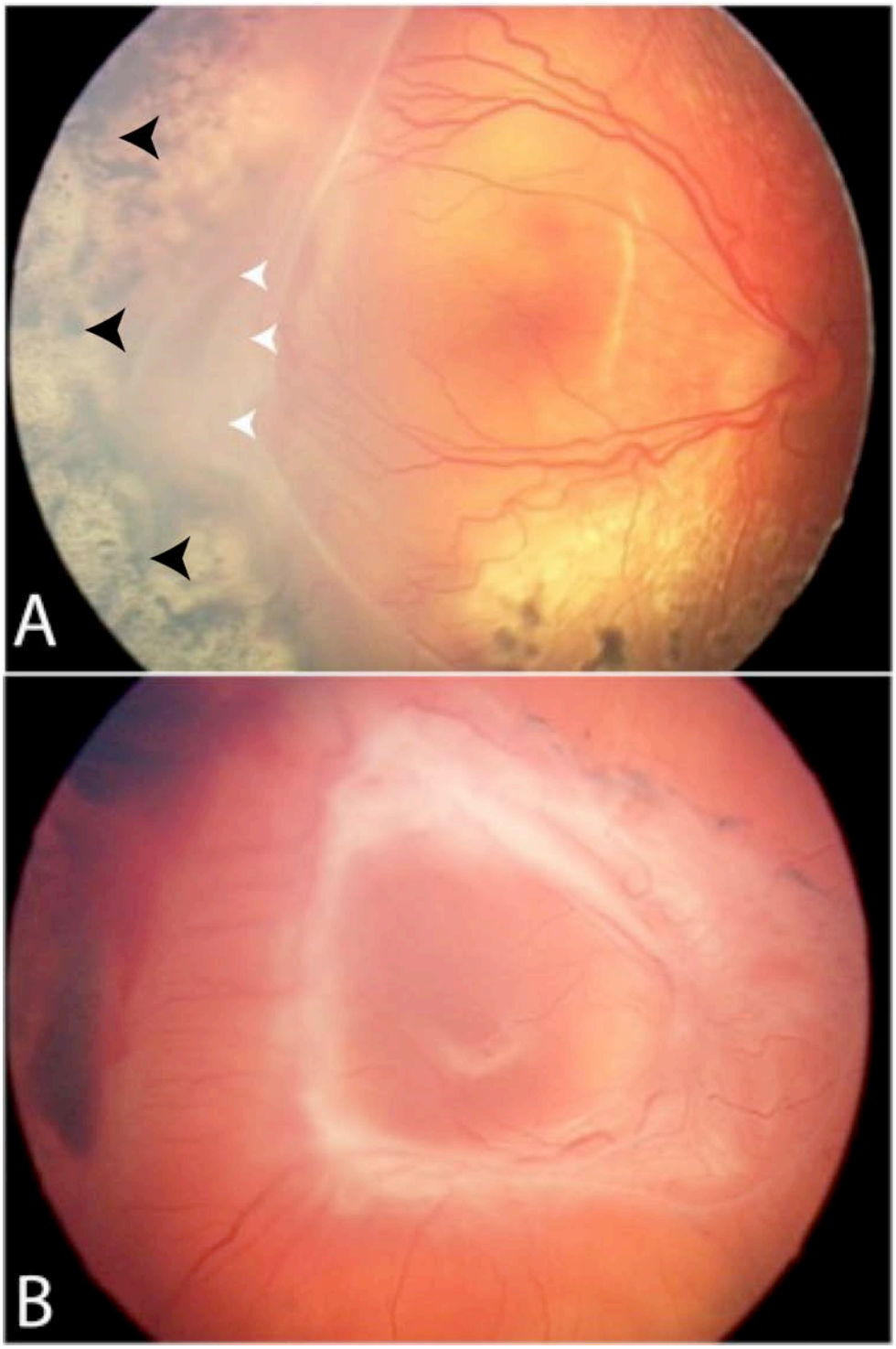

Figure 1.7: Stage 4 and stage 5 ROP

(A) Stage 4 ROP is characterised by the presence of a partial tractional retinal detachment (white arrowheads). Note the extensive scarring present from previous laser burns (black arrowheads) applied to the avascular retina (B) Stage 5 ROP is characterised by the presence of a total tractional retinal detachment.

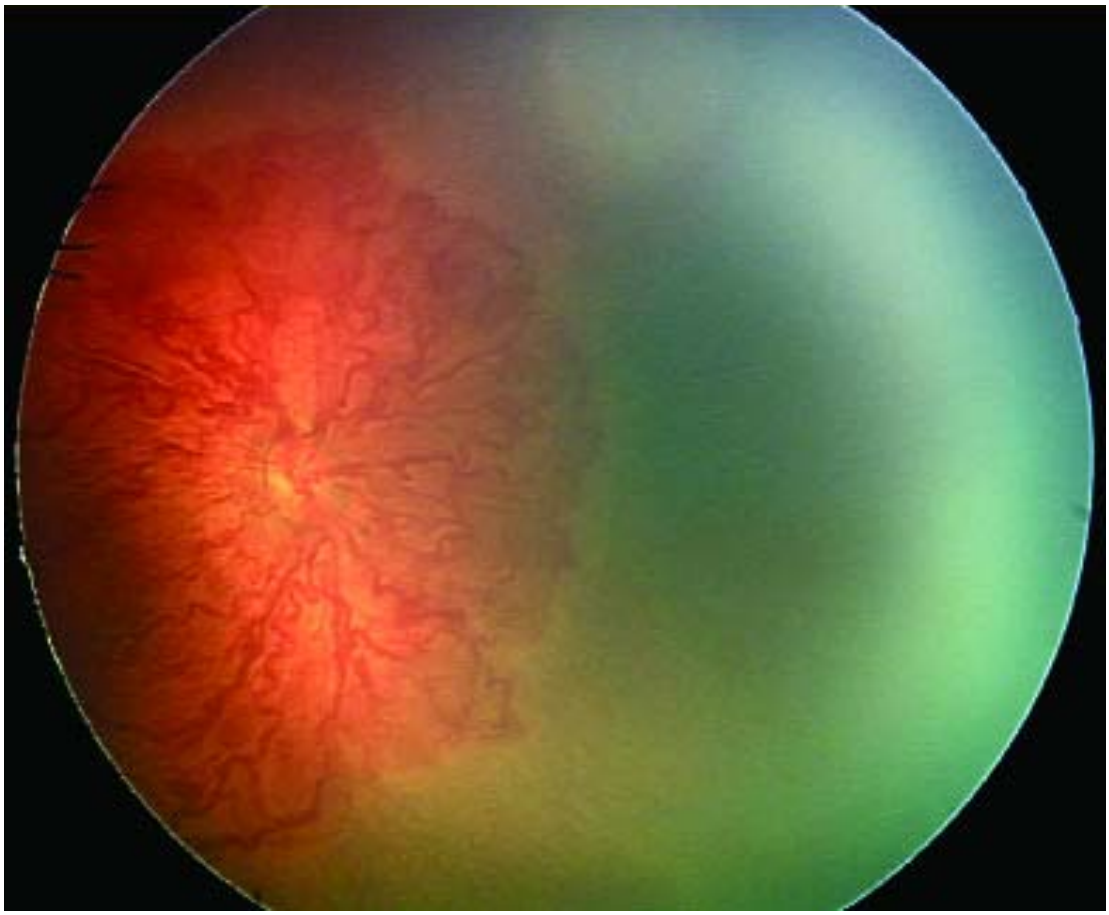

Figure 1.8: Aggressive posterior ROP

This form of ROP is characterised by its location in zone I or posterior zone II, ill-defined nature of the peripheral retinopathy, and prominent plus disease out of proportion to the peripheral findings (Wilson, Head, Fielder and Wilkinson, 2008, p21).

For the purpose of defining the location of the retinopathy, three concentric zones of retinal involvement have been described with the zone designation based on the findings at the time of examination (Figure 1.9) [5]. Zone I (the innermost zone) consists of a circular area, which extends from the center of the optic disc to twice the distance from the center of the optic disc to the center of the macula. Zone II consists of a circular area that extends from the border of zone I to the nasal ora serrata (at the

3 o'clock position in the right eye and the 9 o'clock position in the left eye), and zone III includes the remainder of the retina outside zones II.

The extent of disease is recorded as hours of the clock (Figure 1.9) [5]. The 3 o'clock position is to the right and nasal in the right eye and temporal in the left eye, and the 9 o'clock position is to the left and temporal in the right eye and nasal in the left eye.

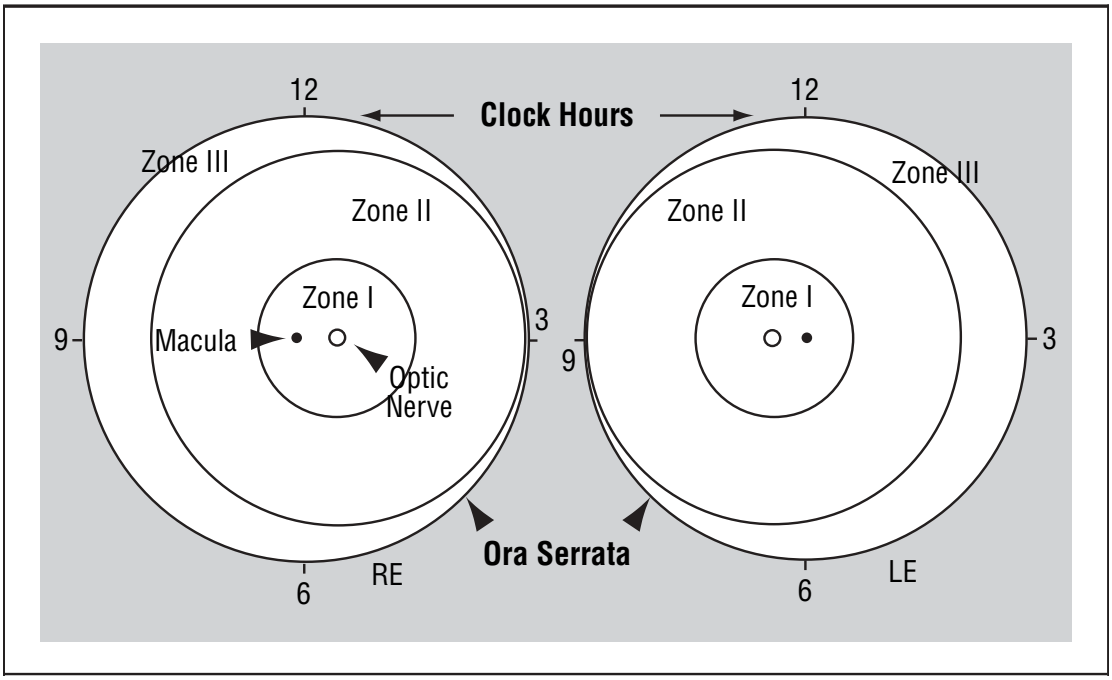

Figure 1.9: Zone borders and clock hours used to describe the location and extent of ROP (The international committee for the classification of retinopathy of prematurity, 2005, p992).

Plus disease is characterised by the presence of marked venous dilatation and arteriolar tortuosity of the posterior pole retinal vasculature in at least two quadrants of the eye (Figure 1.10) [5]. Pre-plus disease is abnormal dilatation and tortuosity of the posterior pole vessels, but less than that seen in plus disease.

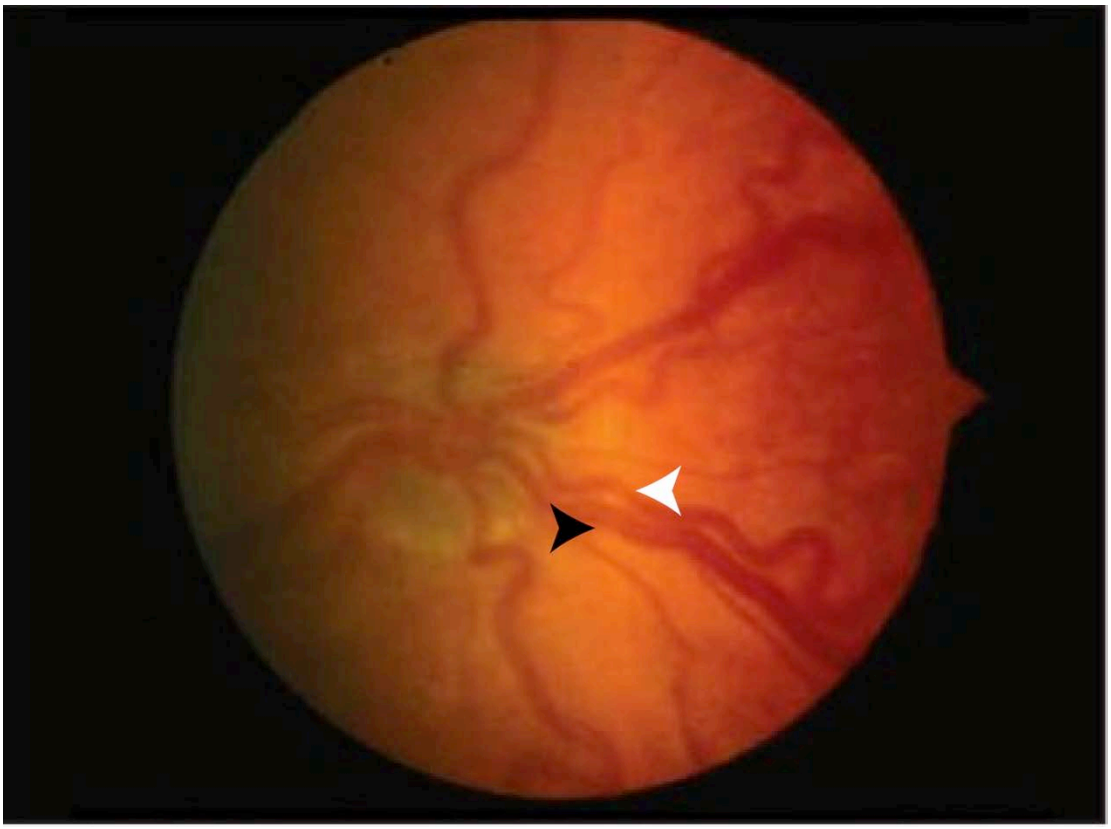

Figure 1.10: Plus disease

Plus disease is characterised by venous dilatation (black arrowhead) and arteriolar tortuosity (white arrowhead) of the retinal vessels in at least two quadrants of the fundus (The international committee for the classification of retinopathy of prematurity, 2005, p996).

1.2.1.2. Screening

The United Kingdom (UK) ROP guideline currently recommend that a retinal examination be performed on all premature infants who have a gestational age (GA) of less than 32 weeks or a birth weight (BW) of less than 1500 grams [6]. GA is measured from the first day of the last menstrual period to the day of birth. For infants born before 27 weeks GA, the first ROP screening examination should be undertaken at 30 to 31 weeks postnatal age (PNA). PNA is measured from the day of birth to the day of retinal examination. For infants born at or after 27 weeks GA, the first ROP

screening examination should be undertaken between 4 to 5 weeks PNA [6]. Follow up examinations should be done every 1 to 2 weeks thereafter until retinal vessels have grown normally into zone III. Examinations should be performed more frequently, either weekly or twice a week, if the normal retinal blood vessels stop growing into the periphery of the retina or if ROP begins to develop.

1.2.1.3. Treatment

Treatment guidelines have been created based on the results of several multicenter ROP trials [7, 8]. Laser treatment to the avascular retina is the treatment of choice for ROP in the UK. The current UK ROP guideline advocates laser treatment of any stage of ROP in zone I associated with plus disease, any Zone I, stage 3 ROP with or without plus disease, and any zone II, stage 3 ROP with plus disease, and suggesting serious consideration for treatment of any infant with zone II, stage 2 ROP with plus disease [6]. A prospective randomised multicenter trial in 2011 showed effective treatment of stage 3 ROP in zone I with intravitreal bevacizumab (Avastin; Roche, Grenzach, Germany) [9].

1.2.2. Incontinentia Pigmenti

Incontinentia pigmenti (IP), also known as Bloch-Sulzberger syndrome, is an X-linked dominant disease with ocular, central nervous system, dermatologic, and dental abnormalities. It is associated with a mutation in the NEMO gene located on Xq28 [10]. The resulting protein regulates the activity of the NF-kB transcription factor complex, increasing a cell's sensitivity to apoptotic signals and resulting in increase endothelial cell death [11].

The cutaneous manifestations of IP are distinctive and appear at birth or within a few weeks after. Classically, the dermatological features are described in four stages

but not all stages necessarily occur and several stages may overlap. The first stage is an erythematous vesicular rash, usually on the extremities, and typically persists for weeks to months. Subsequently, these evolve into verrucous lesions (stage 2) that last for several months, until groups of small hyperpigmented macules (stage 3) in a characteristic "splashed paint" distribution appear, mostly predominantly on the trunk. Finally, the lesions become pale, atrophic, and scarred (stage 4) [11].

About one-third of patients with IP have neurological problems that may include convulsive disorders, microcephaly, hydrocephalus, cerebral palsy, and retarded mental development [12]. Dental abnormalities including partial or total anodontia, late dentition, and pegged and otherwise malformed teeth are found in approximately two-thirds of cases [12].

Ocular manifestations, often asymmetric, are described in one-quarter to one-third of cases [13], typically in the form of a proliferative retinal vasculopathy that closely resembles ROP. The clinical features of the retinopathy of IP include incomplete peripheral retinal vascularisation, arteriovenous anastomoses, neovascular proliferation, fibrous membrane formation and tractional retinal detachment (Figure 1.11) [13, 14]. Microphthalmos, strabismus, nystagmus, cataract, foveal hypoplasia, and optic atrophy occur occasionally, representing secondary consequences of end stage retinopathy in most if not all cases [13].

The retinopathy of IP has been managed by laser photocoagulation or cryotherapy in a small number of cases, with varying degrees of success [13, 14, 15]. Treatment is usually applied primarily to the avascular peripheral retina, which is very similar to the currently preferred approach to management of ROP.

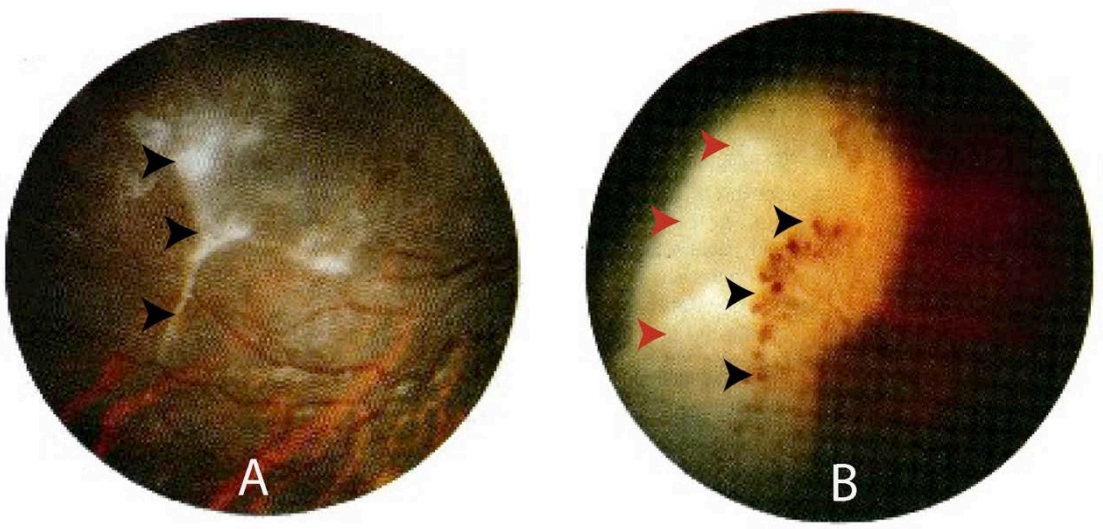

Figure 1.11: Retinal pathologies in incontinentia pigmenti (Rahi and Hungerford, 1990, p378)

(A) Colour fundus photograph of the temporal periphery of the right eye of an infant with IP showing a fibrovascular membrane (black arrowhead). (B) Colour fundus photograph of the temporal periphery of the right eye of an infant with IP showing neovascular proliferations (black arrowheads) at the border of the zone of avascular retina (red arrowheads).

1.2.3. Familial Exudative Vitreoretinopathy

Familial exudative vitreoretinopathy (FEVR) describes a group of inherited disorders with premature arrest of retinal angiogenesis and vascular differentiation resulting in incomplete vascularisation of the peripheral retina. The failure to fully vascularise the retina may be asymptomatic, but in the presence of significant retinal ischaemia, secondary changes can include peripheral retinal neovascularisation, retinal exudate, retinal folds, retinal fibrosis, and tractional retinal detachment (Figure 1.12) [16]. The clinical appearance varies considerably, with severely affected

patients often registered as blind during infancy and mildly affected patients having few or no visual problems.

FEVR can be inherited as an autosomal recessive, autosomal dominant, and X-linked disorder, with all the genes identified to date being components of the Wnt-signalling pathway [17].

Due to the low prevalence of the disease, there is an absence of robust data to guide clinicians in managing FEVR patients. In patients who show signs of progression, laser ablation of peripheral ischaemic retina may be indicated [18]. In advanced cases, vitreoretinal surgery may be beneficial [19].

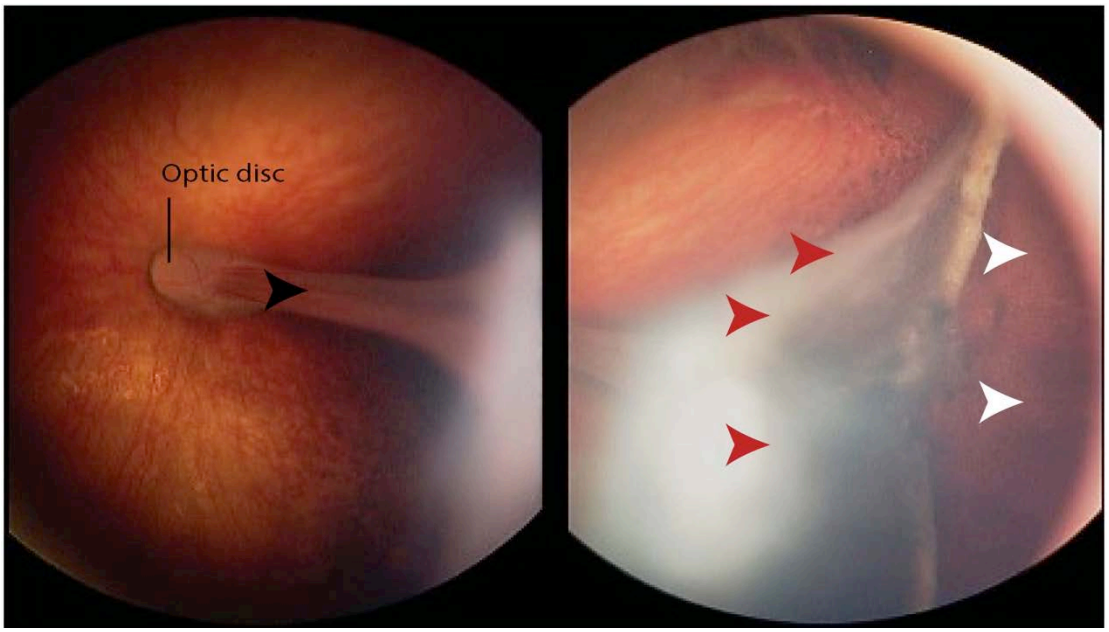

Figure 1.12: Retinal pathologies in familial exudative vitreoretinopathy (Gilmour, 2015, p5)

Colour fundus image of the left eye of an infant with FEVR showing a radial retinal fold (black arrowhead) towards an area of fibrosis (red arrowheads) and temporal avascularity (white arrowhead).

1.3. Diagnostic Approach to Infant Retinal Diseases

1.3.1. Techniques of Clinical Examination

Diagnosing retinal diseases in infants requires a combination of careful clinical examination and specialised imaging techniques. The simplest clinical examination technique is using the direct ophthalmoscope, which provides an upright, monocular, high magnification image of the retina. However, the instruments lack of stereopsis, small field of view, and poor view of the retinal periphery limits its use. These shortcomings are overcome by using the binocular indirect ophthalmoscope (BIO) in combination with a handheld magnifying lens that dramatically increases the field of view with lower magnification (Figure 1.13). The inverted, binocular image of the retina that these provide allows examination of most of the retina. However to see the entire retina, the BIO examination needs to be combined with scleral indentation. The indirect ophthalmoscope is the gold standard method for examining the fundus in infants.

Figure 1.13: Binocular indirect ophthalmoscopy of an infant

1.3.2. Fundus Fluorescein Angiography

Since its first use as a diagnostic tool in the 1960s, fundus fluorescein angiography (FFA) has become an invaluable and increasingly sophisticated tool for studying, understanding, documenting, and treating retinal diseases in infants. During FFA, a rapid sequence of serial photographs of the retina is taken after the intravenous administration of sodium fluorescein to visualise and document choroidal and retinal blood flow. Beyond blood flow, FFA provides information about the integrity of the blood-retinal barrier, the fine details of the RPE, and a glimpse of associated systemic pathology [20].

1.3.2.1. Properties of Sodium Fluorescein

Initially fabricated from plant extract, the fluorescein used in ophthalmic imaging is a hydrocarbon salt of sodium. It has a molecular weight of 376 daltons and is highly water-soluble.

Like all luminescent chemicals, fluorescein has the ability to give off light after exposure to a specific wavelength (excitation wavelength). The dye is able to absorb the energy of the excitation wavelength and subsequently emit the absorbed energy as light of a lower frequency. This is known as the principle of fluorescence. For sodium fluorescein, the excitation wavelength is 465 to 490 nm and the fluorescence wavelength is 520 to 530 nm. In the human blood stream at a pH of 7.4, this absorption wavelength is refined to blue light of 465 nm and the emission wavelength to yellow-green light of 525 nm [21].

A second property of fluorescein that makes it ideal for the study of the retinal vascular properties is its high molecular weight. This molecular weight is large enough to prevent its escape from capillaries of the retina, which have tight junctions between the endothelial cells (this forms the physiologic inner blood-retinal barrier).

Similarly, fluorescein is too large to diffuse through the RPE (this constitutes the physiologic outer blood-retinal barrier). However, fluorescein is able to leak from components of the blood-retina barrier that are pathologically disrupted. This fact is the underlying principle allowing interpretation of hyperfluorescent lesions seen on the fluorescein angiogram.

In the blood stream, 80% of the fluorescein is protein-bound and not available for fluorescence; the remaining 20% is unbound and circulates in the vasculature and tissues of the retina and choroid, where it can be visualised. Fluorescein is eliminated primarily through the liver and kidneys within 24-36 hours via the urine.

1.3.2.2. Side effects and Complications of Fundus Fluorescein Angiography

Various side effects and complications can occur with fluorescein injection. All patients injected with fluorescein have temporary yellowing of the skin and conjunctiva, lasting from 6 to 12 hours after injection, as well as yellow-orange discolouration of the urine, which lasts from 24 to 36 hours [20]. A possible complication of the injection is extravasation of the fluorescein under the skin. This is associated with immediate pain, which is usually self-limited with no long-term sequelae, although in rare instances it has resulted in necrosis of the tissues overlying the site of injection [22]. The application of an ice pack at the site of extravasation may help relieve pain. Nausea is the most frequent side effect of fluorescein injection, occurring in about 5% of patients [23]. Vomiting occurs infrequently, affecting only 0.3-0.4% of patients [23]. During angiography, severe reactions including anaphylactic reactions such as seizures, loss of consciousness, laryngeal oedema, respiratory arrest, and death are possible [24]. The chance of a reaction leading to death is extremely rare, less than 1 in 200,000 [25]. Nonetheless, the possibility of such a reaction requires certain emergency equipment to be available, such as oxygen,

a stethoscope, a blood pressure cuff, an oral airway, intravenous needles, intravenous fluids, and drugs, including adrenaline and an antihistamine.

1.3.2.3. Interpretation of a Fundus Fluorescein Angiogram

Fluorescein enters the eye through the ophthalmic artery, passing into the choroidal circulation through the short posterior ciliary arteries and into the retinal circulation through the central retinal artery. Because the retinal circulation has a longer anatomical course, these vessels fill after the choroidal circulation.

The angiogram may be subdivided into different phases (Figure 1.14). The choroidal phase (Figure 1.14A) is characterised by a lobular, patchy, and mottled filling of the choroid. The arterial phase (figure 1.14B) of the angiogram occurs after the choroidal phase, with filling of the retinal arteries. The arteriovenous phase (Figure 1.14C) begins with complete filling of the retinal arteries and capillaries, and completes with laminar filling of the retinal veins in which the dye appears to line the venous wall leaving a central hypofluorescent strip. In the venous phase (Figure 1.14D), the laminar flow progresses to complete filling of the retinal veins. The late (recirculation) phase (Figure 1.14E) demonstrates the effects of continuous recirculation, dilution and elimination of the dye. With each round of recirculation, the intensity of fluorescence gradually declines.

The macula lutea contains xanthophyll pigments at a higher concentration than the peripheral retina. It is the high concentration of this pigment, in conjunction with the increased density of RPE cells that causes the normal relative hypofluorescence of the macula seen on fluorescein angiography (Figure 1.15). The foveal avascular zone (FAZ) (Figure 1.15), which is readily apparent as a dense hypofluorescent area during fluorescein angiography, is a normal area centered within the fovea that contains no blood vessels. A continuous network of capillaries typically surrounds the FAZ.

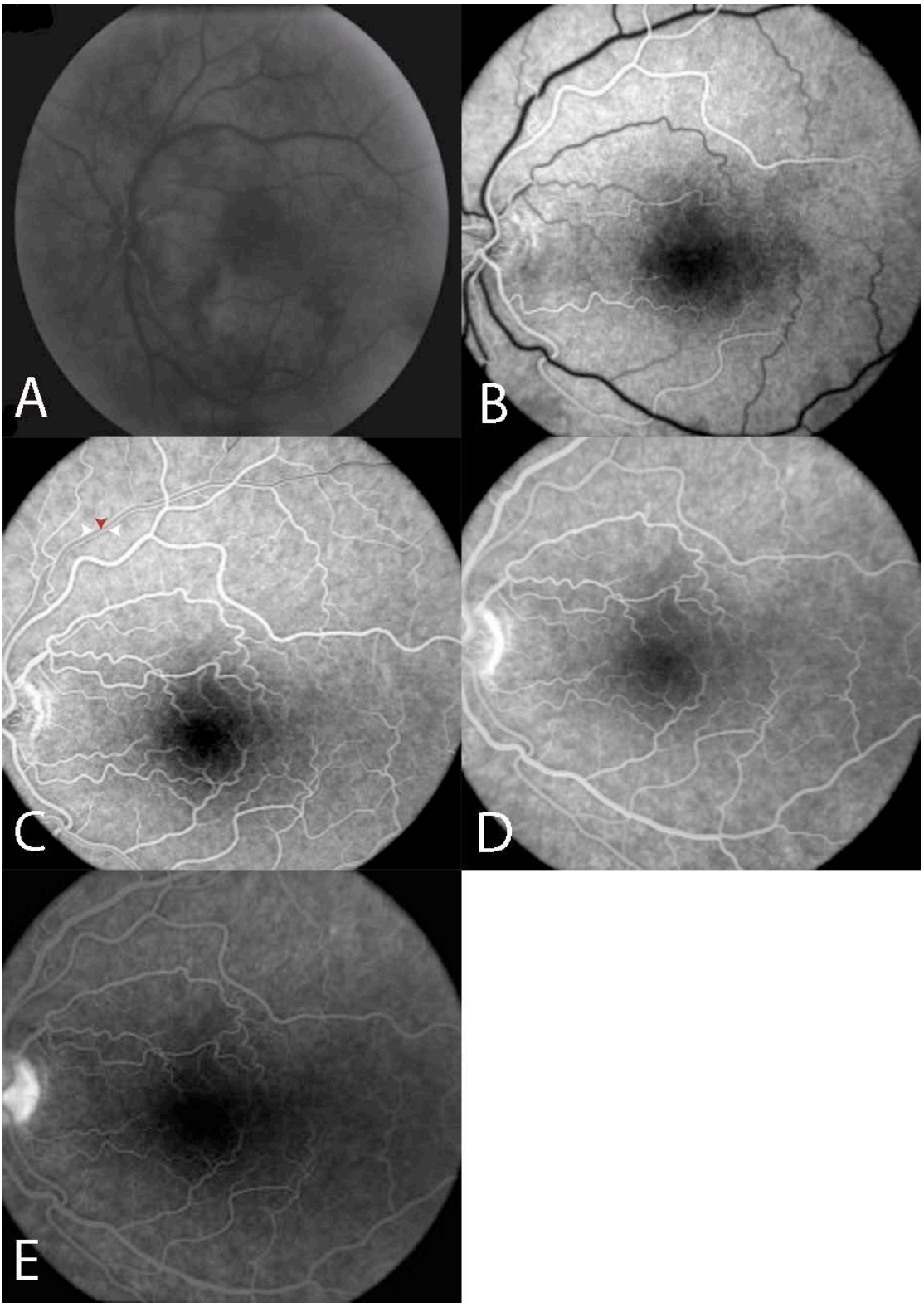

Figure 1.14: Phases of a normal fundus fluorescein angiogram

(A) The choroidal phase is characterised by a lobular, patchy, and mottled filling of the choroid. (B) The arterial phase is characterised by complete filling of the retinal

arteries. The veins remain dark as no dye has yet entered the venous circulation (C) The arteriovenous phase begins with the complete filling of retinal arteries and capillaries, and completes with laminar filling of the retinal veins in which the dye appears to line the venous wall (white arrowheads) leaving a central hypofluorescent strip (red arrowhead). (D) The venous phase is characterised by complete filling of the retinal veins. (E) The late phase demonstrates the gradual elimination of dye from the retinal and choroidal vasculature.

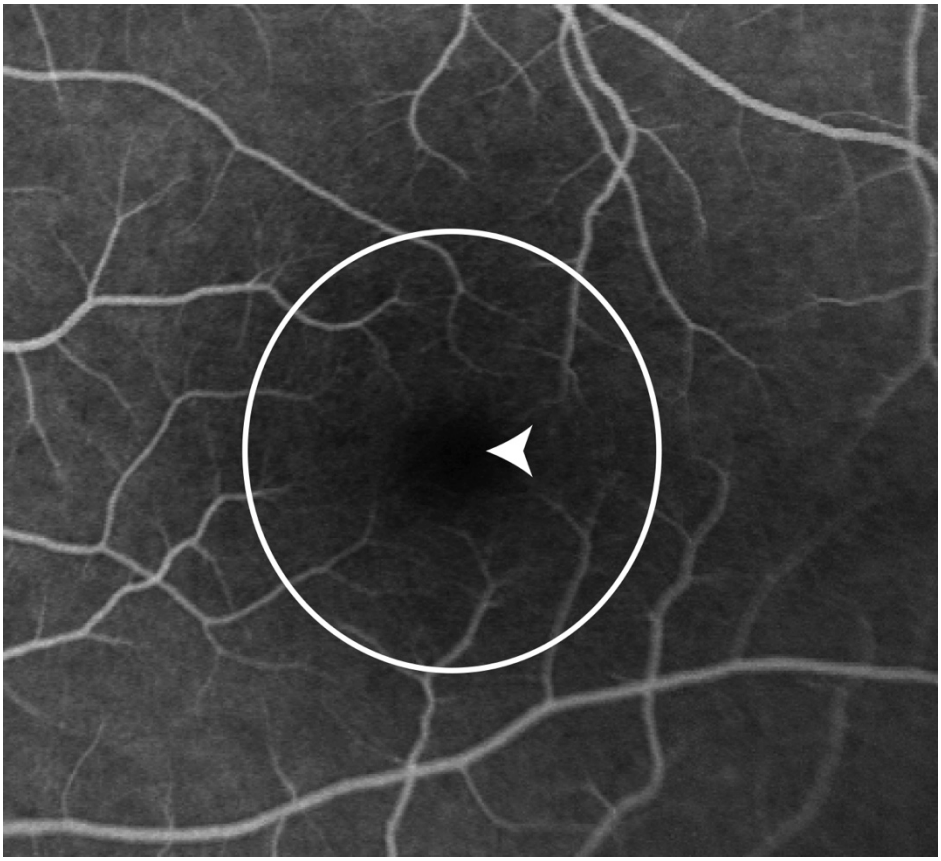

Figure 1.15: Normal fundus fluorescein angiogram of the macula

Relative hypofluorescence (white circle) is normally seen at the macula on fluorescein angiography. The FAZ (white arrowhead) is centered within the fovea and is typically surrounded by a continuous network of retinal capillaries.

Abnormalities seen in FFA can be grouped into 3 categories, associated with one of the following:

(1) Autofluorescence describes the appearance of fluorescence from the fundus captured prior to intravenous fluorescein injection. It is seen with structures that naturally fluoresce, such as optic nerve drusen.

(2) Hyperfluorescence occurs when there is an excess of normal fluorescence. It is seen in several major patterns. *Leakage* (Figure 1.16A,B) refers to the gradual, marked increase in fluorescence throughout the angiogram. It occurs as a result of breakdown of the inner blood-retinal barrier. *Staining* (Figure 1.16C) refers to a pattern of hyperfluorescence where the fluorescence gradually increases in intensity throughout the transit views and persists in late views, but its borders remain fixed throughout the angiogram. Staining results from fluorescein entry into a solid tissue or similar material that retains the fluorescein, such as a scar, optic nerve tissue, or sclera. *Pooling* refers to the accumulation of fluorescein in anatomical space in the retina or choroid. It occurs due to breakdown of the outer blood-retina barrier. A *window defect* refers to a view of the normal choroidal fluorescence through a defect in the pigment or loss of pigment in the RPE.

(3) Hypofluorescence occurs when normal fluorescence is reduced or absent. It is present in 2 major patterns. *Blocked fluorescence* (Figure 1.17A) occurs when the visualisation of the fluorescein is blocked by a barrier such as blood or pigment, producing an absence of normal retinal or choroidal fluorescence in the area. *Vascular filling defects* (Figure 1.17B) occur where the retinal or choroidal vessels do not fill properly, as in non-perfusion of an artery, vein, or capillary in the retina or choroid.

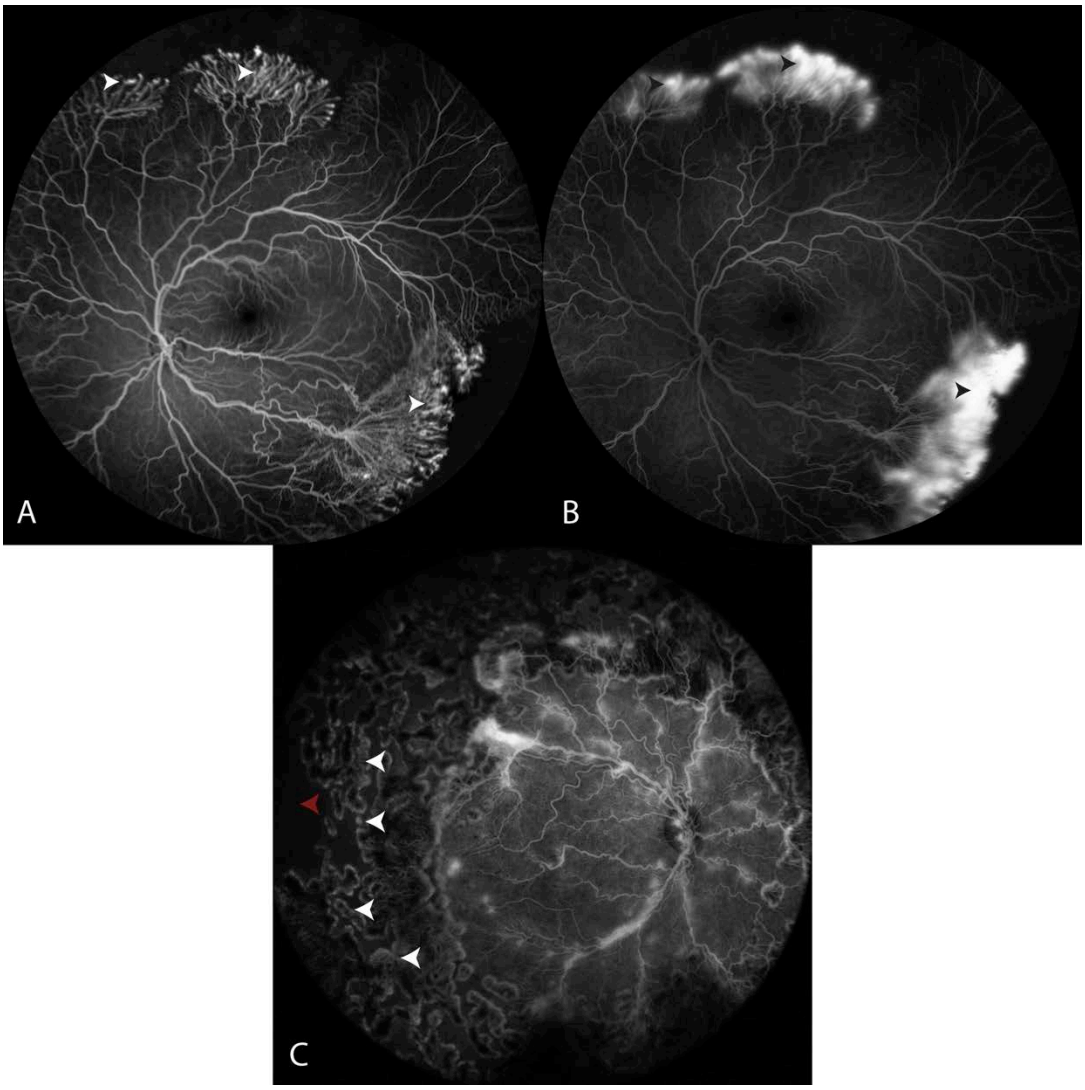

Figure 1.16: Examples of hyperfluorescent abnormalities seen in fundus fluorescein angiography

(A) Venous phase image of a fundus fluorescein angiogram of the left eye of an infant with FEVR demonstrating areas of neovascular tufts (white arrowheads) at the retinal periphery. (B) Late phase image of a fundus fluorescein angiogram of the left eye of the same infant with FEVR demonstrating leakage (black arrowheads) from the neovascular tufts. (C) Late phase image of a fundus fluorescein angiogram of the right eye of an infant with previously treated aggressive posterior ROP demonstrating staining of laser burns (white arrowheads). Note an area of missing laser (skip area) in the retinal periphery (red arrowhead).

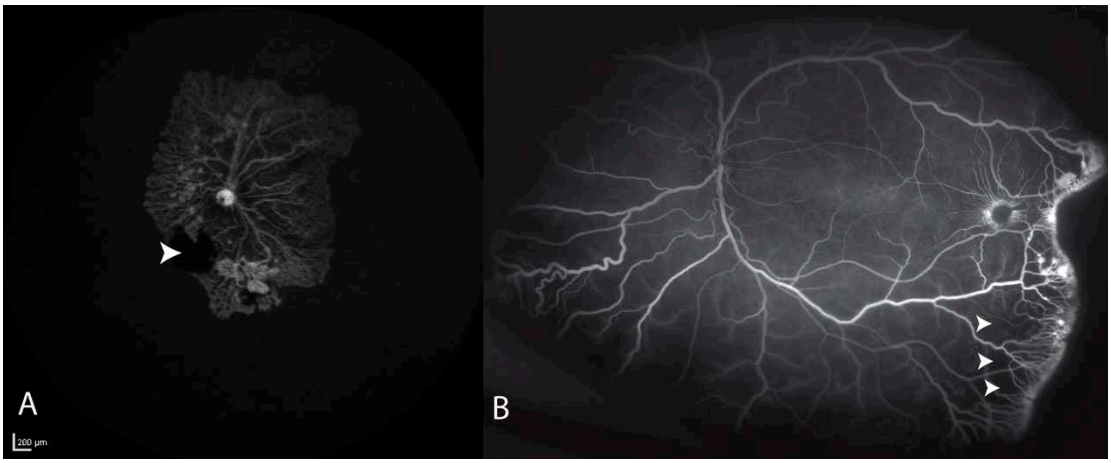

Figure 1.17: Examples of hypofluorescent abnormalities seen in fundus fluorescein angiography

(A) Venous phase image of a fundus fluorescein angiogram of the left eye of an infant with aggressive posterior ROP demonstrating blockage of retinal and choroidal fluorescence by a retinal haemorrhage (white arrowhead). (B) Venous phase image of a fundus fluorescein angiogram of the left eye of an infant with stage 3 ROP in zone 2 demonstrating vascular filling defects caused by areas of capillary non-perfusion (white arrowheads) in the peripheral retina.

1.3.2.4. Role of Fundus Fluorescein Angiography in Retinopathy of Prematurity

In 1969, Flynn et al. [26] began to perform the first large series of FFA for RLF, a late manifestation of the wide spectrum of disease we now call ROP. FFA was used in 122 premature infants to help determine and detail the changes seen in the retinal vasculature of infants with RLF. Building on this study, Lepore et al. [27] conducted FFA in infant eyes with severe ROP that were due to undergo laser photocoagulation to examine systematically the vascular abnormalities of such eyes. By using FFA, they were able to highlight retinal vessels as small as 25 microns and assessed neovascularisation, vessel leakage, loss of capillary beds, and other hypoperfused areas of the retina and choroid (Figure 1.18).

Ng et al. [28] conducted a non-randomised, investigational study to analyse the possible benefits of FFA in the screening and management of ROP. The authors concluded that FFA allowed a more objective assessment of ROP, was helpful in detecting retinal vascular pathology that could not be seen on BIO, and provided a clear observation about regression of ROP.

In 2008, Azad et al. [29] conducted a prospective study to analyse the role of intravenous FFA in the early detection and regression of ROP. In two cases with persistent non-regressing ROP and non-reduction of plus disease, FFA helped to detect previous missed areas of ROP in the peripheral retina and identify missed areas of laser (skip areas) following previous laser photocoagulation. In both of these cases, FFA guided laser photocoagulation helped with regression of ROP.

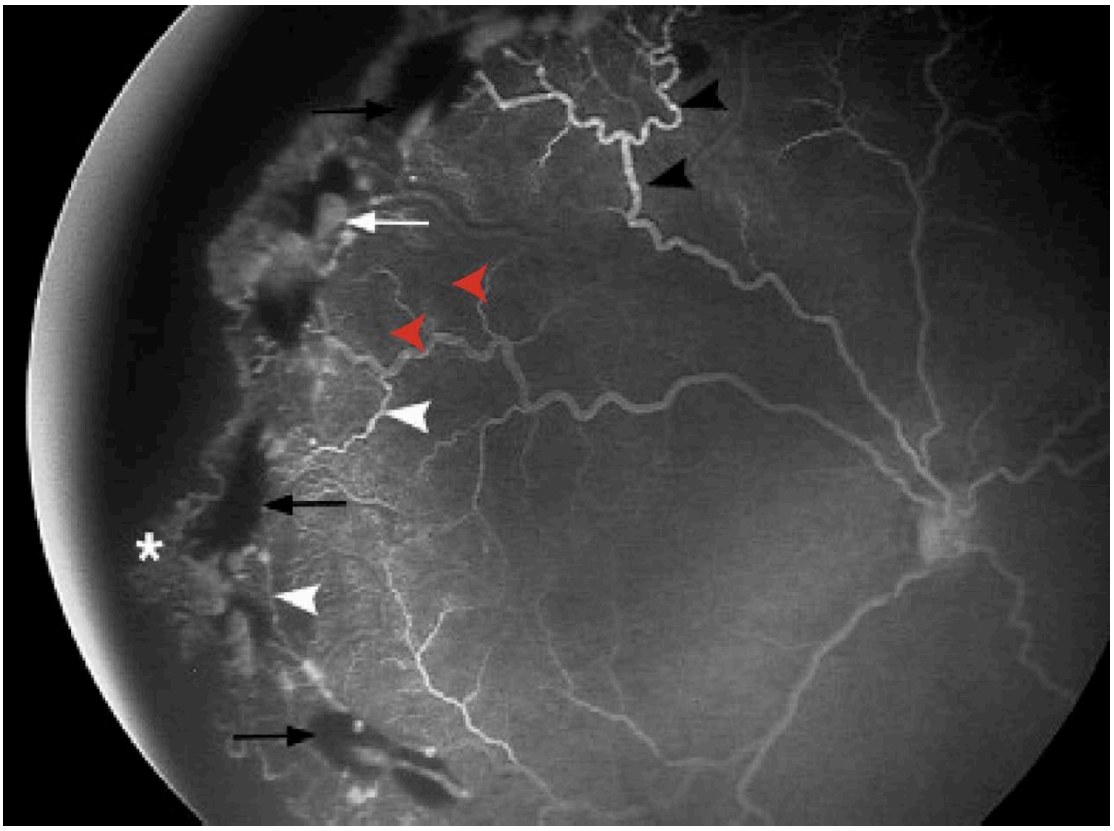

Figure 1.18: Venous phase image of a fluorescein angiogram of the right eye of an infant with severe ROP (Lepore, Molle, Pagliara, Baldascino, Angora, Sammartino and Quinn, 2011, p172)

This image highlights many of the features seen in infants with severe ROP. Retinal haemorrhages (black arrows) and loss of capillary beds (red arrowheads) causing hypofluorescence are seen in the region of the vascular-avascular junction. Hyperfluorescent lesions caused by capillary tufts (white asterix), focal capillary dilatations (white arrowheads), isolated neovascular tufts or 'popcorn' lesions (white arrow), and rosary bead-like lesions (black arrowhead) are also seen towards the vascular-avascular junction.

1.3.2.5. Role of Fundus Fluorescein Angiography in Incontinentia Pigmenti

In 1994, Goldberg [30] carried out FFA in 3 infants with IP under general anaesthesia. He described macula ischaemia, enlargement of the FAZ, anomalous blood vessels traversing the normally avascular foveal center, and tufts of perifoveolar neovascularisation found on FFA, but not on conventional binocular indirect ophthalmoscopy (Figure 1.19). Goldberg concluded that all infants with IP should have their retinas angiographically studied to identify potential severe retinal abnormalities that would be missed with conventional indirect ophthalmoscopy.

Several case reports also described similar findings using FFA in infants with IP [31, 32, 33]. All the cases reported illustrated how binocular indirect ophthalmoscopy, even when performed under general anaesthesia, can miss the subtle peripheral changes that occur in IP. The reports all concluded that angiography is crucial in determining the extent of the disease and should be used as a guide for laser therapy.

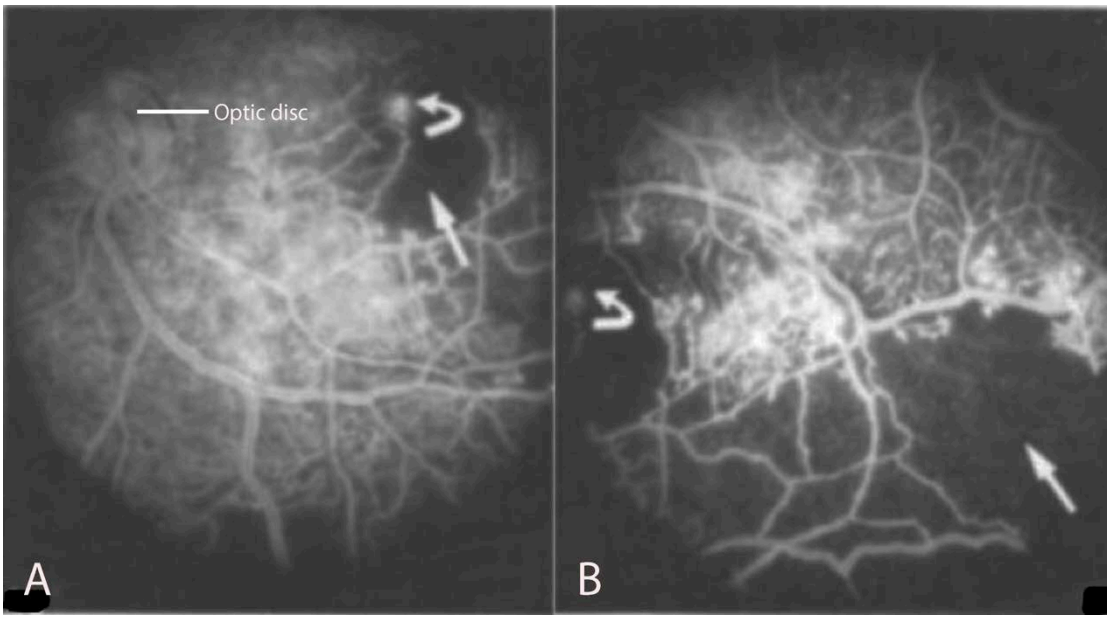

Figure 1.19: Late phase images of a fluorescein angiogram of the left eye of an infant with IP (Goldberg, 1994, p70).

(A) Marked ischaemia of the macula is noted (straight white arrow) with a secondary tuft of perifoveolar neovascularisation (curved white arrow). (B) This photographed area is contiguous with photograph A. Curved white arrow shows tufts of perifoveolar neovascularisation with extensive zone of non-perfusion in adjacent posterior pole (straight white arrow).

1.3.2.6. Role of Fundus Fluorescein Angiography in Familial Exudative Vitreoretinopathy

In 1969, Canny et al. [34] described the fluorescein angiographic findings in 4 patients with FEVR. They demonstrated marked closure of the peripheral retinal vasculature associated with elevated, temporal fibrovascular masses, and stressed the similarity between FEVR and ROP. Building on this, Ober et al. [35] described the fluorescein angiographic findings (Figure 1.20) in 12 affected members of 3 families with autosomal dominant FEVR. Of the 12 patients, they found that 7 had no ocular

symptoms and had no detectable clinical signs with indirect ophthalmoscopy. However on FFA, all 7 patients had pre-equatorial non-perfusion of retinal vessels, indicating the abnormal genotype. Fluorescein angiography easily demonstrated the peripheral non-perfusion, which was difficult to detect ophthalmoscopically. The authors emphasised that FEVR may be asymptomatic and non-progressive, and that clinical abnormalities may only be detectable with FFA.

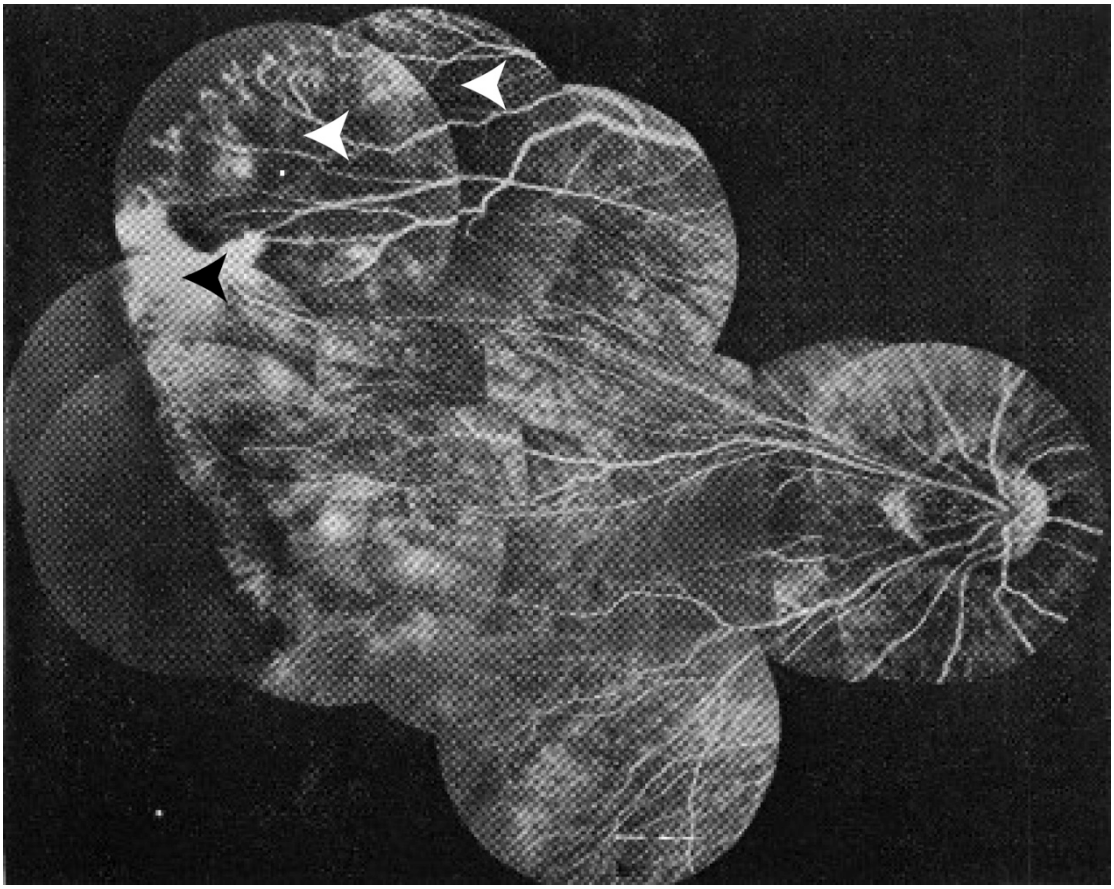

Figure 1.20: Late phase image of a fluorescein angiogram of the right eye of an infant with FEVR (Ober, Bird, Hamilton and Sehmi, 1980, p113)

This image demonstrates distortion of the retinal vessels and peripheral vessel closure (white arrowheads), with diffuse leakage from the peripheral retinal vessels and from the forward vessels (black arrowhead).

1.3.3. Retinal Imaging Techniques in Infants

Traditionally, retinal pathologies were observed using a direct ophthalmoscope or a BIO and documented by freehand drawings. Though ophthalmoscopy still remains the initial technique for examination of the infant retina, the clinician now has at his disposal a sophisticated range of imaging techniques that have dramatically increased the ability to document and investigate infant retinal pathologies.

Imaging of the infant eye using specialised imaging systems has several advantages over ophthalmoscopy. Firstly, images provide a more accurate representation of retinal pathology, which is not dependent on an artistic drawing. Secondly, images can capture subtle retinal pathologies that are not apparent on ophthalmoscopy. Thirdly, the ability to reference and compare images over time allows for better management of retinal disease and better assessment of response to treatment. Lastly, the instant visualisation of retinal pathology on an external monitor is ideal for teaching students, ophthalmic trainees, and other allied health professionals.

1.3.3.1. Traditional Fundus Camera

Traditional fundus cameras specify the area of retina imaged by referring to the external angle of the light source as it enters the eye [36]. In 1926, the Carl Zeiss Company produced its first commercially available fundus camera that provided a 20-degree field of view. The same company later expanded the field of view to 30 degrees (Figure 1.21), which became the standard for the traditional fundus camera. In 1969, Bulpitt et al. [37] documented the first attempts at imaging the retina in infants using a vertically mounted Carl Zeiss fundus camera (Figure 1.22). The infants were positioned on a trolley before the vertically mounted fundus camera was wheeled into position. One team member held the infants head with the eyelids

manually opened whilst another team member performed the photography. Using this imaging method, the authors had difficulty obtaining clear images of the peripheral retina.

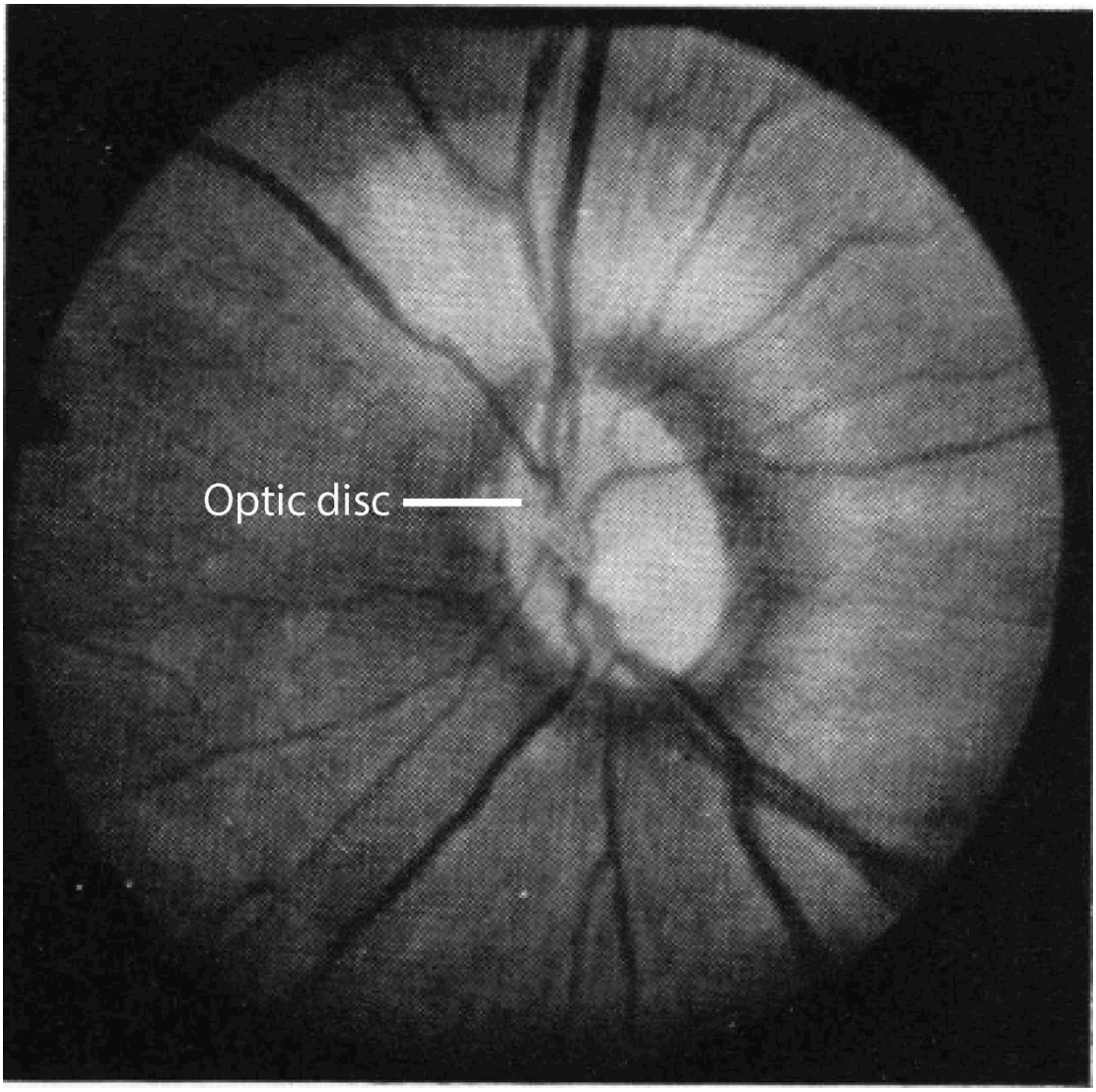

Figure 1.21: Traditional fundus photograph of the left eye of an infant, centered on the optic disc, illustrating the standard 30-degree field of view (Bulpitt and Baum, 1969, p501)

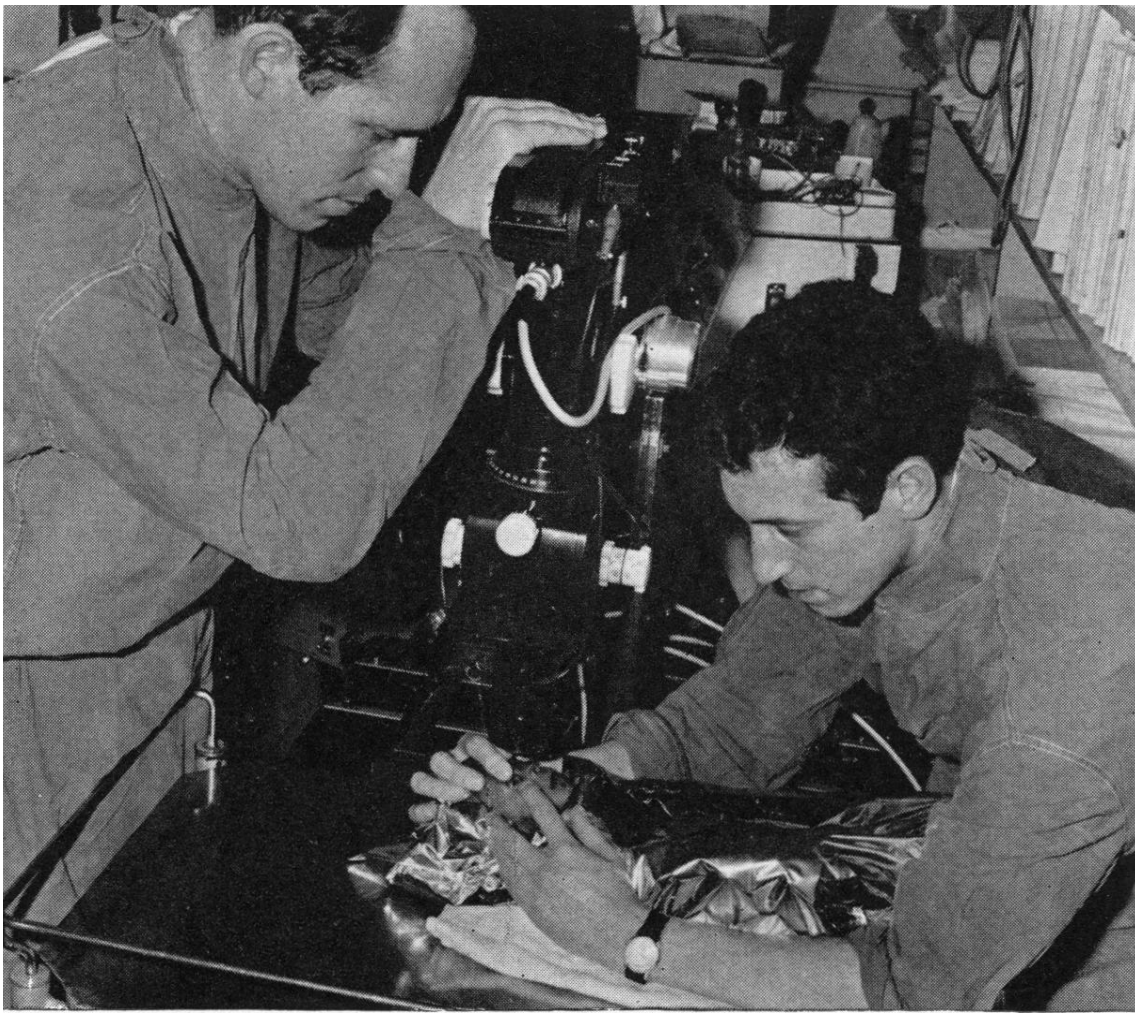

Figure 1.22: Imaging the retina of an infant in 1969 using a vertically mounted Zeiss fundus camera

The earliest documented attempt of imaging the retina of an infant was in 1969 using a vertically mounted Carl Zeiss fundus camera (Bulpitt and Baum, 1969, p500). One team member holds the infant's head and opens the eyelids whilst the other team member performs the photography.

1.3.3.2. Binocular Indirect Ophthalmoscopy Digital Photographic System

The Vantage Plus LED Digital Binocular Indirect Ophthalmoscope system (Keeler Instruments Inc, Broomall, Pennsylvania, USA) consists of a BIO with an integrated camera that can capture still and dynamic colour fundus images during the examination of an infant, which can be stored in various digital formats for later review. The field of view obtained is similar to that seen during the standard examination with indirect ophthalmoscopy (Figure 1.23) [38]. The retinal images obtained from the binocular indirect ophthalmoscopy digital photographic system have predominantly been used to screen and grade infants with ROP [39].

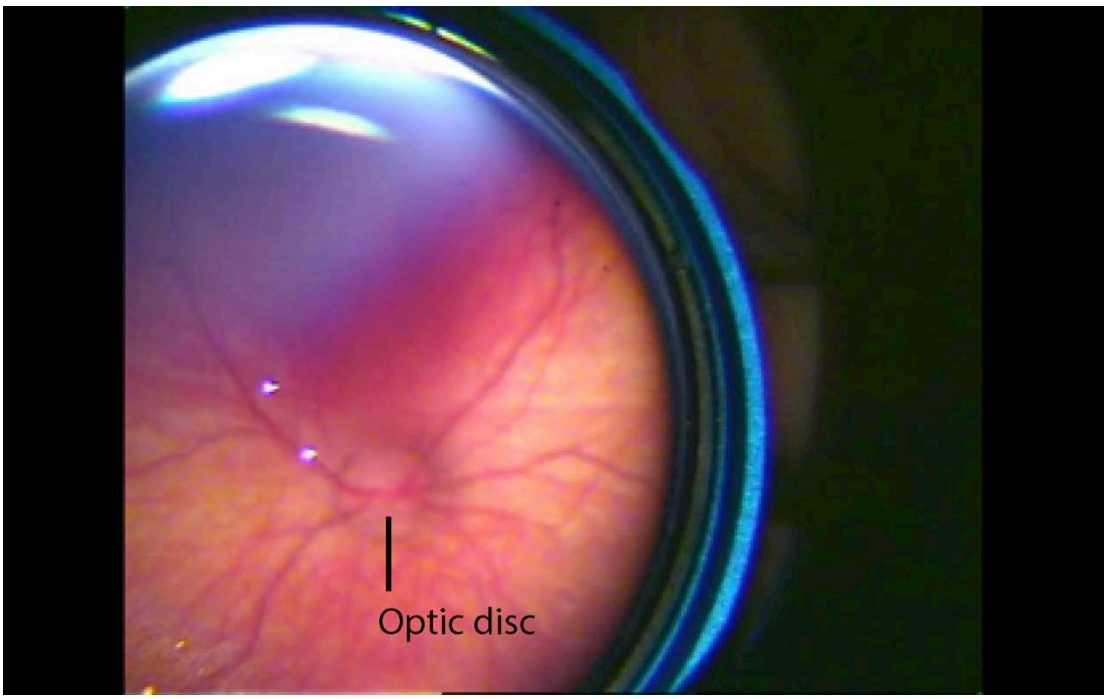

Figure 1.23: Retinal image from the digital binocular indirect ophthalmoscope

A typical image of the retina in an infant obtained with the digital binocular indirect ophthalmoscope (Fung, Smith and Patel, 2014, p144).

1.3.3.3. NIDEK Digital Fundus Camera

The NIDEK NM200D camera (NIDEK Inc, Aichi, Japan) is a non-contact handheld camera that captures a 30-degree field of view of the retina (Figure 1.24) [40]. It is capable of capturing colour fundus photos only. The retinal images obtained from the NIDEK NM200D camera has been used predominantly to screen infants for plus disease in ROP [40].

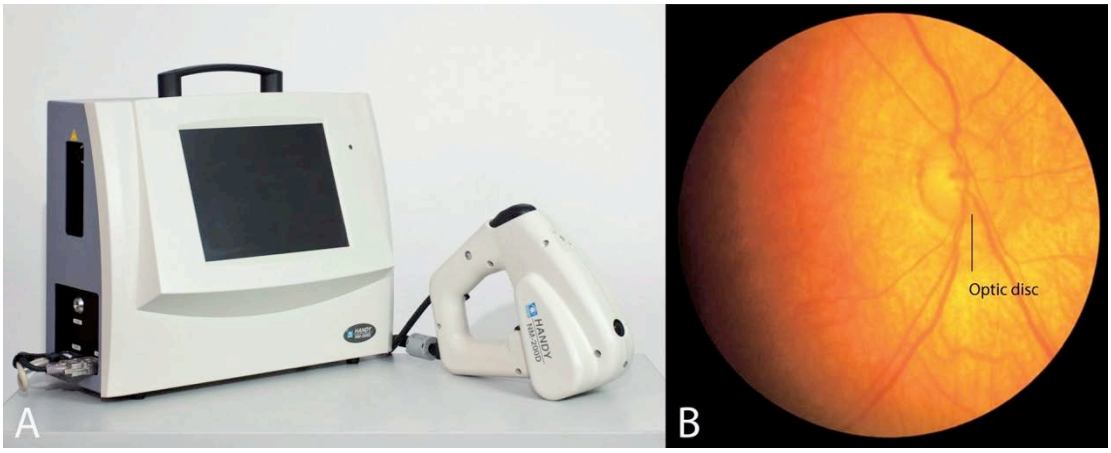

Figure 1.24: NIDEK fundus camera

(A) The NIDEK NM200D fundus camera. (B) Typical 30-degree field of view image of the right retina obtained in an infant with the NIDEK fundus camera (Johnson, Mills, Karp and Grunwald, 2007, p724).

1.3.3.4. Pictor Digital Fundus Camera

The Volk Pictor (Volk Optical Inc, Mentor, Ohio, USA) is a non-contact hand-held digital imaging device that has the capability for both anterior segment and retinal imaging. For retinal imaging, it can record colour and red-free images of the retina simultaneously (Figure 1.25) [41], which can then be stored digitally for subsequent review. The fundus images captured have a field of view of 45 degrees.

The Volk Pictor has been successfully used to document pre-plus and plus disease in infants with ROP (41).

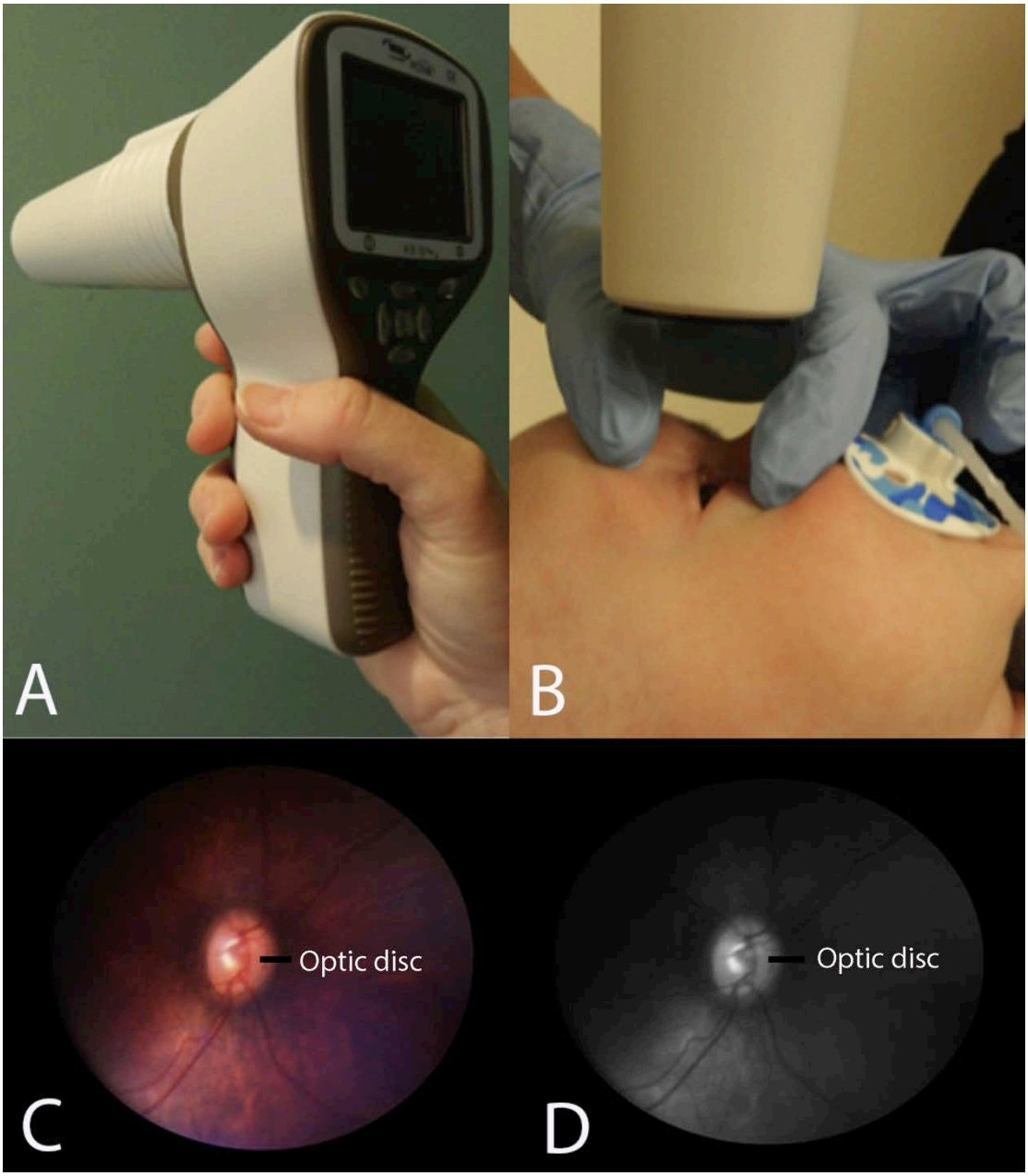

Figure 1.25: Pictor digital fundus camera

(A) The Volk Pictor digital imaging device (Prakalapakorn, Wallace and Freedman, 2014, p322). (B) The Volk Pictor is a hand-held non-contact camera that is held in front of the infant's eye for image capture (Prakalapakorn, Wallace and Freedman, 2014, p322). (C) An example of a typical colour image obtained in an infant with the

Volk Pictor (Prakalapakorn, Wallace and Freedman, 2014, p323). (D) An example of a typical red-free image obtained in an infant with the Volk Pictor (Prakalapakorn, Wallace and Freedman, 2014, p323).

1.3.3.5. RetCam Digital Fundus Camera

The RetCam (Clarity Medical Systems, Pleasanton, California, USA) is a wide-field digital ophthalmic camera that uses fiberoptic illumination to provide clear, high-resolution, real time images of the retina. The RetCam imaging system (Figure 1.26) consists of a hand held camera, which is connected by a fiberoptic cable to an electro-optical box housed in a moveable cart. A foot pedal is provided to allow control of illumination intensity, camera focus, and image acquisition.

The RetCam can capture fundal imaging angles of up to 130-degrees, producing wide-field images of the central and part of the peripheral retina. It is currently the gold standard imaging tool used to acquire retinal images in infants. In addition to colour fundus photography (Figure 1.27), it can also be used for FFA (Figure 1.28).

Prior to taking a RetCam wide-field retinal image it is necessary to instill pupil dilating drops and topical anaesthesia. The eyelids are held open with a lid speculum and the camera probe is applied with a contact lens gel to gently applanate the corneal surface over the dilated pupil. Real time images of the retina are viewed on an external monitor, and the retina is photographed with the use of a foot pedal, providing instant documentation of retinal findings.

As the RetCam can visualise and document the central and a small part of the peripheral retina, it is commonly used in screening for ROP [42] and the documentation of retinal findings in non-accidental injuries in infants [43].

The main advantage of the RetCam imaging system is its ability to provide a panoramic view of the retina, yielding a good perspective of the ocular condition

imaged. Another advantage is the portability of the RetCam imaging unit, which ensures that one can use the camera remotely in telemedicine systems.

There are several limitations to the RetCam system. Firstly despite the 130-degree field of view provided by the RetCam imaging system, peripheral retinal sweeps and montage techniques are often necessary when information about the far retinal periphery is required. These techniques can be labour intensive, require highly skilled photographers, and do not permit the simultaneous capture of the posterior pole and retinal periphery in a single image. Secondly, image quality may be affected by small pupils, corneal scars, lens opacities, and by blood in the vitreous humour [42, 43]. Thirdly, excessive pressure on the infant eye with the camera probe can induce retinal haemorrhages [44, 45], an oculocardiac response with subsequent bradycardia [46], and oxygen desaturation [47]. Excessive pressure on the eye can also affect the diagnosis of plus disease in infants with ROP [48].

Figure 1.26: The RetCam Digital Imaging System

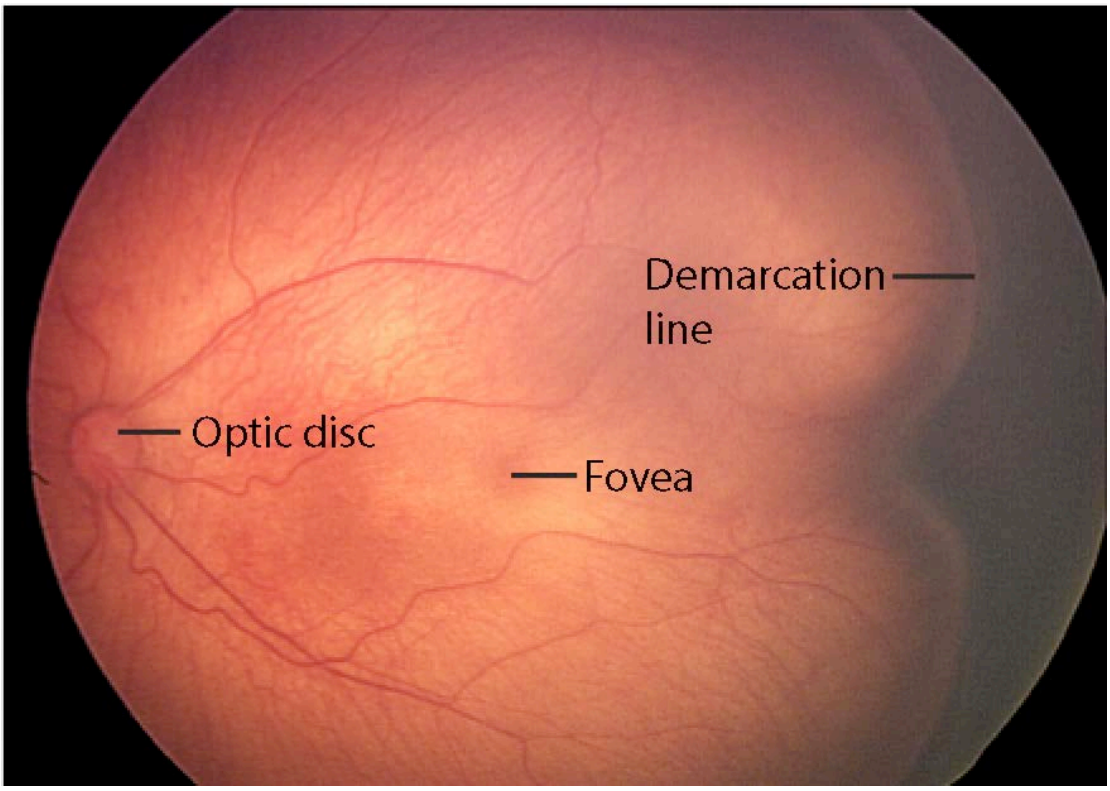

Figure 1.27: An example of a RetCam colour fundus image

This is a colour fundus image of the left eye of an infant with stage 1 ROP in zone 2 illustrates the 130-degree field of view with the RetCam.

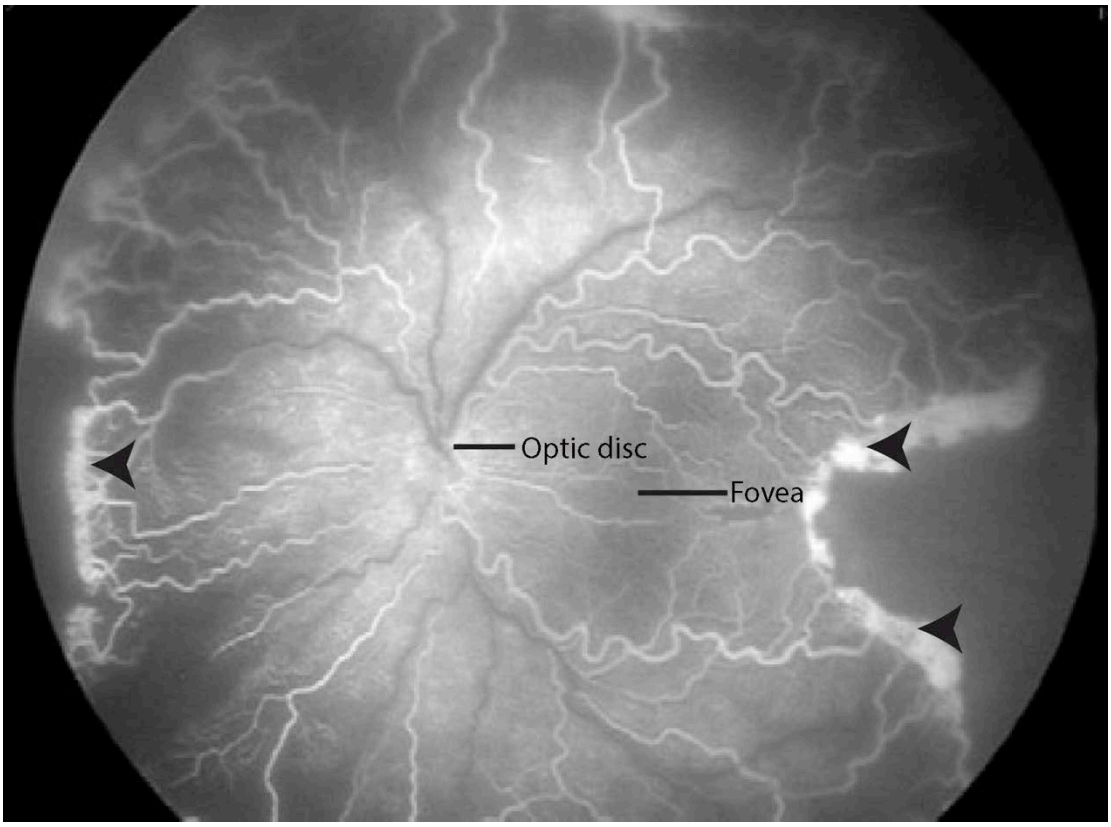

Figure 1.28: An example of a RetCam fluorescein angiographic image (Lepore, Molle, Pagliara, Baldascino, Angora, Sammartino and Quinn, 2011, p172)

This is an arterial phase image of a RetCam fundus fluorescein angiogram of the left eye of an infant with stage 3 ROP in zone 1. Areas of neovascularisation (black arrowheads) are clearly evident in the peripheral retina.

1.4. Ultra-Widefield Retinal Imaging

The field of view obtained with conventional retinal imaging devices was adequate for imaging the optic nerve and the posterior pole but provided a limited view of the peripheral retina. The peripheral retina is the site of pathology in many infant retinal diseases and its evaluation is therefore important for screening, diagnosis, monitoring, and treatment of disease manifestations. A recent technological advance in retinal imaging has been the development of ultra-widefield confocal scanning laser ophthalmoscopy (cSLO) retinal imaging. In comparison to traditional retinal imaging tools, ultra-widefield cSLO retinal imaging technologies are capable of capturing greater fundal imaging angles and provides a more practical method for visualisation and documentation of pathologies in the peripheral retina. The exact definition of ultra-widefield retinal imaging is poorly defined at present.

1.4.1. Confocal Scanning Laser Ophthalmoscopy

Scanning laser ophthalmoscopy (SLO), introduced in the early 1980's, developed as an alternative method to image the ocular fundus [49]. One distinction between digital fundus photography and SLO is that the scanning illumination system samples the retina point by point rather than capturing the image as a whole. A highly collimated narrow laser beam of a specific wavelength is focused on a point on the retina that reflects light back to a detector. A deflector mirror moves the laser beam horizontally so an adjacent point can be imaged. When one line has been acquired, a second deflector mirror moves the beam vertically before acquiring another horizontal line. A two dimensional image is built up in this raster-like fashion, and the digitised image is stored in a computer. The image acquisition is based on confocal optics, a system in which a pinhole in front of the detector is optically conjugate to the focal

plane of the retina being imaged [50]. This ensures that only light reflected from the imaged focal plane reaches the image detector. Reflected light from in front, or behind, the focal plane is prevented from reaching the detector by the pinhole.

Stereoscopic high-contrast images can be produced with and without dyes such as fluorescein and indocyanine green, and altering the laser wavelength permits selective examination and imaging of different tissue depths and structures. SLO is capable of imaging structures at a very high magnification and high frame rate, which allows accurate diagnosis of retinal structures poorly seen by digital fundus cameras and does so using low levels of light exposure and improved contrast.

1.4.2. Optos Ultra-Widefield Retinal Imaging

One of the most widely available ultra-widefield cSLO retinal imaging devices is the Optos Panoramic 200MA (Optos PLC, Dunfermline, Scotland, UK) (Figure 1.29). This imaging device consists of a large scan head, which is connected by an arm to the scan head monitor. The scan head is supported by a scan head table, which can be raised and lowered to adjust the scan head height. A hand control is linked to the scan head monitor and is used to adjust the scan head height, to capture images, and to align the eyes with the imaging system. A headrest, which is made up of a forehead strap and adjustable chin cup, is linked to the scan head and supports the patient's head while images are being captured. All images captured are stored and available for viewing in the Optos V2 vantage software.

Using an internal ellipsoid mirror (Figure 1.30), the scanner can capture fundal imaging angles of up to 200-degrees, or more than 80% of the entire retina, in a single image [51]. No eye contact is required and the image is produced in the correct orientation. A single image can be captured in 0.25 seconds. In comparison to most digital fundus cameras, which produce colour images of the retina using white light as

the illumination source, the Optos Panoramic 200MA produces false or pseudocolour colour images of the retina (Figure 1.31) using a combination of a green laser light (532 nm, red-free light) and a red laser light (633 nm). The red (Figure 1.32) and green (Figure 1.33) laser components of the retinal image can be separated. The green light (red-free) image predominantly highlights the anterior retinal structures and the retinal vasculature, whereas the red light image predominantly highlights the choroidal vasculature. Fluorescein angiography (Figure 1.34) and autofluorescence imaging are other retinal imaging modes available with the Optos Panoramic 200MA. The Optos Panoramic 200MA has a laser power of 4mW at the patient's eye and includes a laser safety system that would prevent the system being used if the lasers were operating at unsafe levels.

The Optos ultra-widefield confocal scanning laser imaging device has been predominantly used in the adult patient population to evaluate and manage various retinal diseases including diabetic retinopathy [51], diabetic macular oedema [52], retinal venous occlusions [53], and retinal vasculitis [54].

There have only been limited studies demonstrating the use of Optos ultra-widefield imaging for paediatric patients with retinal diseases. In 2013, Tsui et al. [55] successfully used the Optos ultra-widefield retinal imaging system for pseudocolour fundus photography and FFA in 16 paediatric patients with a mean age of 9.3 years (range 5 to 12 years). A spectrum of paediatric retinal diseases encompassing uveitis, hereditary retinal dystrophies, childhood retinal vascular diseases, trauma, infection, and tumours were imaged. The authors concluded that ultra-widefield imaging with the Optos device was feasible in cooperative paediatric patients. The macula and periphery were adequately imaged in all patients and was able to help with documentation, diagnosis, and management. A further study performed ultra-widefield pseudocolour fundus photography and FFA with the Optos Panoramic

200MA on 8 paediatric patients with a mean age of 11.6 years (range 9 to 14 years) [56]. In this study, 5 children had FEVR and 3 children had coat's disease. The authors reported that ultra-widefield colour fundus photography and FFA could be used successfully as an outpatient procedure in the cooperative paediatric patient population without the necessity of examination under anaesthesia and can aid the physician in the documentation and evaluation of peripheral retinal pathology. The authors also found that ultra-widefield FFA can assist in directing laser photocoagulation in the treatment of paediatric retinal vascular diseases.

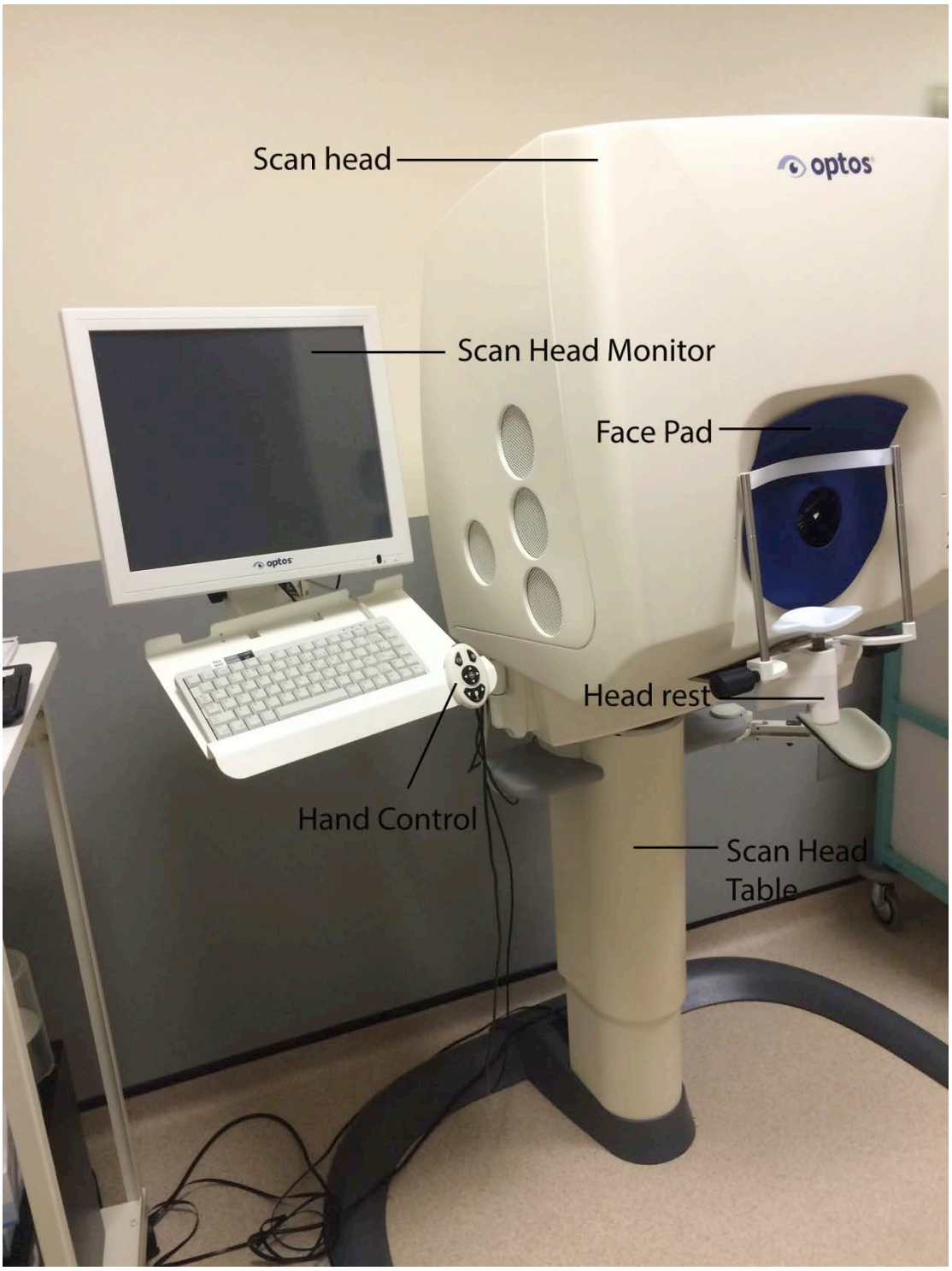

Figure 1.29: The Optos Panoramic 200MA

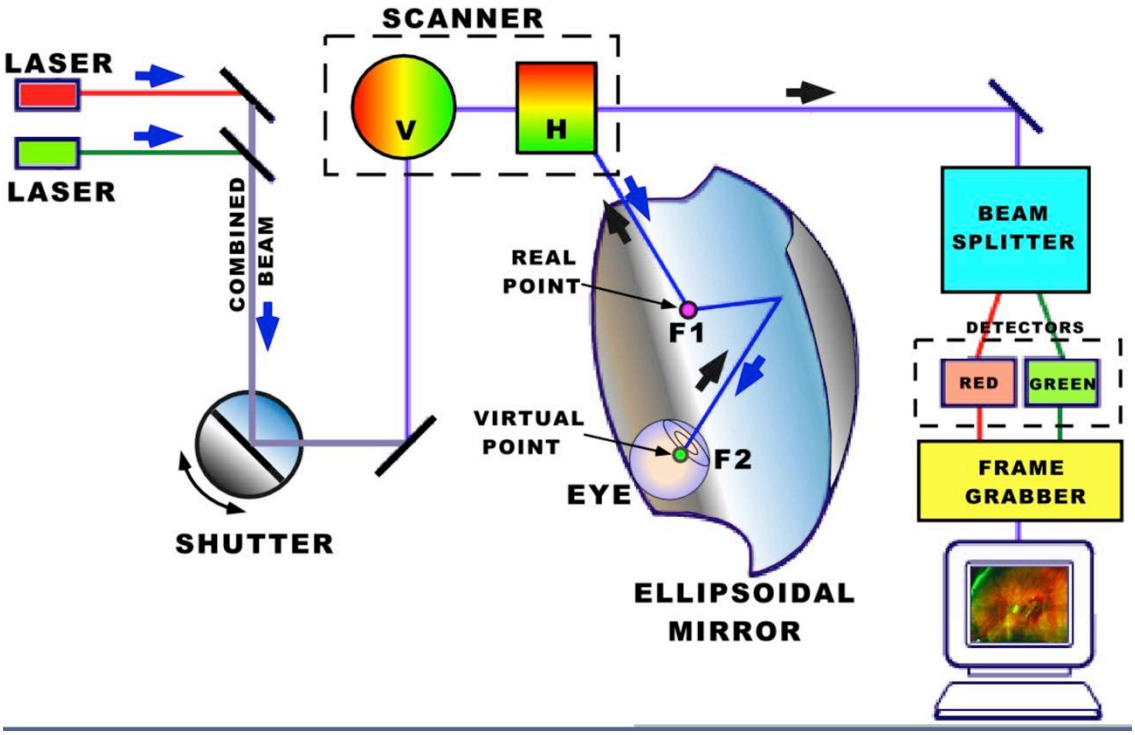

Figure 1.30: Optics of the Optos Panoramic 200MA

The Optos Panoramic 200MA utilises the optics of an ellipsoid mirror to create ultra-widefield images of the retina. The ellipsoid mirror contains two focal points. The lasers of the Optos Panoramic 200MA are directed through the 'real' focal point, while the patients eye is positioned so that the 'virtual' focal point is located posterior to the patient's iris plane.

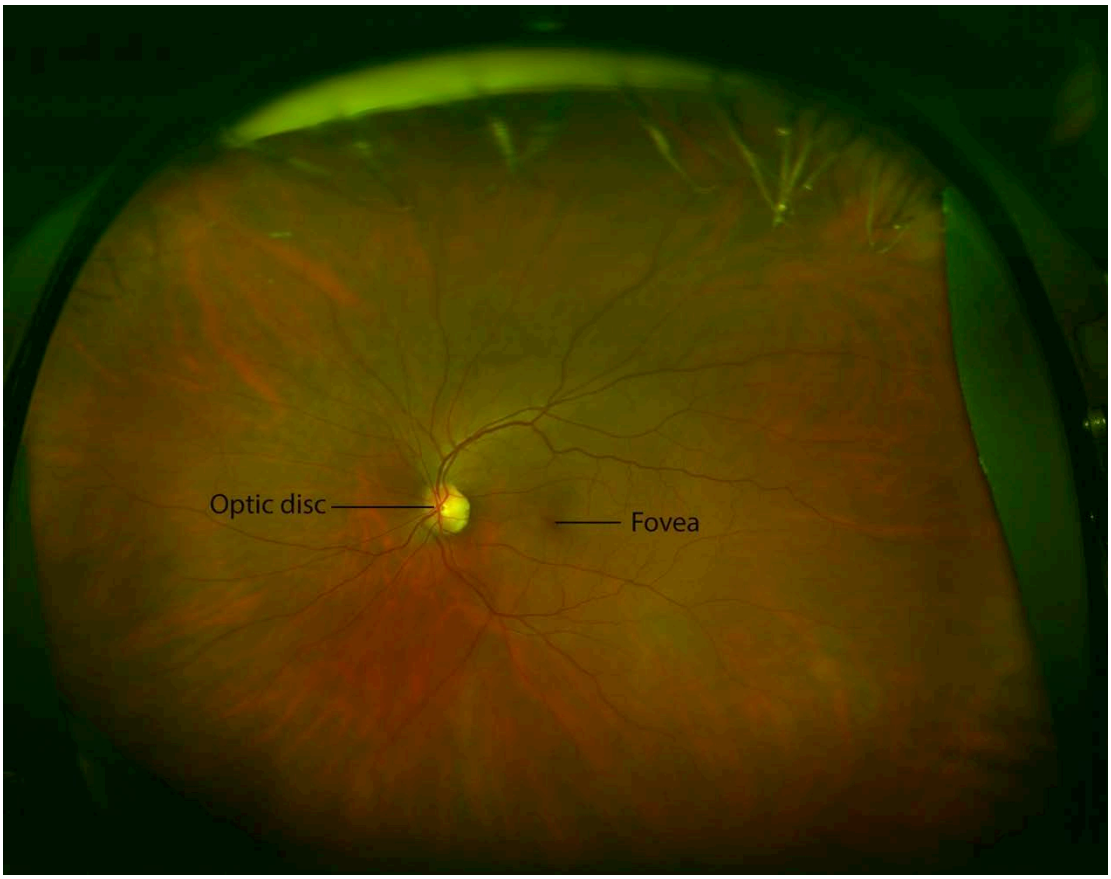

Figure 1.31: An example of an Optos ultra-widefield pseudocolour fundus image

This pseudocolour fundus image of the left eye illustrates the 200-degrees of field of view with the Optos Panoramic 200MA. The pseudocolour fundus image is produced from a combination of the red laser light and the green laser light of the Optos Panoramic 200MA.

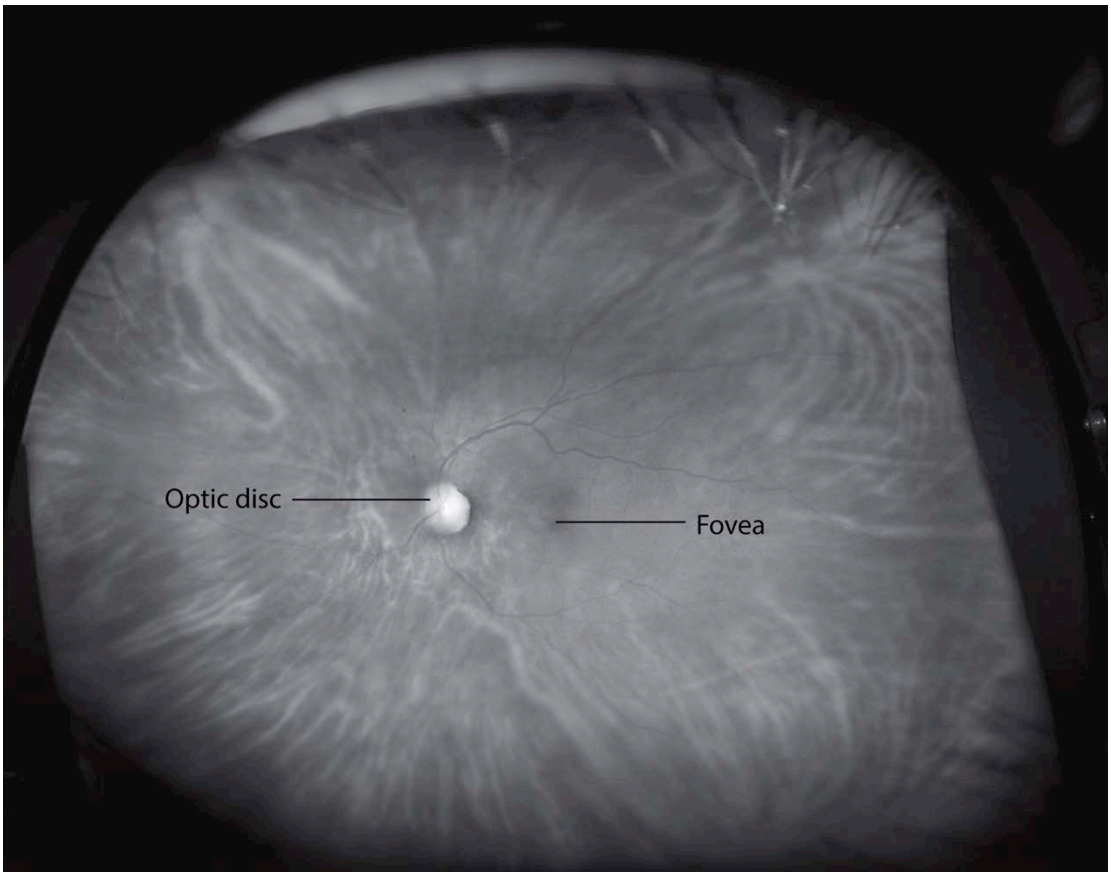

Figure 1.32: An example of an ultra-widefield fundus image from only the red laser light of the Optos Panoramic 200MA

This ultra-widefield image of the left eye is produced from only the red laser light of the Optos Panoramic 200MA. The red laser light image is predominantly used to visualise and image the choroidal vasculature.

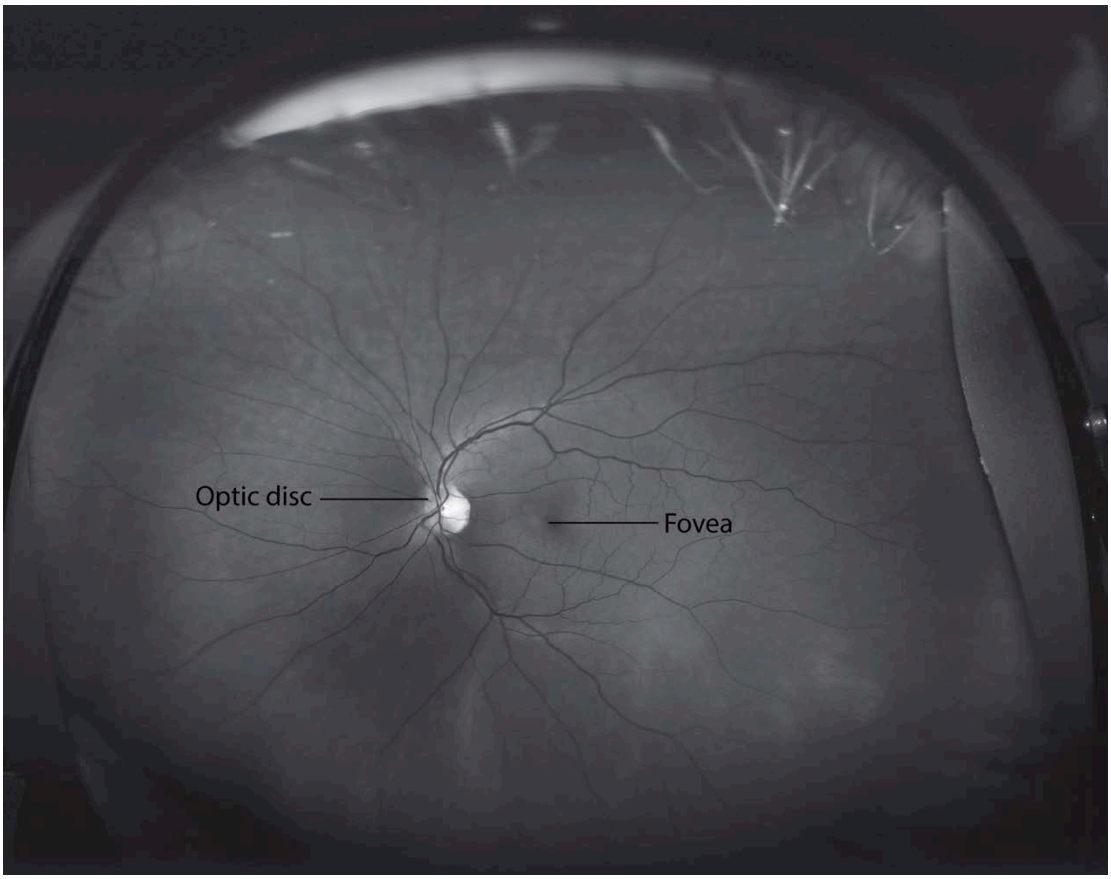

Figure 1.33: An example of an ultra-widefield fundus image from only the green laser light of the Optos Panoramic 200MA

This ultra-widefield image of the left eye is produced from only the green laser light of the Optos Panoramic 200MA. The green laser light image is predominantly used to visualise and image the anterior retinal structures and vasculature.

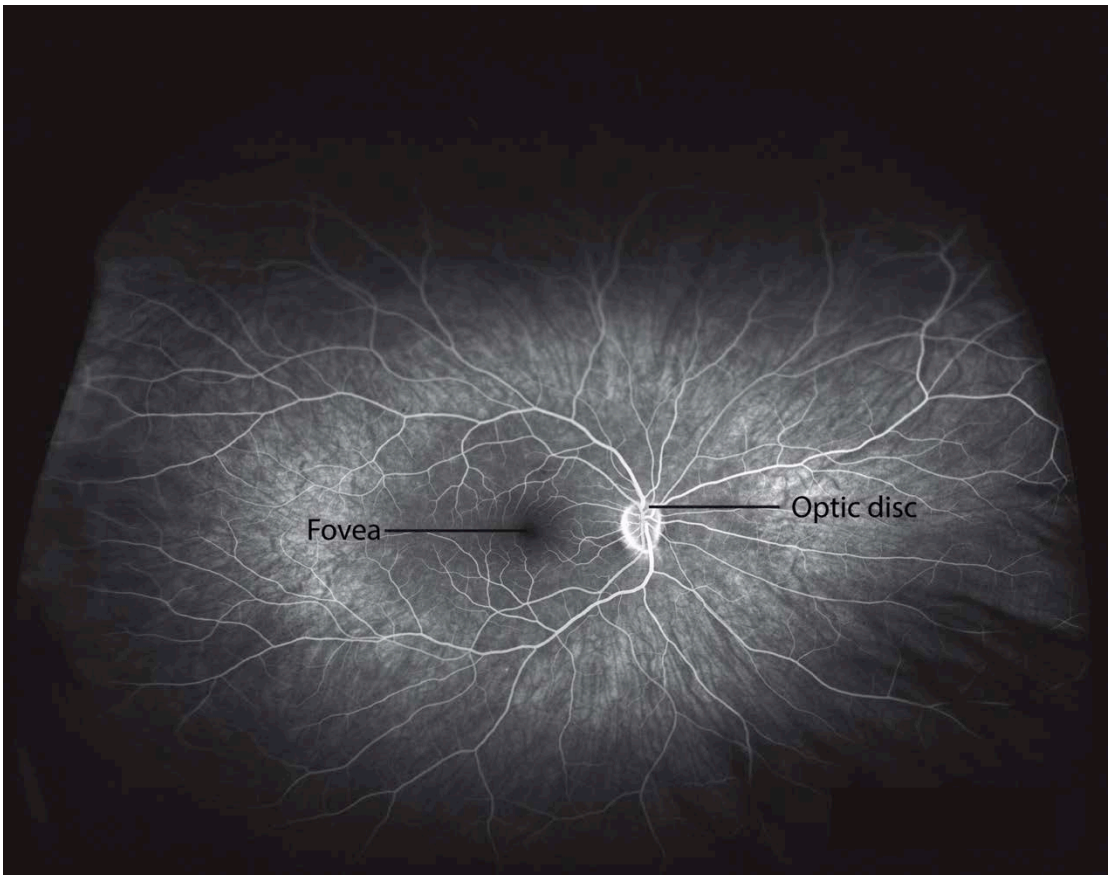

Figure 1.34: An example of an ultra-widefield fundus fluorescein angiographic image acquired with the Optos Panoramic 200MA

This is a normal late phase fluorescein angiographic image of the right eye demonstrating the 200-degrees of field of view with the Optos Panoramic 200MA.

1.4.2.1. Optos Ultra-Widefield Retinal Imaging in Infants

In July 2012, a 3-month-old infant born at term was referred to the Oxford Eye Hospital (OEH), Oxford, UK, for the management of a retinal detachment secondary to IP [57]. Clinical examination with the BIO showed fleeting fundus views of the right and left eyes, indicating the presence of a tractional retinal detachment in the left eye and an intact posterior pole in the right eye. Determining the extent of the peripheral retinal vascular abnormalities and ischaemia by clinical examination alone, however, proved difficult. Fluorescein angiography was deemed necessary to assist with planning the laser photocoagulation of the retina. At the OEH, a RetCam Shuttle is available for capturing colour fundus photos. However this model of RetCam does not have fluorescein angiography capabilities. In view of this, colour fundus photography and fluorescein angiography was attempted for the first time in both eyes using the Optos Panoramic 200MA in the outpatients department. High-resolution ultra-widefield pseudocolour and fluorescein angiographic images were successfully obtained in both eyes of the infant. Optos ultra-widefield imaging provided accurate identification of retinal neovascularisation and avascular retinal zones that enabled targeted laser treatment to be applied to areas of retinal capillary non-perfusion.

A few weeks later, a premature infant with aggressive posterior ROP was treated at the OEH with an intravitreal injection of bevacizumab. RetCam colour fundus imaging is normally used at the OEH to monitor the objective response to laser treatment of ROP. However as RetCam imaging requires contact with the eye, there were concerns about increased infection risk when using it in the early post-intravitreal injection period. A clinical decision was therefore taken not to use RetCam imaging to objectively monitor the therapeutic response following the intravitreal injection of bevacizumab. Based on the previous success of obtaining non-contact ultra-widefield images in the infant with IP, a clinical decision was made to

use Optos ultra-widefield imaging to objectively monitor the therapeutic response following the intravitreal injection of bevacizumab [58]. Ultra-widefield images were successfully obtained in both eyes of the infant and enabled adequate objective documentation of the response to treatment.

In both the cases described above, the quality of non-contact ultra-widefield imaging was judged to be superior to that of RetCam imaging in many ways. On the basis of these clinical experiences, the Optos Panoramic 200MA gradually became the standard imaging modality used at the OEH in infants with retinal diseases. At the OEH, colour fundus photography and fluorescein angiography with the Optos Panoramic 200MA is used in infants with retinal diseases to guide retinal treatment and to document objectively retinal disease findings and response to treatment.

The non-portable nature of the Optos Panoramic 200MA necessitates that all infants are imaged at the outpatients department of the OEH. Prior arrangements are made to ensure that adequate staffing is available on the day of retinal imaging. In addition to an ophthalmologist, whose presence is required to hold and position the infant during the imaging process, an ophthalmic photographer familiar with the Optos Panoramic 200MA is needed to capture the images. A neonatal nurse or doctor trained in newborn and paediatric resuscitation is also required during the imaging process to monitor the oxygen saturations, heart rate, and respiratory efforts of the infant. The cardiorespiratory monitors are connected to the infant during the imaging process and are provided by the neonatal team. Retinal imaging would cease should the infant experience any apnoeic or bradycardic episodes during the imaging process. A resuscitation trolley with paediatric and neonatal equipment is available outside the imaging room at the OEH should it be required in an emergency situation. No routine monitoring of the infant is required post-retinal imaging with the Optos Panoramic 200MA. Prior arrangements with the neonatal unit (NNU) are made for those infants

that need to be transported from the NNU to the outpatients department for retinal imaging with the Optos Panoramic 200MA. The decision about whether an infant is suitable and safe for transport to the outpatients department rests with the neonatal team caring for the infant. In general, any infant who is mechanically ventilated through an endotracheal tube or who suffers from regular apnoeic and bradycardic episodes is not suitable for transport to the outpatients department for retinal imaging. Infants with stable cardiorespiratory functions and who require no oxygen support can be imaged in the outpatients setting. Infants with stable cardiorespiratory functions but who require oxygen support with nasal prongs or a nasal continuous positive airway pressure device can also be imaged in the outpatients department. These devices do not need to be removed for the imaging process to take place. Infants in the NNU are transported to the outpatients department in a pram or an incubator depending on their clinical needs, and are accompanied by a neonatal nurse or doctor. Oxygen tanks and concentrators are transported with the infant and neonatal team to the outpatients department. Following retinal imaging, the infant can be immediately transported from the outpatient department back to the NNU.

It is necessary to ensure that all infant's pupils are sufficiently dilated, as adequate dilation is imperative to get clear ultra-widefield retinal images. Pupil dilation is achieved with cyclopentolate 0.5% and phenylephrine 2.5%. One drop of each solution is instilled in the eyes at least 30 minutes prior to retinal imaging. If after 10 minutes adequate dilation has not been achieved, a second set of drops would be placed in the eyes. At times a third set of drops may be necessary, particularly in a very dark eyed infant.

No sedatives are routinely given to infants for retinal imaging with the Optos Panoramic 200MA. However for infants who are difficult to image with the Optos

Panoramic 200MA, an oral form of sedation such as chloral hydrate may be considered (50 mg/kg).

For an infant who requires fluorescein angiography, peripheral venous cannulation by a neonatal or paediatric member of staff is performed prior to the infant attending the outpatient department for retinal imaging. Many sites are available for cannulation including the dorsal hand veins, forearm veins, and the antecubital vein; however, as a rapid injection improves contrast and facilitates interpretation of the arm-to-retina time, the antecubital location is preferred [59].

The decision to image an infant's retina with the Optos Panoramic 200MA is based solely on clinical necessity and no ethical approval is therefore required for image acquisition and subsequent analysis. To gain informed consent for pseudocolour fundus imaging, the parents of the infants are contacted and an explanation is provided about the clinical need for taking colour photographs of the retina. The Optos pseudocolour fundus imaging procedure (see section 1.4.2.2) is explained and discussed. Once the procedure has been explained, the parents are asked if they have any questions, and the questions are answered to the parent's satisfaction. In accordance with the OEH consent policy, only verbal consent is required from the parents for colour fundus imaging. To gain informed consent for fluorescein angiography, the parents are contacted and an explanation is provided about the clinical need for taking fluorescein angiographic images. The parents are informed about the expected temporary yellowish discolouration of the skin, eyes, nails, and urine after administration of the dye and the possible occurrence of nausea and vomiting immediately following fluorescein injection. The other possible side effects and complications of fluorescein angiography, as described in detail in section 1.3.2.2, are also discussed. Once the procedure has been explained, the parents are asked if they have any questions, and the questions are answered to the parent's

satisfaction. In accordance with the OEH consent policy, an informed consent form for fluorescein angiography is filled out and the parent's signature is sought.

1.4.2.2. Optos Ultra-Widefield Pseudocolour Fundus Imaging Technique in Infants

The headrest and the face pad covering the scan head mirror are removed prior to imaging. Removal of these ensures that the infant can be moved close enough to the mirror for image acquisition. It is necessary to ensure that the internal ellipsoid mirror is clean and free of debris such as dust before each infant is imaged. Dust and other debris collected on the scan head mirror can impair image quality. The internal mirror can be cleaned with cleaning wipes provided by the manufacturers. The scan head table is adjusted so that the height of the scan head is at a level comfortable for the ophthalmologist holding the infant in front of the scan head mirror.

Under topical anaesthesia (proxymetacaine 0.5%), the eyes of the infant are held open with a paediatric lieberman adjustable eyelid speculum (Duckworth & Kent LTD, Baldock, Hertfordshire, UK), with the speculum stabilised by taping its handle to the infant's cheek or temple. To optimise image clarity, the cornea needs to be hydrated with 0.9% normal saline drops prior to starting image acquisition. Further hydration may be necessary whilst imaging an infant if the cornea begins to dehydrate. This can be noticed on the head scan monitor whilst images are captured. When corneal desiccation begins, the retinal images seen on the head scan monitor becomes blurred and distorted.

The infant is held up to the scan head mirror in the "flying baby" position (Figure 1.35) [57, 58, 60]. One hand is used to support the body and chin of the infant, with the legs of the infant straddling the forearm. The other hand is used to support the head of the infant. The neck of the infant is fractionally extended to maximise the

field of imaging before the head is advanced towards the scan head mirror until the dorsal surface of the hand supporting the body and chin of the infant touches the cheek rest of the scan head mirror aperture (Figure 1.36) [60]. The cheek rest acts as a stable reference point from which fine adjustments of the infant's head and body position can be made. The "flying baby" position was developed based on the technique customarily used to examine an infant on a slit lamp biomicroscope (Figure 1.37) [61]. To examine an infant on a slit lamp, a parent is asked to support the infant in a prone position, with one hand under the infant's tummy whilst the other hand is steadying the chin of the infant. The parent is instructed to rest the infant's forehead against the slit lamp headrest. When performing retinal imaging with the Optos Panoramic 200MA, holding the infant in a more upright position with the legs straddling the forearm was deemed more comfortable for the person holding the infant and offered better support of the infant's head, chin and body.

Holding an infant in the "flying baby" position for retinal imaging with the Optos Panoramic 200MA involves a learning curve for the ophthalmologist. In general, imaging of 3 to 5 infants is typically required to become familiar and competent with the technique.

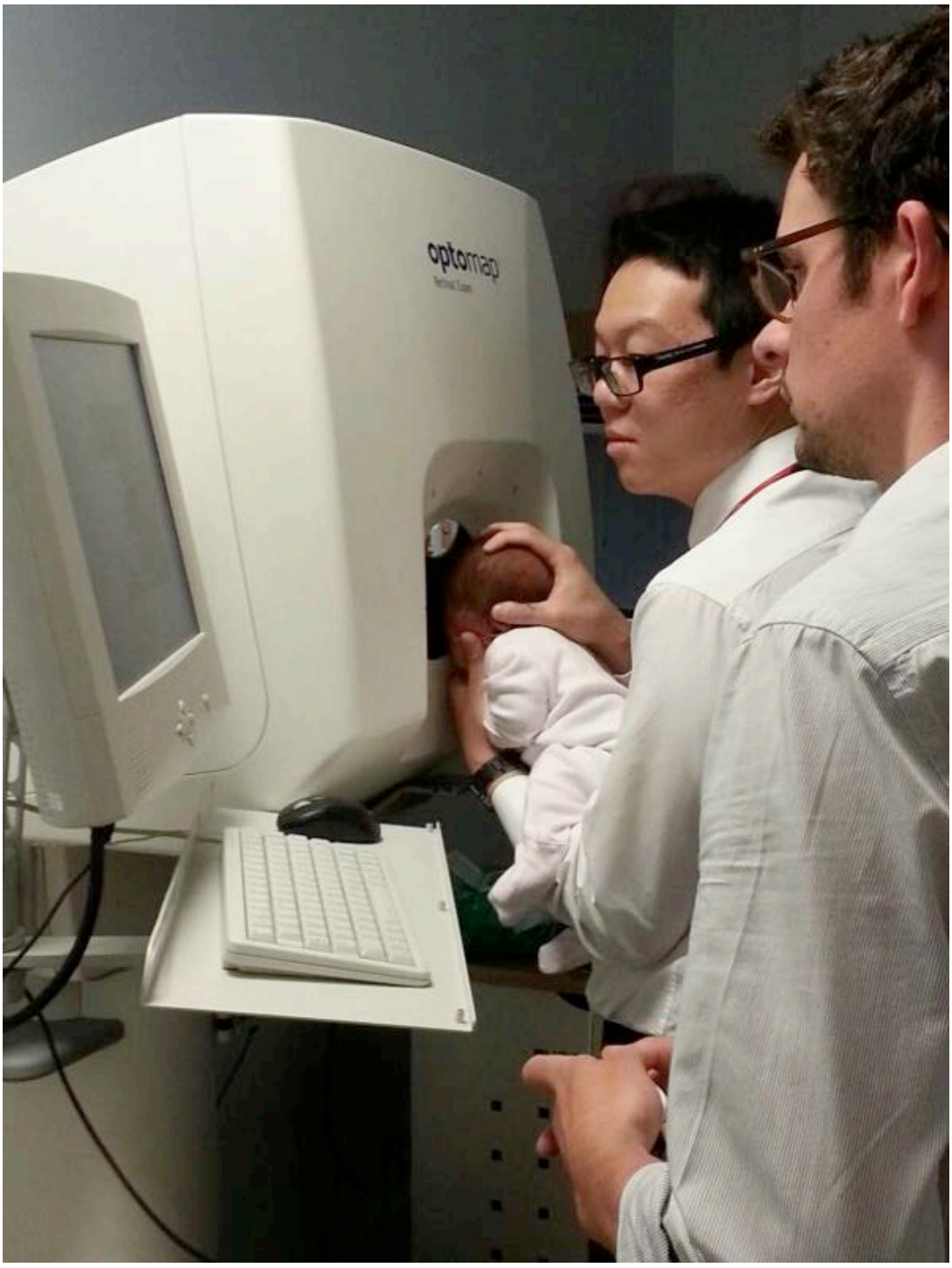

Figure 1.35: The 'flying baby' position for Optos ultra-widefield retinal imaging in infants (Fung, Yusuf, Smith, Brett, Weston and Patel, 2014, p303)

In the 'flying baby' position, one hand is used to support the body and chin of the infant, with the legs of the infant straddling the forearm. The other hand is used to support the head of the infant.

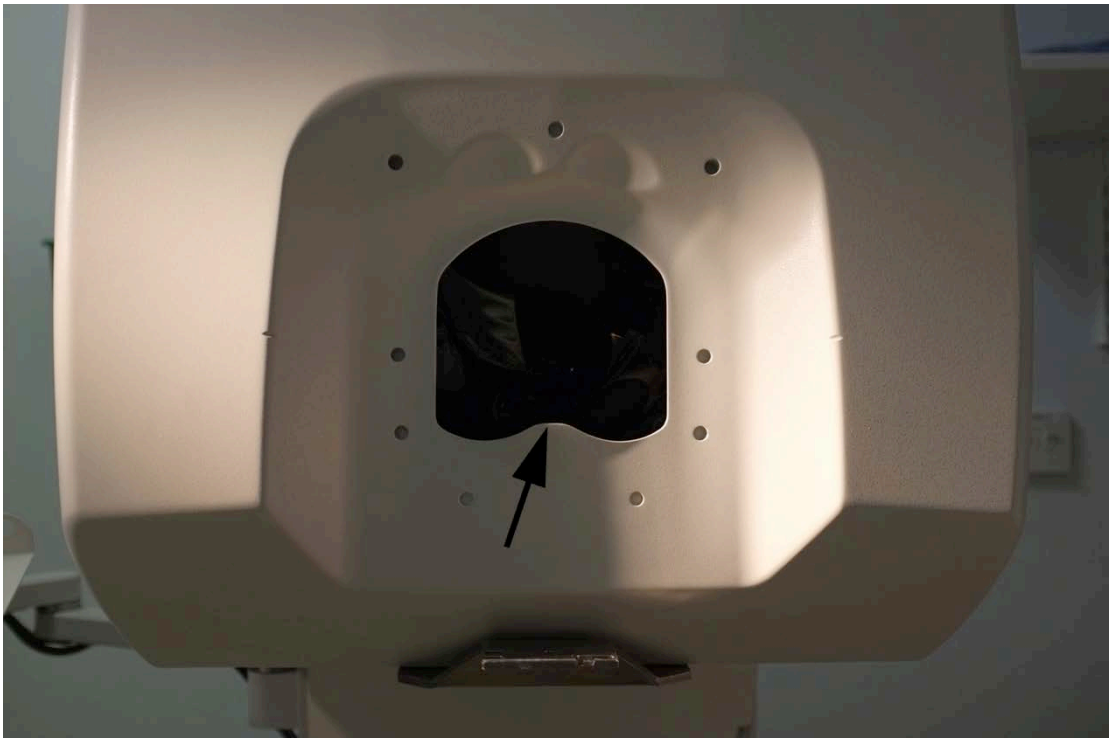

Figure 1.36: Cheek rest reference point of the Optos Panoramic 200MA for retinal imaging in infants (Fung, Yusuf, Smith, Brett, Weston and Patel, 2014, p303)

During retinal imaging, the head of the infant is advanced towards the scan head mirror until the dorsal surface of the hand supporting the infant's body and chin touches the exposed cheek rest (black arrow) of the Optos Panoramic 200MA. The cheek rest provides a stable reference position from which fine adjustments can be made to optimise alignment of the infant pupil with the Optos imaging system.

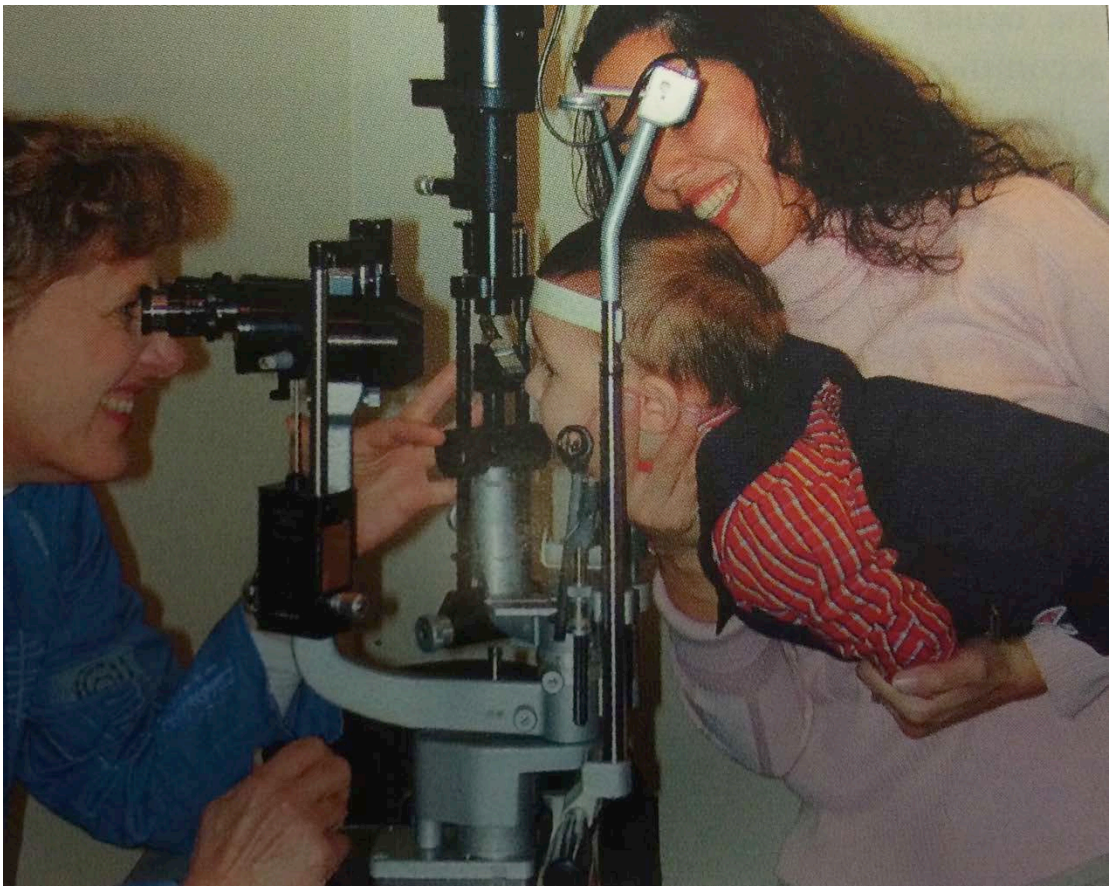

Figure 1.37: Method for examining an infant at the slit lamp (Hoyt and Taylor, 2012, p51)

For infants, the parent or clinic assistant is asked to support the infant in a prone position, with the palm steadying the chin. The parent or assistant is instructed to rest the infant's forehead against the slit lamp headrest.

Accurately aligning the infants' eyes with the Optos imaging system is the key to capturing good ultra-widefield images of the retina. The infant's eye is aligned so that the center ring seen on the scan head monitor is in the center of the pupil and the 3 and 9 o'clock sides of the limbus ring cover the infant's limbus (Figure 1.38). The infant is moved closer to the mirror when a positive sign (+) is displayed in the center ring, and moved further away from the mirror when a negative sign (-) is displayed. Buttons on the hand control used by the photographer and fine adjustments of the infant's head and body position by the person holding the infant can help align the infant's eye with the rings. The device is optimally aligned with the infant's eye when the ring changes colour from red to green and the center ring is filled. As the infant's eye moves, small adjustment of the infant's head and body position in relation to the scan head mirror is necessary to maintain alignment. Once alignment is optimal, the photographer captures an image by pressing the capture button on the hand control. Following image acquisition in one eye, the process is repeated for the fellow eye. An example of an Optos ultra-widefield pseudocolour fundus image acquired in an infant is shown in Figure 1.39.

Accurate alignment of an infant eye with the Optos Panoramic 200MA involves a learning curve for both the ophthalmologist and the ophthalmic photographer. In general, imaging of 5 to 10 infants is typically required to become competent and accurate with alignment. However if the head movements of an infant cannot be well controlled with the baby held in the "flying baby" position, optimal alignment of the infant eye with the Optos imaging device may not be possible, making image acquisition difficult.

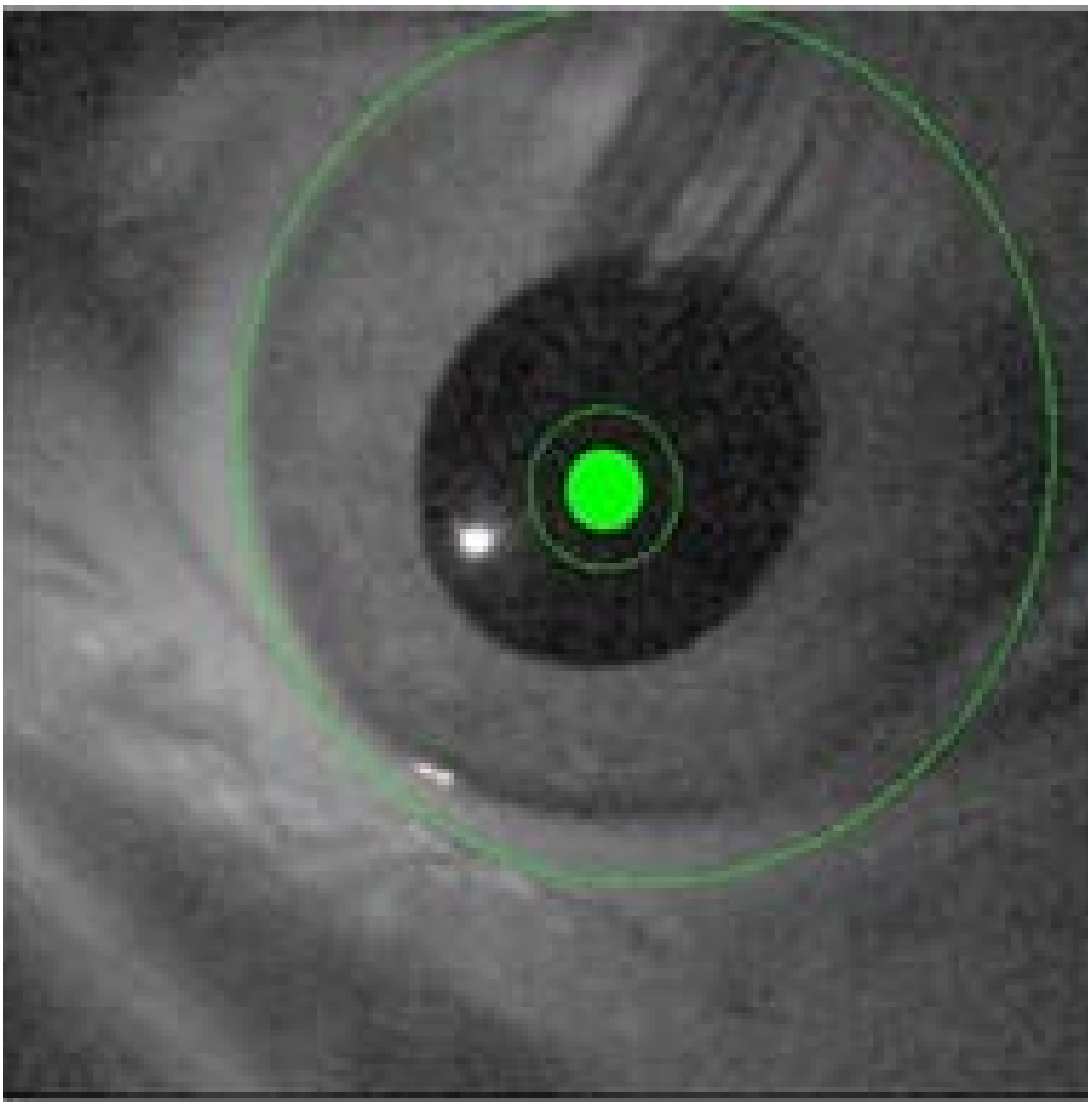

Figure 1.38: Alignment of the infant's eye with the Optos imaging system

The infant's eye is aligned so that the center ring seen on the scan head monitor is in the center of the pupil and the 3 and 9 o'clock sides of the limbus ring cover the infant's limbus. The Optos device is aligned with the infant's eye when the rings are green in colour and the center ring is filled.

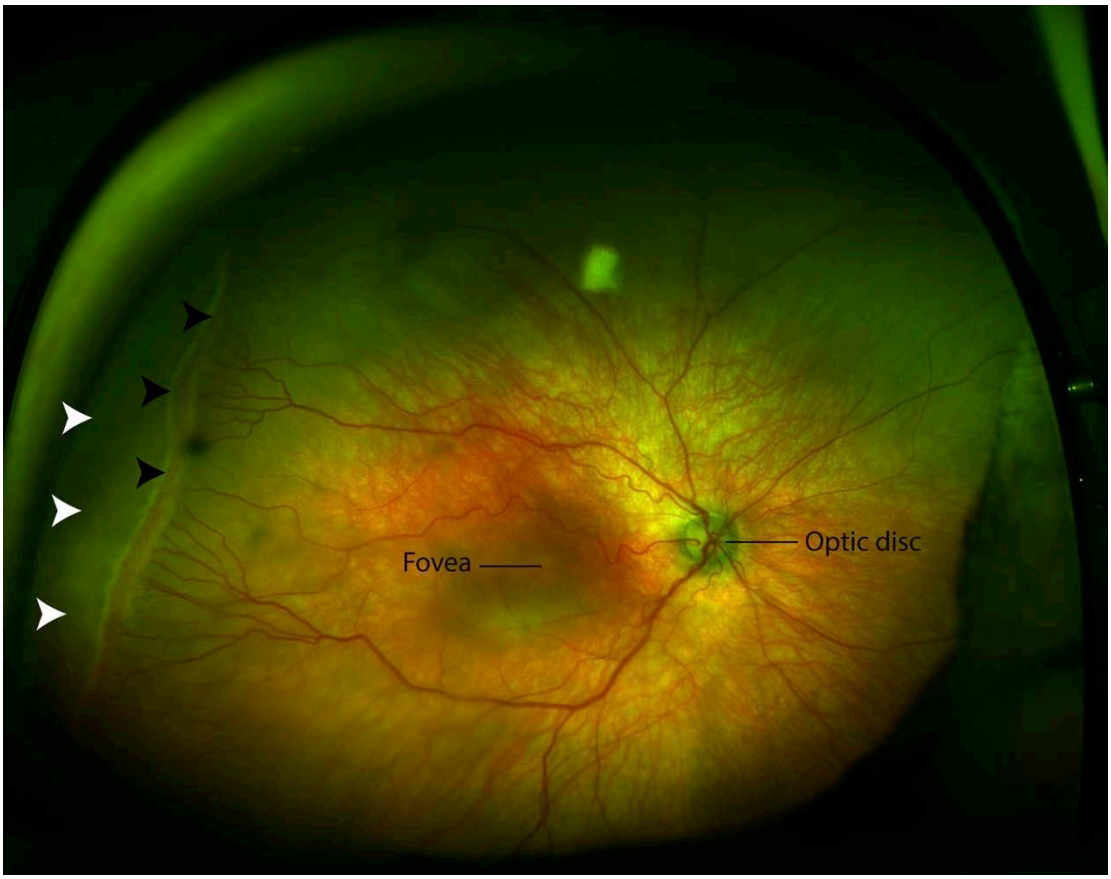

Figure 1.39: An example of an Optos ultra-widefield pseudocolour fundus image acquired in an infant

This is a pseudocolour fundus image of the right eye of an infant with stage 3 ROP in zone 2 with plus disease. The neovascular ridge (black arrowheads) and areas of avascular retina (white arrowheads) are clearly seen in the periphery.

1.4.2.3. Optos Ultra-Widefield Fundus Fluorescein Angiography Technique in Infants

The headrest and the face pad covering the scan head mirror are removed prior to imaging. The internal ellipsoid mirror is cleaned before each infant is imaged. The scan head table is adjusted so that the height of the scan head is at a level comfortable for the ophthalmologist holding the infant in front of the scan head mirror.

Under topical anaesthesia (proxymetacaine 0.5%), the eyes of the infant are held open with a paediatric lieberman adjustable eyelid speculum.

To optimise image clarity, the cornea is hydrated with 0.9% normal saline drops prior to starting image acquisition. Further hydration may be necessary whilst imaging an infant if the cornea begins to dehydrate.

The infant is held up to the Optos Panoramic 200MA scan head mirror in the "flying baby" position (see section 1.4.2.2). Obtaining high quality images of the early phase of the angiogram requires that the infant be correctly positioned at the imaging camera prior to dye injection. This can be facilitated by first obtaining the pseudocolour fundus photographs so that the photographer and the ophthalmologist holding the infant is familiar with positioning prior to starting the active phase of the angiogram. The eye of primary interest should be identified for the photographer and should be correctly aligned with the imaging camera at the commencement of the angiogram. The technique for ensuring correct alignment of the infant's eye with the Optos imaging system is described in detail in section 1.4.2.2. An injection of 10% sodium fluorescein at a dose of 0.1 ml/kg of body weight [26] is administered once the infant's eyes are aligned. Immediately after the fluorescein injection, the peripheral venous cannula is flushed with 1 to 2 mL of 0.9% normal saline. The photographer begins capturing the early-phase images using the image capture button on the hand control. Once the early-phase capture has completed or stopped in one

eye, mid-phase images of the fellow eye are captured. Late-phase images are then captured several minutes later from each eye. A resuscitation trolley, drugs for treatment of anaphylaxis, and a receiver in case of vomiting is available in the OEH outpatients department for the possible adverse effects of fluorescein injection.

In instances where venous access is not possible, the 10% sodium fluorescein dye used for intravenous fluorescein angiography is diluted to 2% by adding infant formula milk. This solution is then administered to the infant at a dosage of 25 mg/kg of body weight [57, 62]. The diluted dye is given as a fluid for the infant to suck from a feeding bottle. Image capture begins 30 minutes after ingestion of the dye. This method of oral fluorescein angiography makes adequate documentation of the early phase of the angiogram impossible and limits capture to late-phase images only.

An example of an Optos ultra-widefield fundus fluorescein angiographic image acquired in an infant is shown in Figure 1.40.

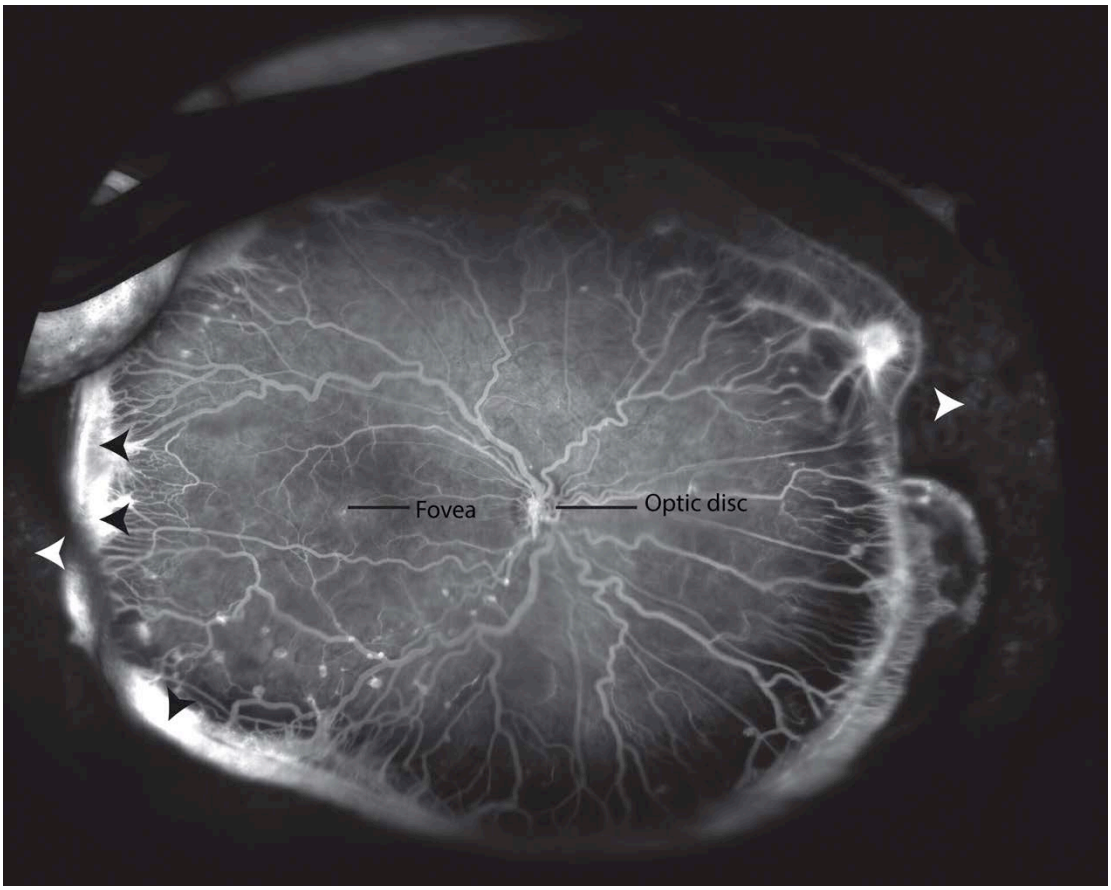

Figure 1.40: An example of an Optos ultra-widefield fundus fluorescein angiographic image acquired in an infant

This is a venous phase image of the right eye of an infant with stage 3 ROP in zone 2 with plus disease. Areas of neovascularisation (black arrowheads) and staining from previous laser burns (white arrowhead) are clearly evident in the peripheral retina.

1.4.3. Heidelberg Spectralis Ultra-Widefield Retinal Imaging

Another widely available ultra-widefield cSLO retinal imaging system is the Heidelberg Spectralis (Heidelberg Engineering, Heidelberg, Germany). This imaging system is a table based chin-rest system consisting of a laser-scanning camera head, which is connected by a flexible fiberoptic cable to a monitor, a personal computer (PC), a power supply and an isolating transformer housed in a cart (Figure 1.41). The scanning laser camera head is attached by a setscrew to the base of the camera unit, which is bolted down to a table (Figure 1.42). A touch panel (Figure 1.42), linked to the laser-scanning camera head and the PC, is used to access different image acquisition modes and acquire images. All images captured are stored and available for viewing on the Heidelberg eye explorer software.

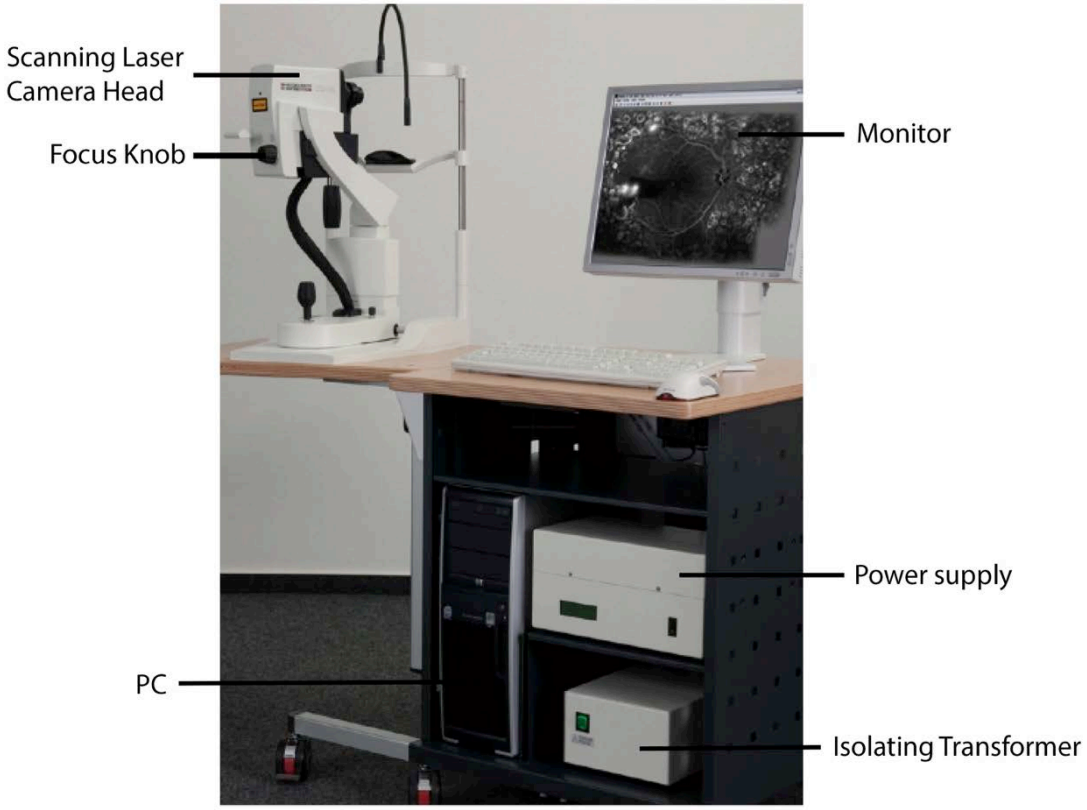

Figure 1.41: Heidelberg Spectralis imaging system

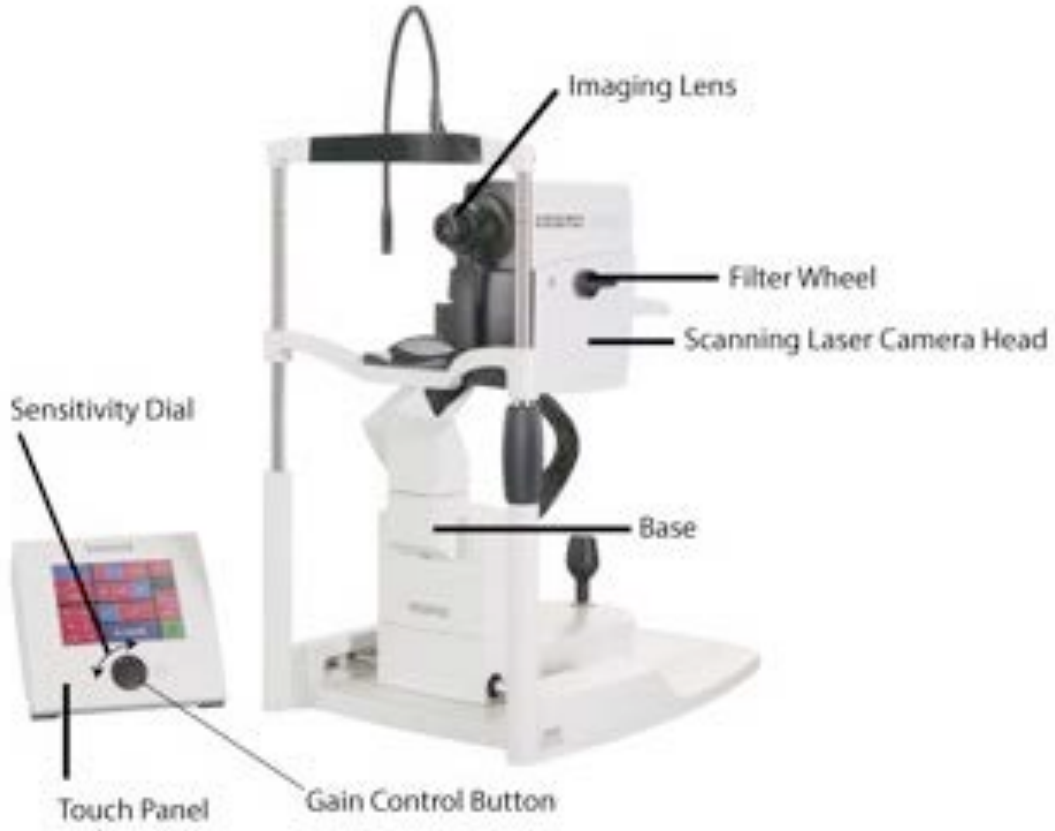

Figure 1.42: Heidelberg Spectralis scanning laser camera head and touch panel

The Heidelberg Spectralis is capable of producing a multi-modal range of images of the retina using different laser sources that emit laser lights with different wavelengths. No eye contact is required and the images produced are in the correct orientation. A diode laser at a wavelength of 815 nm is used for infrared (IR) reflectance imaging (Figure 1.43A). IR reflectance imaging is a variation of fundus photography that uses near infrared light rather than white light for illumination. Near infrared light has the advantage of being able to penetrate unclear ocular media better than white light. Additionally, as near infrared light is invisible to the human eye, patients are spared the flash that accompanies traditional fundus photography. This may be particularly valuable for light sensitive patients. An infrared beam of a super luminescence diode at a wavelength of 870 nm is used for optical coherence tomography (OCT) technology to provide cross sectional images of human retinal morphology in vivo (Figure 1.43B). A blue diode laser at a wavelength of 486 nm is used to create auto-fluorescent and blue reflectance (red free) images (Figure 1.43C). The blue light used to illuminate the retina in blue reflectance imaging accentuates the visibility of blood vessels and enhances the contrast of certain structures on the surface of the retina such as the retinal nerve fiber layer, rendering them easier to see compared to white light illuminated images. The same blue laser wavelength is used with a barrier filter at 500 nm for fluorescein angiography. A diode laser at a wavelength of 786 nm is used with a barrier filter at 830 nm for indocyanine green angiography (ICG). A multi-colour scanning laser image of the fundus can be produced by simultaneously imaging the retina with multiple laser colours (Figure 1.43D).

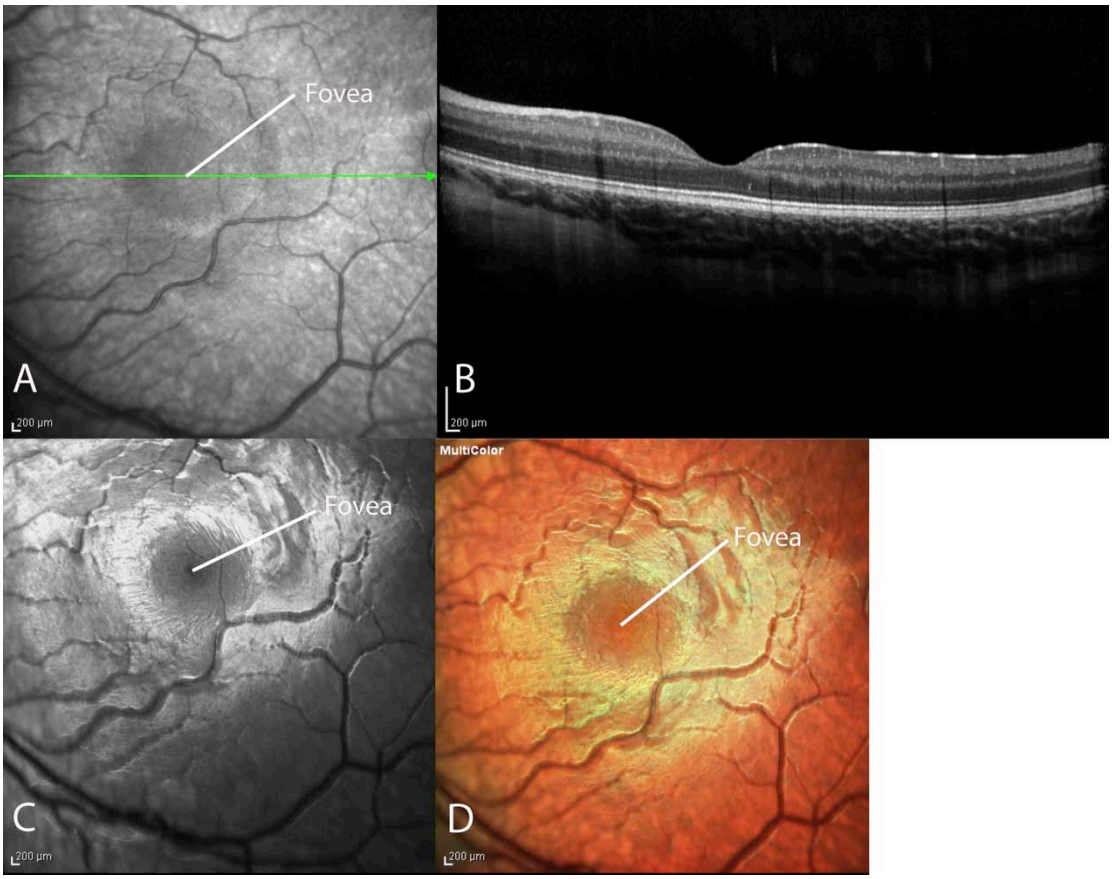

Figure 1.43: Multi-modal range of images of the retina that can be captured with the Heidelberg Spectralis imaging system

(A) Infrared image of the left foveal region. (B) Optical coherence tomography image of the left foveal region. (C) Blue reflectance image of the left foveal region. (D) Multi-colour scanning laser image of the left foveal region. All images shown were obtained with the 30-degree imaging lens.

The addition of an imaging lens to the Heidelberg Spectralis scanning laser camera head is necessary to capture images of the retina. Several lenses that capture different fundal imaging angles are available for the scanning laser camera head (Figure 1.44). The 30-degree and 55-degree imaging lenses are adequate for obtaining images of the optic disc and the posterior pole, but provide a limited view of the peripheral retina. The ultra-widefield imaging lens, first made commercially available in 2012, can capture the posterior pole and the periphery of the retina in a one shot image [63]. The 30-degree and 55-degree imaging lenses can be used to capture all the multi-modal range of retinal images described above. However, in contrast to the 30-degree and 55-degree imaging lenses, the ultra-widefield imaging lens is only capable of acquiring infrared, fluorescein and indocyanine green angiographic images of the retina. OCT, blue reflectance and multi-colour scanning laser imaging of the retina is not compatible at present with the ultra-widefield imaging lens.

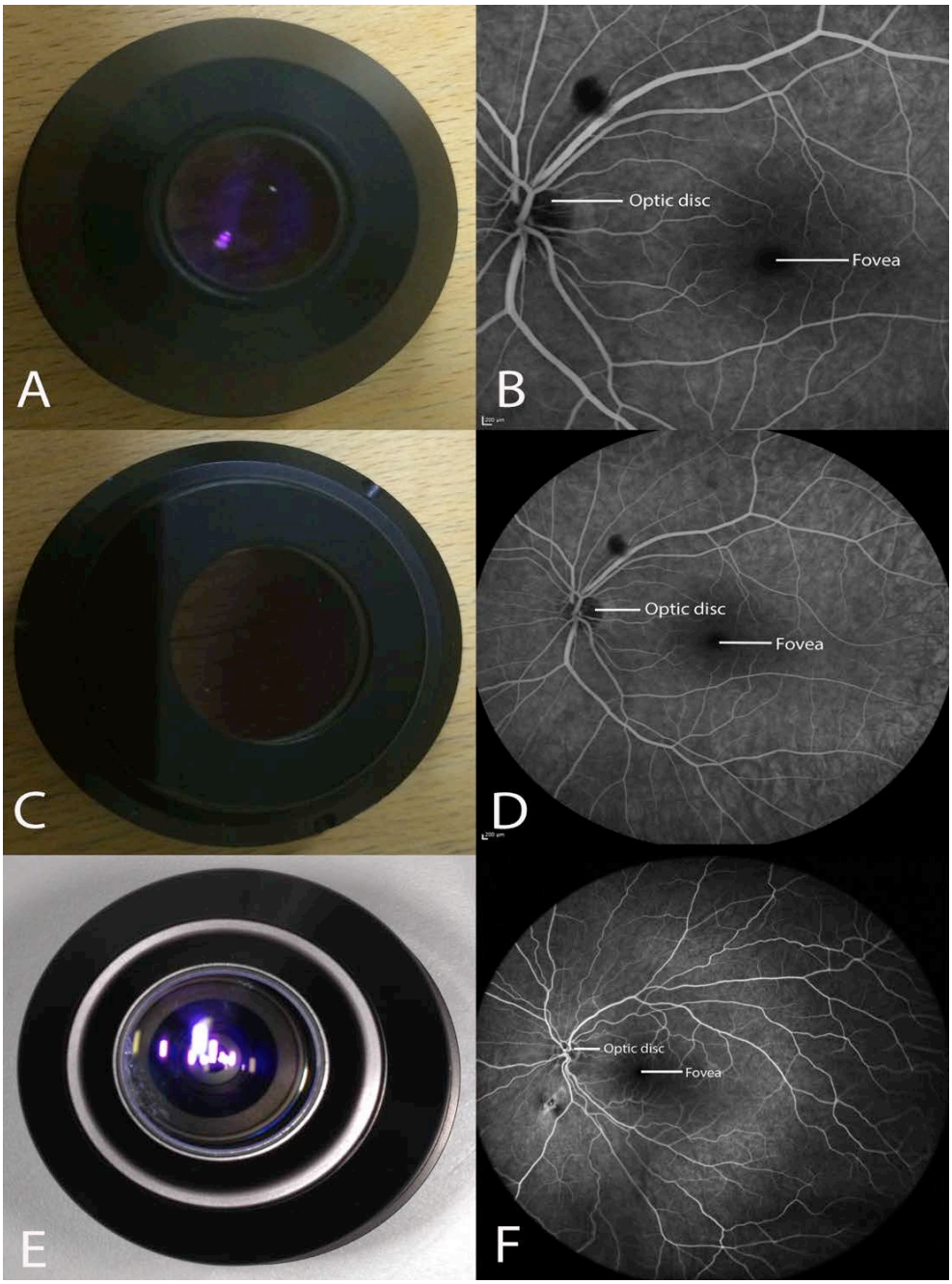

Figure 1.44: Imaging lenses available with the Heidelberg Spectralis

(A) The 30-degree imaging lens. (B) Fluorescein angiogram of the left fundus illustrating the field of view with the 30-degree imaging lens. (C) The 55-degree imaging lens. (D) Fluorescein angiogram of the left fundus illustrating the field of view with the 55-degree imaging lens. (E) The ultra-widefield imaging lens. (F) Fluorescein angiogram of the left fundus illustrating the field of view with the ultra-widefield lens.

The use of the Heidelberg Spectralis to image the infant retina has been limited. This has been primarily related to the fact that the Heidelberg Spectralis scanning laser camera head is vertically oriented in a tabletop, chin rest system and disallows the imaging of supine, non-anaesthetised, and uncooperative infants. In 2010, Vinekar et al. [64] described a method for converting the Heidelberg Spectralis tabletop chin rest system into a hand held device (Figure 1.45). By removing the setscrew connecting the scanning laser camera head to its base, the Heidelberg Spectralis scanning laser camera head can be freed and utilised as a mobile hand held device. The hand held Heidelberg Spectralis scanning laser camera head was successfully utilised for OCT retinal imaging on 4 non-anaesthetised infants with aggressive posterior ROP [64].

Figure 1.45: The use of the Heidelberg Spectralis scanning laser camera head as a mobile hand held device to image supine infants

Following disassembly, the Heidelberg Spectralis scanning laser camera head is utilised as a hand held device and is pointed downwards in alignment with an infant's eye (Vinekar, Sivakumar, Shetty, Mahendradas, Krishnan, Mallipatna and Shetty, 2010, p380). Imaging occurs at the head end of the infant and the resulting images are laterally inverted.

1.4.3.1. Heidelberg Spectralis Ultra-Widefield Retinal Imaging in Infants

Due to difficulty with patient cooperation in the infant population, adequate examination of the entire retina using fluorescein angiography often requires an examination under anaesthesia (EUA). RetCam is currently the only widely available imaging modality used to perform FFA on a supine infant under general anaesthesia. A RetCam with fluorescein angiography capability is not available at the OEH for imaging anaesthetised infants in the operating room. At the OEH, a Heidelberg Spectralis is available and has been used in the operating room since July 2012 to acquire ultra-widefield fundus fluorescein angiographic images in anaesthetised infants with retinal diseases. At the OEH, ultra-widefield fluorescein angiography with the Heidelberg Spectralis is currently used in anaesthetised infants with retinal diseases to demonstrate disease progression and regression following retinal treatment and to guide laser photocoagulation treatment.

At the OEH, retinal imaging of non-anaesthetised infants in the outpatients department with the Heidelberg Spectralis in a hand-held mode as described by Vinekar et al. [64] was attempted, but obtaining images of the retina consistently was found to be difficult. Regular eye movements and poor eye fixation in non-anaesthetised infants was found to limit imaging with the Heidelberg Spectralis. A sustained period of eye fixation was found to be necessary for the device to focus and lock on to the retina before images can be successfully acquired. In view of this finding, retinal imaging with the Heidelberg Spectralis has only been used in the operating room at the OEH for anaesthetised infants with retinal diseases.

The decision for an infant to have ultra-widefield FFA with the Heidelberg Spectralis in the operating room under general anaesthesia is based solely on clinical necessity. Ethical approval is therefore not required for image acquisition and subsequent analysis.

To gain informed consent for retinal examination and imaging of an infant under general anaesthesia, the parents of an infant are contacted and an explanation is provided about the clinical need to examine and to take photographs of the retina under general anaesthesia. The examination and imaging procedure is explained (see section 1.4.2.3) and the possible side effects and complications of fluorescein injection (see section 1.3.2.2) are discussed. In accordance with the OEH consent policy, an informed consent form for fluorescein angiography is filled out and the parent's signature is sought. The anaesthetic team discusses the possible side effects and complications of the general anaesthetic with the parents.

To consistently image the infant retina in the supine position using the Heidelberg Spectralis, a custom-made arm was developed (Base Design Limited, Great Dunmow, Essex, UK) and added to the existing table based imaging system (Figure 1.46) [65]. The setscrew connecting the scanning laser camera head to its base is removed and the camera head is mounted onto a multi-positional bracket at the end of the custom made arm and tightened by a handle bolt (Figure 1.47). This converts the orientation of the scanning laser camera head from vertical to horizontal. Adjustable wheels on the arm (Figure 1.48) allow four degrees of freedom of movement of the scanning laser camera head to optimise alignment with an infant's eye. The modified Heidelberg Spectralis is based in the outpatients department and is transported to the operating room on the day an infant needs to be imaged with the device.

Figure 1.46: Modified Heidelberg Spectralis for retinal imaging in infants

A custom made arm (black arrowhead) was developed and added to the existing table based imaging system. To image an anaesthetised infant in the supine position in the operating room, the scanning laser camera head is disconnected from its base and transferred onto a bracket towards the end of the arm, converting its orientation from vertical to horizontal. The wheels at the base of the table (red arrowheads) enable transportation of the modified system from the outpatient's department to the operating room.

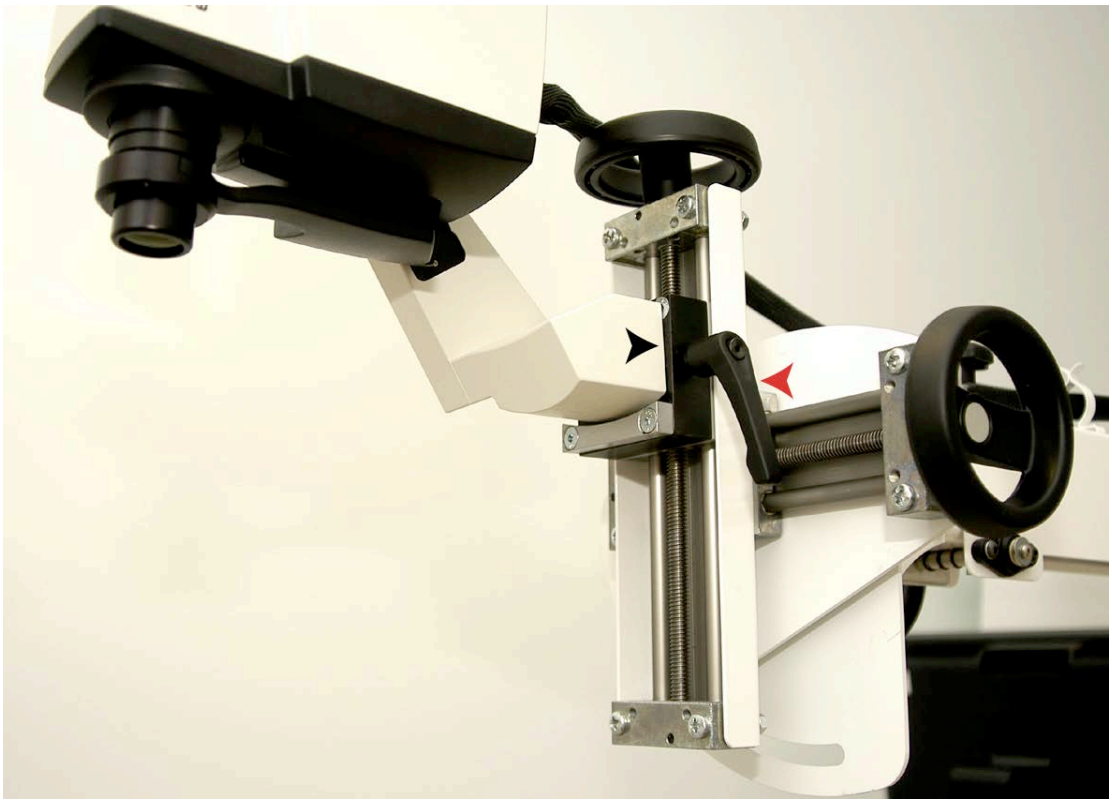

Figure 1.47: Multi-positional bracket of the modified Heidelberg Spectralis imaging system

The Heidelberg Spectralis scanning laser camera head is mounted onto a multi-positional bracket (black arrowhead) at the end of the custom made arm and tightened into place by a handle bolt (red arrowhead).

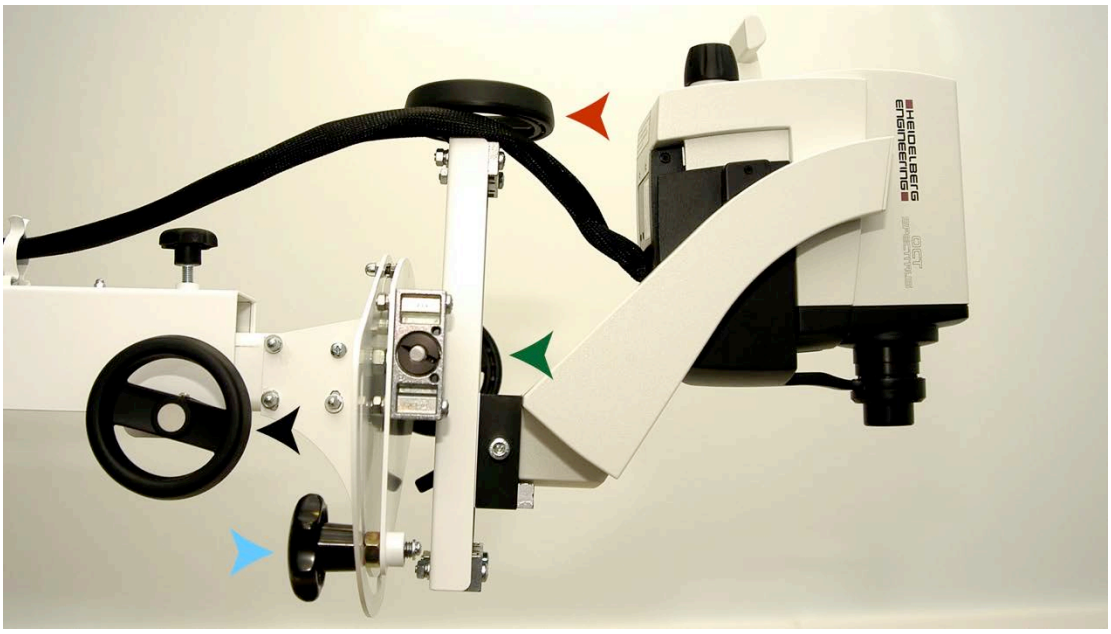

Figure 1.48: Movement wheels of the custom made arm of the modified Heidelberg Spectralis imaging system

Adjustable movement wheels at the end of the custom arm allow rotational (blue arrowhead), superior-inferior (red arrowhead), lateral-medial (green arrowhead), and anterior-posterior (black arrowhead) movements of the scanning laser camera head.

1.4.3.2. Heidelberg Spectralis Ultra-Widefield Fundus Fluorescein Angiography Technique in Infants

Before the fluorescein angiography procedure begins, ensure that the filter wheel on the scanning laser camera head is placed in the 'A' position (Figure 1.49). The ultra-widefield imaging lens needs to be connected to the scanning laser camera head and must be clean and free from any debris before each infant is imaged.

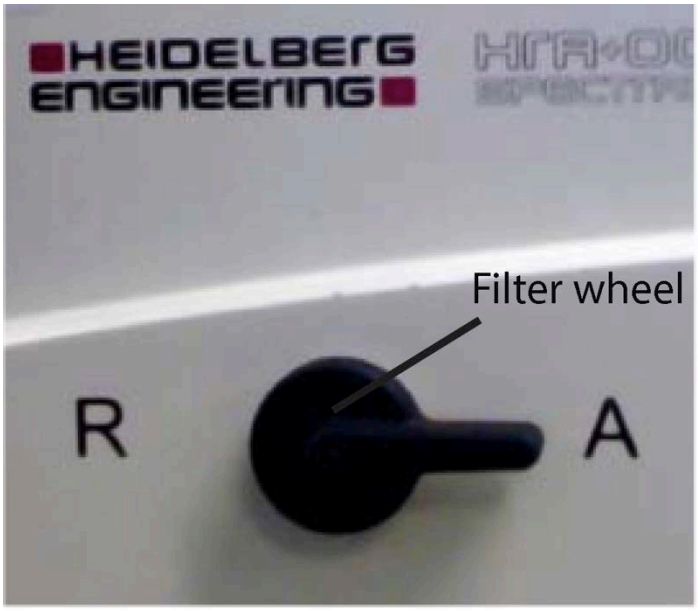

Figure 1.49: Position of the filter wheel of the Heidelberg Spectralis scanning laser camera head for fluorescein angiography

It is necessary to ensure that the pupils are dilated, as adequate dilation is vital to get clear ultra-widefield fluorescein angiographic images. Pupil dilation is achieved with cyclopentolate 0.5% and phenylephrine 2.5%. One drop of each solution is instilled in the eyes at least 30 minutes prior to retinal imaging.

The eyes of the infant are held open with a paediatric lieberman adjustable eyelid speculum. To optimise image clarity and to preserve the integrity of the corneal

surface, hydration of the cornea with 0.9% normal saline drops are necessary prior to and during image acquisition. The eye of primary interest should be identified for the photographer before the fluorescein angiography procedure begins. The scanning laser camera head with the ultra-widefield imaging lens attached is aligned with the center of the infant's pupil at the head end of the infant (Figure 1.50). To ensure correct alignment, the 'IR' acquisition mode on the touch panel is selected and an IR image of the infant's fundus is visualised on the computer monitor. Altering the position of the imaging lens using the movement wheels on the arm can make fine adjustments to the IR fundus image position. The IR fundus image position should encompass the retinal pathological area of interest, and will be the area where fluorescein angiographic images are subsequently acquired. The image brightness can be adjusted with the sensitivity dial on the touch panel (Figure 1.42). The correct working distance of the imaging lens to the eye produces an IR fundus image that is evenly illuminated on the computer monitor with no dark corners (Figure 1.50A). The imaging lens needs to be moved closer to the pupil if an unevenly illuminated IR fundus image with dark corners is seen on the computer monitor (Figure 1.50B). The focus of the imaging lens is adjusted by using the knob on the back of the scanning laser camera head until the smallest blood vessels seen on the monitor are at its sharpest. Once the IR fundus image is exposed and focused properly, the 'FA' acquisition mode button is pressed on the touch panel. The automatic real time (ART) mean function is activated in order to obtain the highest resolution images by pressing the black gain control button on the touch panel (Figure 1.42). The injection of 10% sodium fluorescein dye at a dose of 0.1 mL/kg of body weight [26] is given and single fluorescein angiographic images are acquired by pressing the "ACQUIRE' button on the touch panel. Readjustment of the sensitivity dial and focus knob for optimal brightness and sharpness of vessels respectively may be required. Once images have

been acquired in one eye, the process is repeated for the fellow eye. When all the images have been acquired, the images are saved to the Heidelberg Eye Explorer software. As imaging occurs at the head end of an infant, all the resultant images are laterally inverted. During image acquisition, the scanning laser camera head with the imaging lens is stabilised by resting a hand on the custom made arm to keep movement of the arm and the camera head with the imaging lens to a minimum. Imaging of the retina up to the ora serrata can be made possible by rotating the globe with a toothed forceps and indenting the sclera with a squint hook.

Ultra-widefield fundus fluorescein angiographic imaging in infants using the modified Heidelberg Spectralis involves a learning curve for the ophthalmologist. In general, imaging of 3 to 5 infants is typically required to become familiar and competent with the technique. Condensation of the ultra-widefield imaging lens can occur during imaging because of the close working distance between the lens and the infant eye, but can be easily dealt with by creating an air current near the eye.

An example of a Heidelberg Spectralis ultra-widefield fundus fluorescein angiographic image acquired in an infant is shown in Figure 1.52.

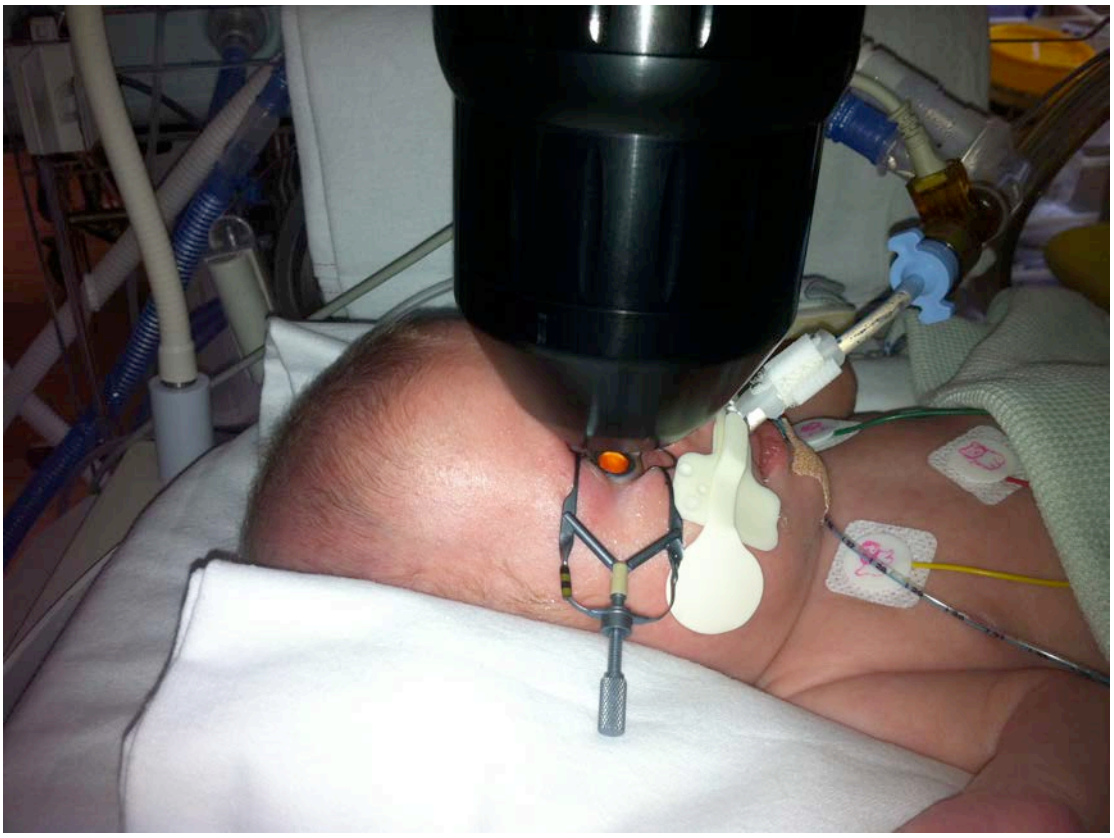

Figure 1.50: Imaging of an infant with the Heidelberg Spectralis ultra-widefield imaging lens

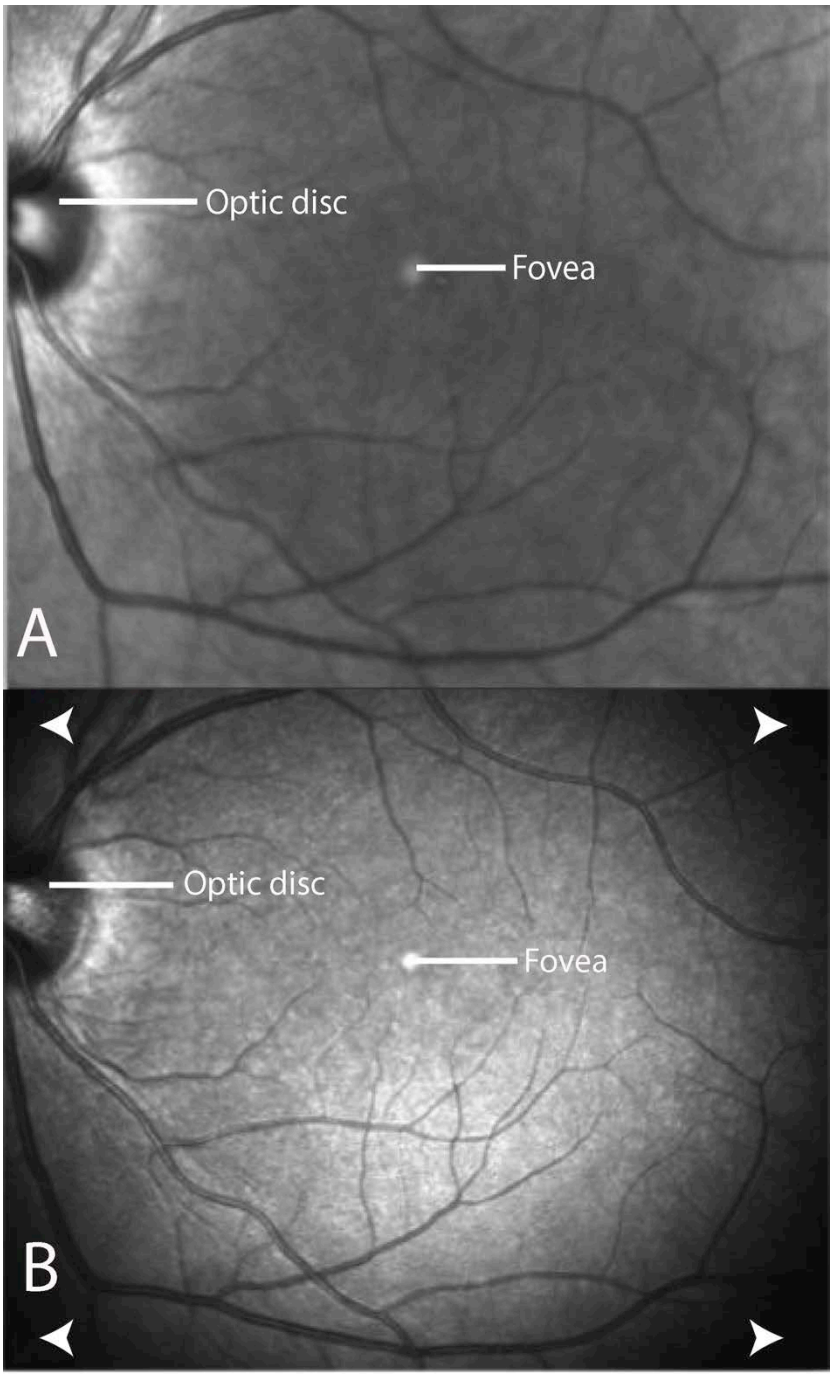

Figure 1.51: Correct working distance of the Heidelberg Spectralis imaging lens with an infant's eye

(A) The correct working distance of the imaging lens to the eye produces an infrared fundus image that is evenly illuminated with no dark corners. (B) An unevenly illuminated infrared fundus image with dark corners (white arrowheads) means the imaging lens needs to be moved closer to the eye.

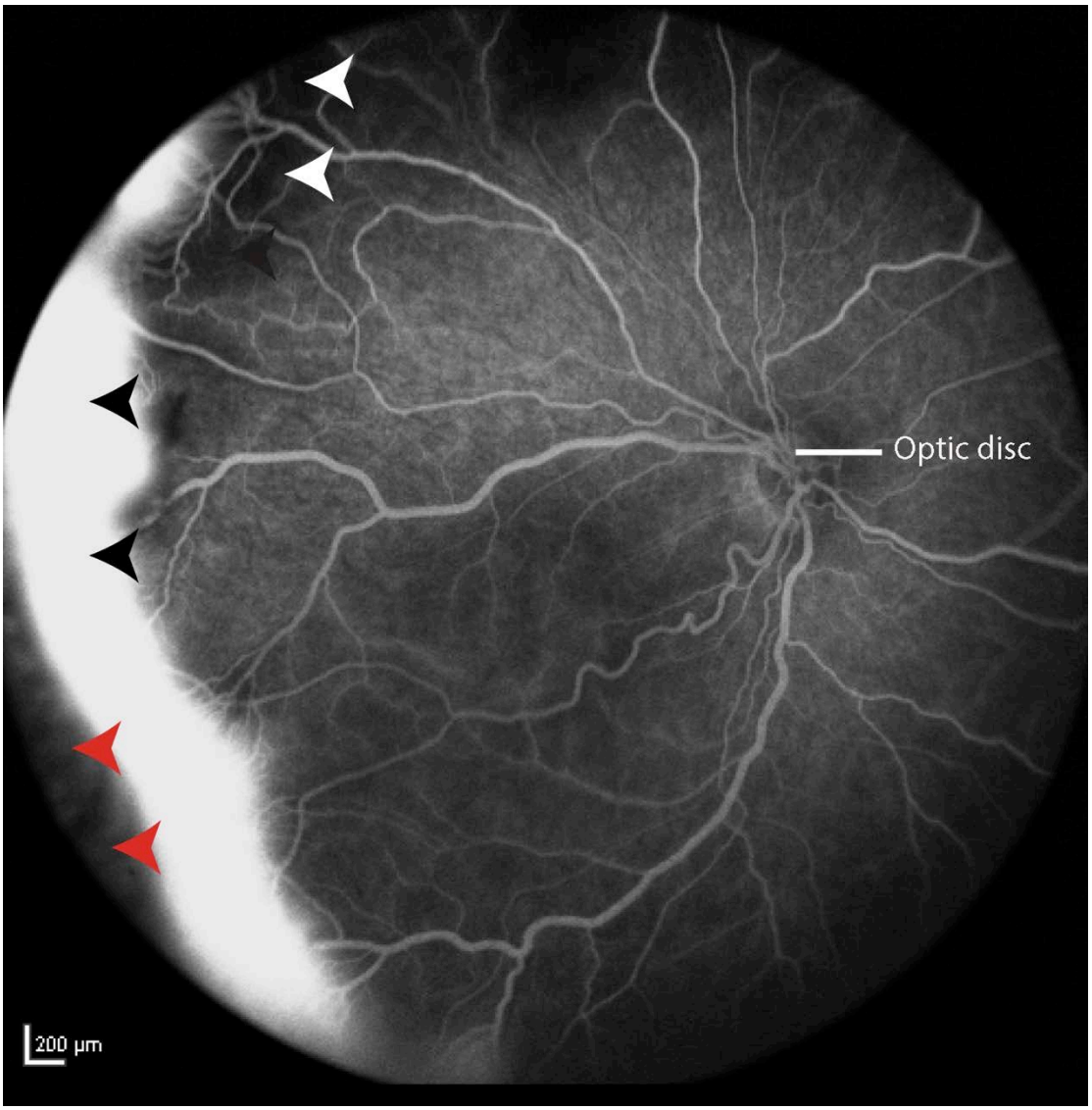

Figure 1.52: An example of a Heidelberg Spectralis ultra-widefield fundus fluorescein angiographic image acquired in an infant

This is a venous phase image of the right eye of an infant with stage 3 ROP in zone 2 with plus disease. Areas of leakage (black arrowheads), capillary non-perfusion (white arrowheads), and staining from previous laser burns (red arrowheads) are clearly evident in the peripheral retina.

1.5. Research Aims

There has been no previous evaluation of retinal imaging with the Optos and Heidelberg Spectralis ultra-widefield imaging modalities in infants with retinal diseases. The aims of this thesis are:

1. To evaluate ultra-widefield pseudocolour fundus imaging with the Optos Panoramic 200MA in infants with a range of retinal diseases.
2. To evaluate ultra-widefield fundus fluorescein angiography with the Optos Panoramic 200MA in infants with a spectrum of retinal diseases.
3. To evaluate ultra-widefield fundus fluorescein angiography with the Heidelberg Spectralis in infants with a range of retinal diseases.

1.6. Outline of Chapters

- **Aim 1** will be addressed in Chapter 2: "Evaluation of Optos Ultra-Widefield Pseudocolour Fundus Imaging in Infants"
- **Aim 2** will be addressed in Chapter 3: "Evaluation of Optos Ultra-Widefield Fundus Fluorescein Angiographic Imaging in Infants"
- **Aim 3** will be addressed in Chapter 4: "Evaluation of Heidelberg Spectralis Ultra-Widefield Fundus Fluorescein Angiographic Imaging in Infants"

Chapter 5 will summarise the results of this thesis and discuss potential future work.

Chapter 2

Evaluation of Optos Ultra-Widefield Pseudocolour Fundus Imaging in Infants

2.1. Introduction

Non-contact ultra-widefield retinal imaging with the Optos Panoramic 200MA (Optos PLC, Dunfermline, Scotland, UK) in an outpatient setting has been successfully performed in cooperative children with a variety of paediatric retinal diseases [55, 56]. However very little work has been carried out on imaging uncooperative infants with retinal diseases using the Optos Panoramic 200MA. As previously discussed in section 1.4.2.1, since July 2012 the Optos Panoramic 200MA has been used at the Oxford Eye Hospital (OEH) for acquiring ultra-widefield retinal images as part of the routine clinical care and management of infants with retinal diseases.

The purpose of this study was to evaluate non-contact ultra-widefield pseudocolour fundus imaging with the Optos Panoramic 200MA in infants with a variety of retinal diseases.

2.2. Methods

2.2.1. Infants

A retrospective review of all infants with retinal diseases who had ultra-widefield pseudocolour fundus imaging at the outpatients department of the OEH between July 2012 and July 2014 was conducted. An infant was defined as any child from birth to the end of the first year of life. Medical records of all infants were reviewed with information collected on age, gender, diagnosis, use of any sedation for pseudocolour fundus imaging, and any respiratory or cardiovascular complications that occurred during the pseudocolour fundus imaging process (see section 1.4.2.2). For infants who were born premature (defined as an infant born before a gestational age of 37 completed weeks), additional information on gestational age (GA) (measured from the first day of last menstrual period to the day of birth), postnatal age (PNA) (measured from the day of birth to the day of retinal imaging), and birth weight (BW) were collected. A term infant was defined as any infant born with a gestational age between 37 and 42 completed weeks.

2.2.2. Image analysis

Ultra-widefield pseudocolour fundus images were reviewed with the Optos V2 Vantage Pro Review software version 2.8.0.4. The number of ultra-widefield pseudocolour fundus imaging sessions and the number of ultra-widefield pseudocolour fundus images acquired per imaging session were recorded for each infant. The quality of each individual ultra-widefield pseudocolour fundus image was determined as adequate or inadequate, based on field definition. An image was classed as adequate quality if the optic disc, the posterior pole (area of the retina located between the superior and inferior temporal arteries), and the peripheral retina

(area of the retina that extends from the border of the posterior pole to the ora serrata) were all visible (Figure 2.1). An image was classed as inadequate quality if at least one of the optic disc, the posterior pole, or the peripheral retina were not visible (Figure 2.2). All adequate quality ultra-widefield pseudocolour fundus images were chosen for analysis of captured peripheral retinal features and artefacts.

Image acquisition time was determined for each ultra-widefield pseudocolour fundus imaging session by calculating the time difference between the first and last pseudocolour fundus image captured. The time a pseudocolour fundus image is captured with the Optos Panoramic 200MA is automatically recorded and stored on the Optos V2 Vantage Pro Review software.

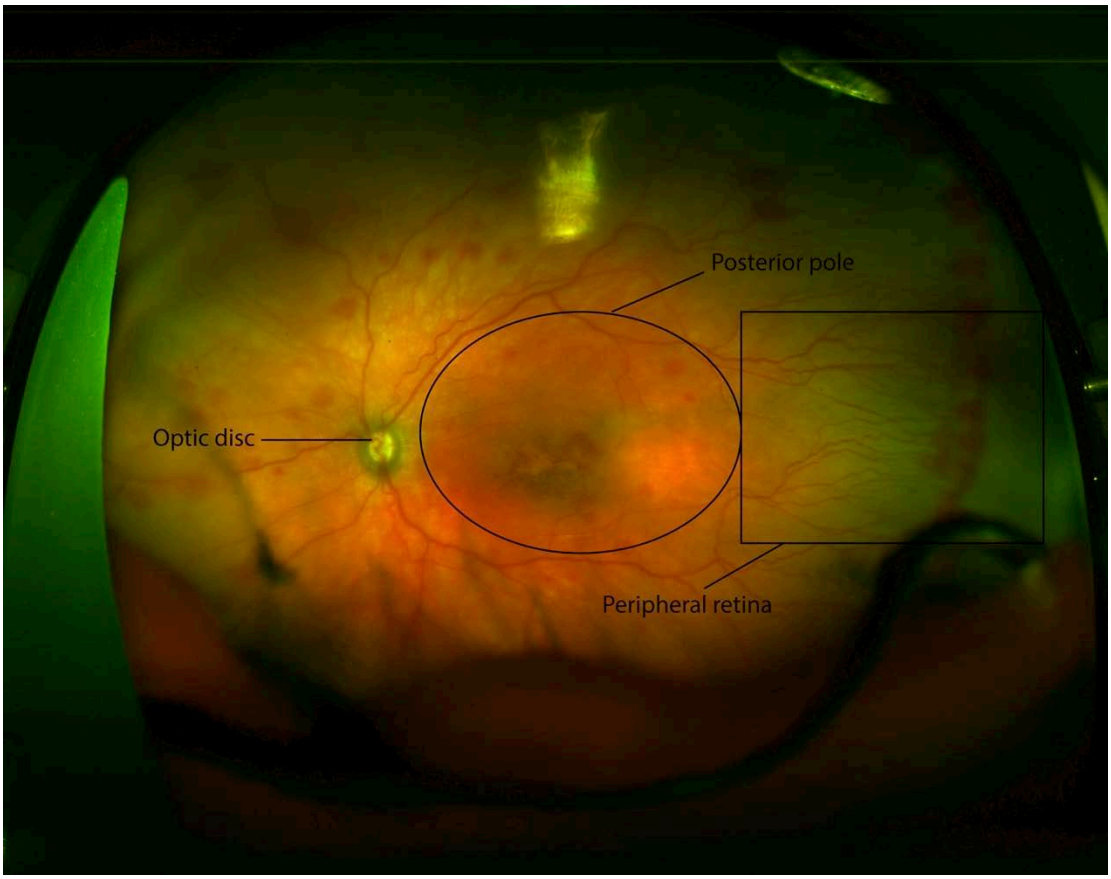

Figure 2.1: An example of an adequate quality Optos pseudocolour fundus image

In this pseudocolour fundus image of the left eye of an infant with stage 3 ROP in zone 2, the optic disc, the posterior pole, and the peripheral retina are all visible.

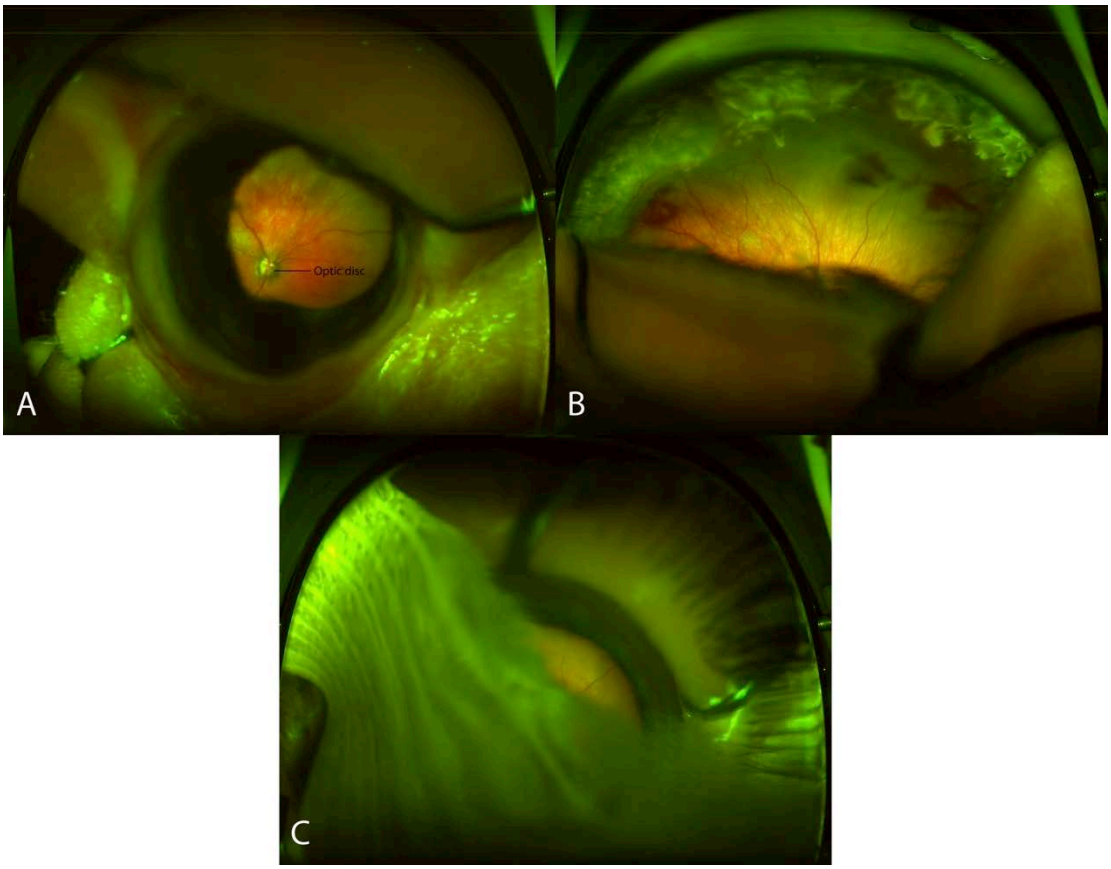

Figure 2.2: Examples of inadequate quality Optos pseudocolour fundus images

(A) In this pseudocolour fundus image of the right eye of an infant only the optic disc is visible. (B) In this pseudocolour fundus image of the right eye of an infant only the peripheral retina is visible. (C) In this pseudocolour fundus image no regions of the retina are visible.

2.3. Results

2.3.1. Infants

Over a 2-year period, a total of 42 infants with retinal diseases had ultra-widefield pseudocolour fundus imaging with the Optos Panoramic 200MA at the outpatients department of the OEH. There were 20 male and 22 female infants. Of the 42 infants, 2 were term infants with incontinentia pigmenti (IP) and 1 was a term infant with a diagnosis of familial exudative vitreoretinopathy (FEVR). The characteristics of the 3 term infants are provided in Table 2.1. Thirty-nine of the infants were diagnosed with retinopathy of prematurity (ROP). The characteristics of the 39 infants with ROP are provided in Table 2.2. Of the 39 infants with ROP, 27 were inpatients on the neonatal unit (NNU) and were transported to the outpatients department of the OEH for ultra-widefield pseudocolour fundus imaging. The mean GA was 25 weeks (range 23-29 weeks) and the mean BW was 811 grams (range 550-1150 grams). The mean PNA at ultra-widefield pseudocolour fundus imaging was 41 weeks (range 36-48 weeks). Seven infants transported from the NNU to the outpatients department of the OEH required oxygen support through a nasal continuous positive airway pressure (CPAP) device. The remaining 12 infants with ROP had ultra-widefield pseudocolour fundus imaging as part of their outpatient clinic appointment at the OEH. The mean GA was 25 weeks (range 24-30) and the mean BW was 787 grams (range 520-1510 grams). The mean PNA at ultra-widefield pseudocolour fundus imaging was 47 weeks (range 36-73 weeks). No infants had reduced oxygen saturations or altered cardiovascular parameters that required cessation of ultra-widefield pseudocolour fundus imaging. No infants required the use of any sedation for ultra-widefield pseudocolour fundus imaging.

Table 2.1: Characteristics of 3 term infants who had pseudocolour fundus imaging with the Optos Panoramic 200MA

Characteristic	Infant 1	Infant 2	Infant 3
Age (months)	3	6	2
Gender	Female	Female	Female
Diagnosis	IP	IP	FEVR

IP = incontinentia pigmenti; FEVR = familial exudative vitreoretinopathy

Table 2.2: Characteristics of 39 premature infants with ROP who had pseudocolour fundus imaging with the Optos Panoramic 200MA

Characteristic	**NNU Infants (N = 27)**	**Outpatient Infants (N = 12)**
Birth weight, grams		
Mean (SD)	811 (159.1)	787 (255.8)
Range	550-1150	520-1510
Gestational age, weeks		
Mean (SD)	25 (1.6)	25 (1.7)
Range	23-29	24-30
Postnatal age, weeks		
Mean (SD)	41 (5.9)	48 (12.3)
Range	36-48	36-73
Gender		
Male	N = 14	N = 6
Female	N = 13	N = 6

ROP = retinopathy of prematurity; NNU = neonatal unit; N = number of infants; SD = standard deviation

2.3.2. Image analysis

A total of 100 ultra-widefield pseudocolour fundus imaging sessions were conducted for 191 eyes, 96 right and 95 left, of 42 infants. The mean number of ultra-widefield pseudocolour fundus imaging sessions per infant was 2 (range 1-7) and 9 infants (21%) had 4 or more ultra-widefield pseudocolour fundus imaging sessions. The mean number of ultra-widefield pseudocolour fundus images captured per imaging session was 21 (range 1-75).

A total of 2147 individual ultra-widefield pseudocolour fundus images were captured in 100 ultra-widefield pseudocolour fundus imaging sessions. Among these images, 517 (24%) were classed as adequate quality and 1630 (76%) were classed as inadequate quality. For each imaging session, at least 1 adequate quality pseudocolour fundus image was obtained in one or both eyes of an infant.

A total of 517 images were chosen for analysis of captured peripheral retinal features and artefacts. A range of peripheral retinal pathologies was captured (Figure 2.3) including neovascular tissue, ischaemic retina, retinal exudates, retinal haemorrhages, retinal detachments, laser scars, and skip areas from previous laser therapy.

A summary of the image artefacts is provided in Table 2.3. Four hundred and thirty of 517 images had eyelid blocking the superior and/or inferior fundus (Figure 2.4A). Two hundred and seventy of 517 images had eyelashes obscuring the inferior fundus (Figure 2.4B). In 193 of 517 images, the nose obscured the temporal fundus (Figure 2.4C). Forty-eight of 517 images had an artefact from a nasal CPAP device obscuring the temporal fundus (Figure 2.4D).

Capturing of all pseudocolour colour fundus images took a mean time of 3 minutes (range 1-5 minutes) per imaging session.

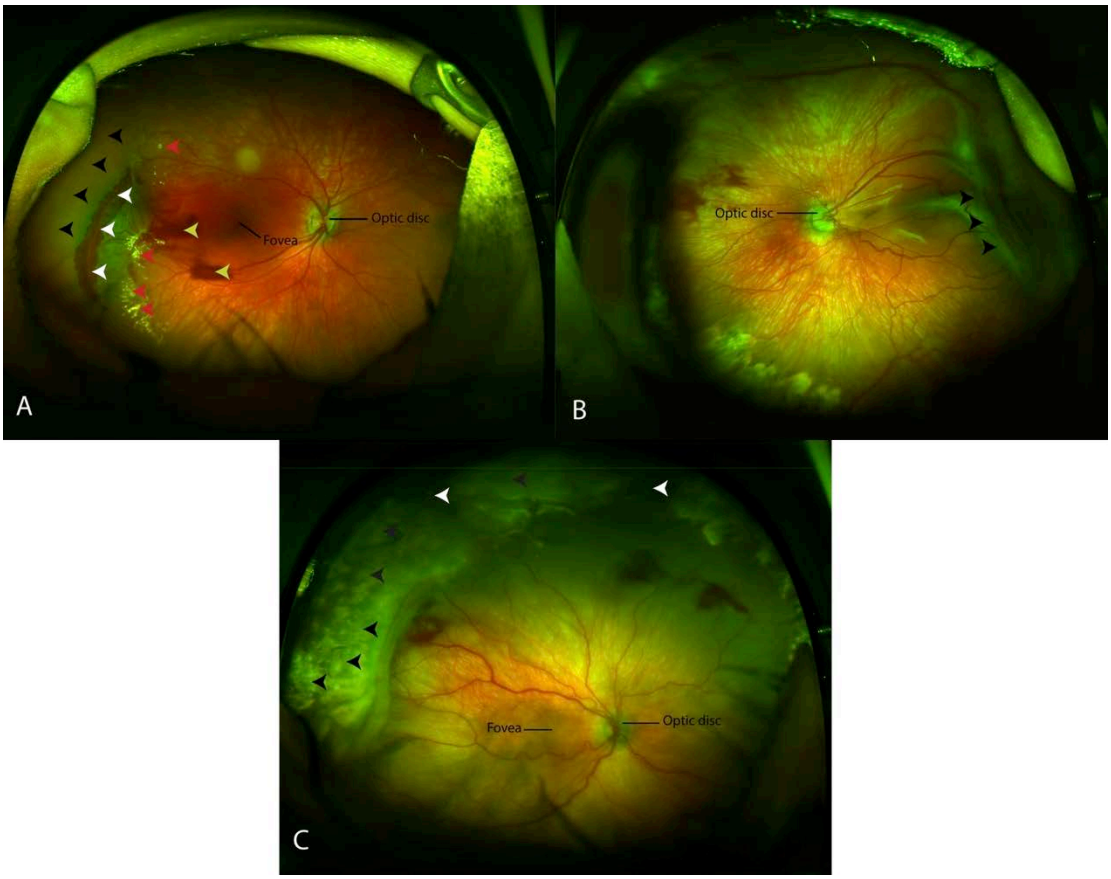

Figure 2.3: Examples of peripheral retinal features captured with Optos ultra-widefield pseudocolour fundus imaging in infants with retinal diseases

(A) Optos ultra-widefield pseudocolour fundus image of the right eye of an infant with FEVR demonstrating areas of peripheral ischaemia (black arrowheads), neovascularisation (white arrowheads), retinal exudates (red arrowheads), and retinal haemorrhages (yellow arrowheads). (B) Optos ultra-widefield pseudocolour fundus image of the right eye of an infant with stage 4 ROP demonstrating the presence of a periphery retinal detachment (black arrowheads). (C) Optos ultra-widefield pseudocolour fundus image of the right eye of an infant with stage 3 ROP demonstrating scars from previous laser treatment (black arrowheads) and skip areas from missed areas of laser treatment (white arrowheads).

Table 2.3: Artefacts from Optos ultra-widefield pseudocolour fundus images acquired in infants with retinal diseases

Artefact	**Images (N = 517)**
Eyelid blocking	430 (83%)
Eyelashes	270 (52%)
Nose	193 (37%)
CPAP device	48 (9%)

N = number of images; CPAP = continuous positive airway pressure

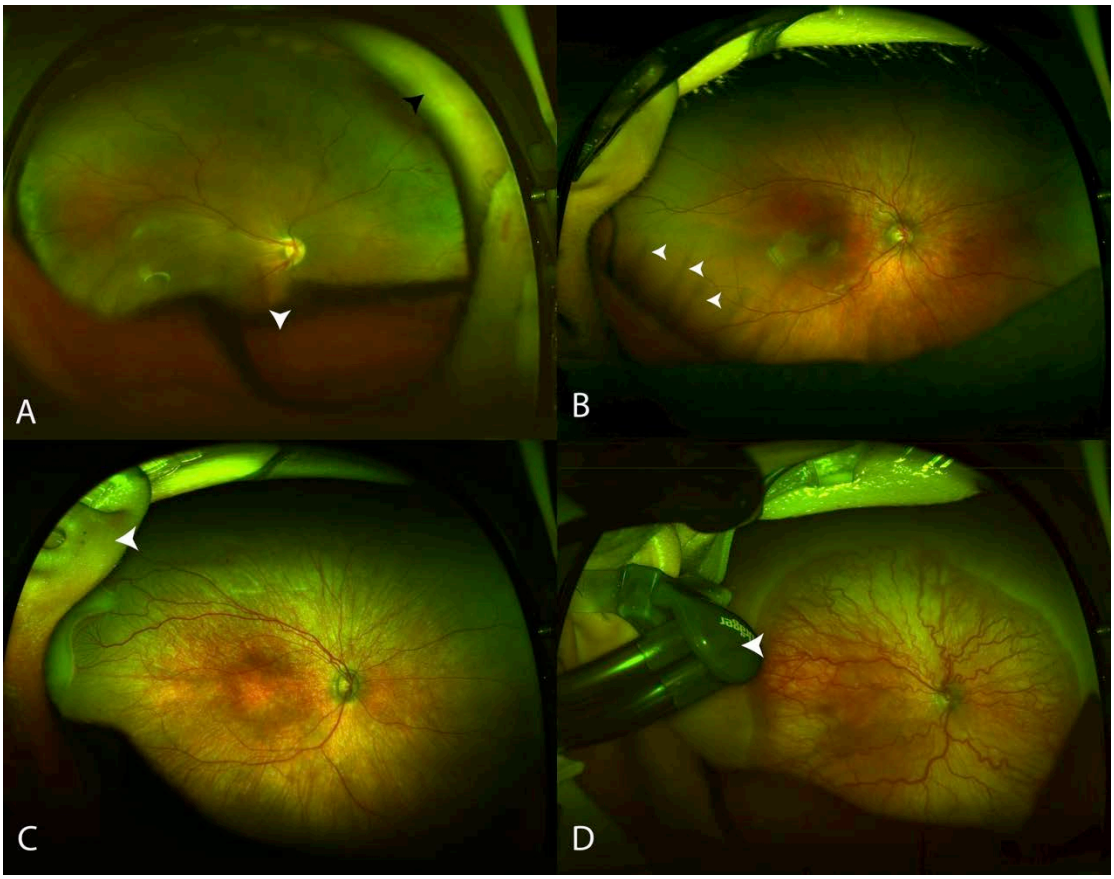

Figure 2.4: Examples of image artefacts from Optos ultra-widefield pseudocolour fundus imaging in infants with retinal diseases

(A) Optos ultra-widefield pseudocolour fundus image of a right eye of an infant demonstrating eyelid artefacts blocking the superior (black arrowhead) and inferior (white arrowhead) aspects of the fundus. (B) Optos ultra-widefield pseudocolour fundus image of a right eye of an infant demonstrating eyelash artefacts (white arrowheads) obscuring the inferior view of the fundus. (C) Optos ultra-widefield pseudocolour fundus image of a right eye of an infant demonstrating obstruction of the temporal fundus from a nose artefact (white arrowhead). (D) Optos ultra-widefield pseudocolour fundus image of the right eye of an infant showing an artefact from a continuous positive airway pressure device (white arrowhead), which obscures part of the temporal aspect of the fundus.

2.4. Discussion

To the best of our knowledge, we have evaluated for the first time non-contact ultra-widefield pseudocolour fundus imaging with the Optos Panoramic 200MA in an ophthalmic outpatient setting in infants with a range of retinal diseases. The Optos Panoramic 200MA was capable of acquiring clinically useful, high-resolution, ultra-widefield pseudocolour fundus images in infants with ROP, FEVR, and IP without the use of sedation. The ultra-widefield pseudocolour fundus images acquired were able to document a range of peripheral retinal features. There were no adverse changes in physiological parameters in any infant that necessitated cessation of ultra-widefield pseudocolour fundus imaging.

There are several advantages of using the Optos Panoramic 200MA for colour fundus photography in infants with retinal diseases. Firstly, the Optos Panoramic 200MA provides a 200-degree field of view, which covers approximately 80% of the retina in a single view. This ensures that only a single retinal image per eye of an infant is required with the Optos Panoramic 200MA to adequately document pathologies in the posterior pole and the far retinal periphery. With other imaging techniques (see section 1.3.3) multiple images are required to capture the far retinal periphery, which may then be montaged. Secondly, ultra-widefield pseudocolour fundus imaging with the Optos Panoramic 200MA requires no ocular contact. This may eliminate the risk of inducing retinal haemorrhages and stimulating an oculocardiac response in infants, which are well documented possibilities with imaging techniques that require ocular contact [44, 45, 46, 48]. Retinal imaging techniques that require ocular contact have also been documented to affect the diagnosis of plus disease in infants with ROP [47]. Thirdly, the Optos Panoramic 200MA uses cSLO imaging technology that allows the production of retinal images

with a more uniform focus to multiple retinal locations, which simultaneously increases clarity across the entire retinal field. The cSLO technology with the Optos Panoramic 200MA has been shown to be superior to traditional methods of colour fundus photography in its ability to image through small pupils and media opacities [49]. Lastly, the Optos Panoramic 200MA permits rapid image acquisition (0.25 seconds), overcoming the challenge of ocular movements when imaging mobile, non-sedated infants.

There are several limitations to using the Optos Panoramic 200MA for colour fundus photography in infants. Firstly, the Optos Panoramic 200MA is not portable and is restricted to imaging infants in the outpatients setting. Secondly, the Optos Panoramic 200MA is not currently capable of imaging infants who are required to remain in a supine position. Thirdly, a large proportion of ultra-widefield pseudocolour fundus images obtained in our series of infants have artefacts that decrease the field of view. The most common artefact in our study came from eyelids blocking the superior and inferior views of the fundus. In some infants, we managed to deal with this by ensuring the eyelids were held as wide open as possible with the paediatric lieberman adjustable speculum. Another common artefact in this study came from eyelashes obscuring the view of the inferior fundus. In a few infants, we managed to deal with this by taping down the eyelashes with steri-strips. Other methods have been described to reduce eyelash artefacts, such as placement of a specific disposable speculum [66].

In summary, the Optos Panoramic 200MA is capable of capturing clinically useful, high-resolution, ultra-widefield pseudocolour fundus images in infants with a range of retinal diseases in an ophthalmic outpatient setting.

Chapter 3

Evaluation of Optos Ultra-Widefield Fundus Fluorescein Angiography in Infants

3.1. Introduction

The importance of fundus fluorescein angiography (FFA) in infants with retinal diseases such as retinopathy of prematurity (ROP), incontinentia pigmenti (IP), and familial exudative vitreoretinopathy (FEVR) is well recognised for the diagnosis of peripheral retinal vascular pathologies such as neovascularisation, capillary non-perfusion, and leakage (see section 1.3.2). Infants are incapable of keeping their eyes open and steady for a long time, which is why conventional outpatient FFA is underused.

Non-contact ultra-widefield FFA in the outpatient setting using the Optos Panoramic 200MA (Optos PLC, Dunfermline, Scotland, UK) has been shown to be effective in detecting peripheral retinal vascular pathologies in cooperative paediatric patients with a wide range of retinal disorders [55, 56]. However, very little work has been carried out on ultra-widefield FFA of infants with retinal diseases in the outpatient setting using the Optos Panoramic 200MA.

As previously discussed in section 1.4.1.2, since July 2012 the Optos Panoramic 200MA has been used in the outpatient department of the Oxford Eye Hospital (OEH) for performing ultra-widefield FFA as part of the routine clinical care and management of infants with retinal diseases.

The purpose of this study was to evaluate non-contact ultra-widefield FFA with the Optos Panoramic 200MA in infants with a variety of retinal diseases.

3.2. Methods

3.2.1. Infants

A retrospective review of all infants with retinal diseases who had Optos ultra-widefield intravenous (IV) or oral FFA at the outpatients department of the OEH between July 2012 and July 2014 was conducted. An infant was defined as any child from birth to the end of the first year of life. Medical records of all infants were reviewed with information collected on age, gender, diagnosis, use of any sedation for FFA, and any respiratory or cardiovascular complications that occurred during the FFA imaging process (see section 1.4.2.3). For infants who were born premature (defined as an infant born before a gestational age of 37 completed weeks), additional information on gestational age (GA) (measured from the first day of last menstrual period to the day of birth), postnatal age (PNA) (measured from the day of birth to the day of retinal imaging), and birth weight (BW) were collected. A term infant was defined as any infant born with a gestational age between 37 and 42 completed weeks.

3.2.2. Image analysis

Ultra-widefield fundus fluorescein angiographic images were reviewed with the Optos V2 Vantage Pro Review software version 2.8.0.4. The number of fundus fluorescein angiographic imaging sessions and the number of fundus fluorescein angiographic images acquired per imaging session were recorded for each infant. For each imaging session, all images were evaluated for the presence of angiographic phases (choroidal, arterial, arteriovenous, venous, late). The different phases of a fluorescein angiogram are explained in section 1.3.2.3.

The quality of each individual fluorescein angiographic image was determined as adequate or inadequate, based on field definition. An image was classed as adequate

quality if the optic disc, the posterior pole (area of the retina located between the superior and inferior temporal arteries), and the peripheral retina (area of the retina that extends from the border of the posterior pole to the ora serrata) were all visible (Figure 3.1). An image was classed as inadequate quality if at least one of the optic disc, the posterior pole, or the peripheral retina were not visible (Figure 3.2).

All adequate quality fluorescein angiographic images were chosen for analysis of captured peripheral retinal features and artefacts.

Image acquisition time was determined for each ultra-widefield fundus fluorescein angiographic imaging session by calculating the time difference between the first and last image captured. The time an image is captured with the Optos Panoramic 200MA is automatically recorded on the Optos V2 Vantage Pro Review software.

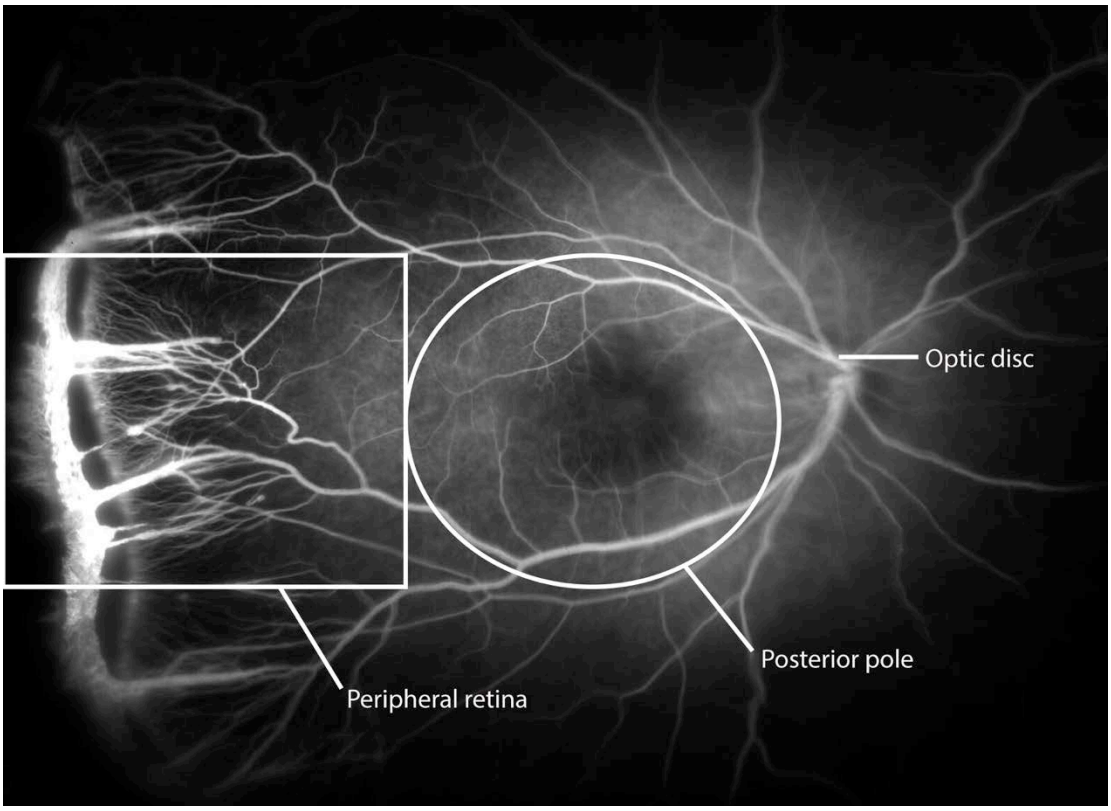

Figure 3.1: An example of an adequate quality Optos ultra-widefield fundus fluorescein angiographic image

In this venous phase image of a fundus fluorescein angiogram of the left eye of an infant with stage 3 ROP in zone 2, the optic disc, the posterior pole, and the peripheral retina are all visible.

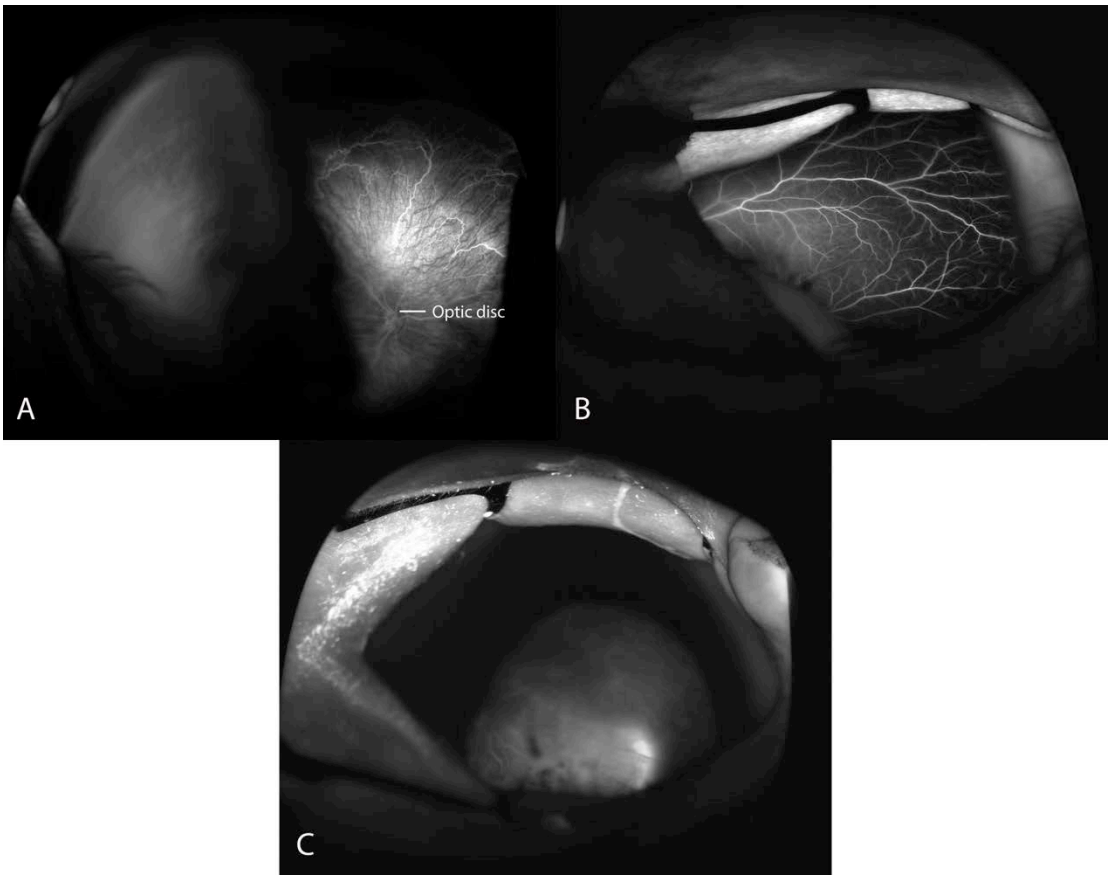

Figure 3.2: Examples of inadequate quality Optos ultra-widefield fundus fluorescein angiographic images

(A) In this late phase image of a fundus fluorescein angiogram of the right eye of an infant the macula is not visible. (B) In this venous phase image of a fluorescein angiogram of the left eye of an infant the optic disc is not visible. (C) In this fluorescein angiographic image no regions of the retina are visible.

3.3. Results

3.3.1. Infants

Over a 2-year period, a total of 29 infants with retinal diseases had non-contact ultra-widefield FFA with the Optos Panoramic 200MA at the outpatients department of the OEH. Optos ultra-widefield intravenous FFA was performed in 23 infants and Optos ultra-widefield oral FFA was performed in 6 infants who had inaccessible veins. There were 14 male and 15 female infants. Of the 29 infants, 2 were term infants with IP and 1 was a term infant with a diagnosis of FEVR. The characteristics of the 3 term infants are provided in Table 3.1. Twenty-six of the infants were diagnosed with ROP. The characteristics of the 26 infants with ROP are provided in Table 3.2. Of the 26 infants with ROP, 21 were inpatients on the neonatal unit (NNU) and were transported to the outpatients department of the OEH for ultra-widefield FFA. The mean GA was 25 weeks (range 23-29 weeks) and the mean BW was 789 grams (range 550-1090 grams). The mean PNA at ultra-widefield FFA was 39 weeks (range 37-45 weeks). Six infants transported from the NNU to the outpatients department of the OEH for FFA required oxygen support through a nasal continuous positive airway pressure (CPAP) device. The remaining 5 infants with ROP had ultra-widefield FFA as part of their outpatient clinic appointment at the OEH. The mean GA was 25 weeks (range 24-30) and the mean BW was 819 grams (range 520-1510 grams). The mean PNA at ultra-widefield FFA was 41 weeks (range 37-47 weeks). No infants had reduced oxygen saturations or altered cardiovascular parameters that required cessation of ultra-widefield FFA. One infant required oral sedation with chloral hydrate to assist with ultra-widefield fundus fluorescein angiographic image acquisition.

Table 3.1: Characteristics of 3 term infants who had non-contact ultra-widefield FFA with the Optos Panoramic 200MA

Characteristic	Infant 1	Infant 2	Infant 3
Age (months)	3	6	2
Gender	Female	Female	Female
Diagnosis	IP	IP	FEVR

IP = incontinentia pigmenti; FEVR = familial exudative vitreoretinopathy

Table 3.2: Characteristics of 26 premature infants with ROP who had non-contact ultra-widefield FFA with the Optos Panoramic 200MA

Characteristic	**NNU Infants (N = 21)**	**Outpatient Infants (N = 5)**
Birth weight, grams		
Mean (SD)	789 (150.1)	819 (150.1)
Range	550-1090	520-1510
Gestational age, weeks		
Mean (SD)	25 (1.6)	25 (1.7)
Range	23-29	24-30
Postnatal age, weeks		
Mean (SD)	39 (3.1)	41 (3.5)
Range	37-45	37-47
Gender		
Male	N = 10	N = 5
Female	N = 11	N = 0

ROP = retinopathy of prematurity; FFA = fundus fluorescein angiography; NNU = neonatal unit; N = number of infants; SD = standard deviation

3.3.2. Image analysis

A total of 38 ultra-widefield IV fundus fluorescein angiographic imaging sessions were conducted for 71 eyes, 36 right and 35 left, of 23 infants. The mean number of ultra-widefield IV fluorescein angiographic imaging sessions per infant was 2 (range 1-4) and 3 infants (10%) had 3 or more ultra-widefield IV fluorescein angiographic imaging sessions. The mean number of ultra-widefield IV fundus fluorescein angiographic images captured per imaging session was 41 (range 33-58). A total of 1586 individual ultra-widefield IV fundus fluorescein angiographic images were captured in 38 ultra-widefield IV fluorescein angiographic imaging sessions. Among these images, 684 (43%) were classed as adequate quality and 902 (57%) were classed as inadequate quality. The results of the angiographic phase evaluation are shown in Table 3.3. In one of 38 imaging sessions (3%), the choroidal filling phase was captured in both eyes of an infant. In all 38 imaging sessions, at least 1 adequate quality fluorescein angiographic image of the arterial, arteriovenous, venous, and late phases were captured in one or both eyes of an infant.

A total of 7 ultra-widefield oral fluorescein angiographic imaging sessions were conducted for 14 eyes, 12 right and 12 left, of 6 infants. The mean number of ultra-widefield oral fluorescein angiographic imaging sessions per infant was 1 (range 1-2). The mean number of ultra-widefield oral fluorescein angiographic images captured per imaging session was 53 (range 7-80). A total of 376 individual ultra-widefield oral fundus fluorescein angiographic images were captured in 7 ultra-widefield oral fluorescein angiographic imaging sessions. Among these images, 64 (17%) were classed as adequate quality and 312 (83%) were classed as inadequate quality. At least 1 adequate quality late phase angiographic image was obtained in both eyes of all 6 infants.

Table 3.3: Fluorescein angiographic phases captured in infants who had non-contact ultra-widefield IV FFA with the Optos Panoramic 200MA

Angiographic phase	**Imaging sessions (N = 38)**
Choroidal	N = 1 (3%)
Arterial	N = 38 (100%)
Arteriovenous	N = 38 (100%)
Venous	N = 38 (100%)
Late	N = 38 (100%)

IV FFA = intravenous fundus fluorescein angiography; N = number of imaging sessions

A total of 684 ultra-widefield intravenous fundus fluorescein angiographic images were chosen for analysis of captured peripheral retinal features and artefacts. A range of peripheral retinal features was captured with intravenous fluorescein angiography (Figure 3.3) including neovascularisation and leakage, capillary non-perfusion, staining of scars from previous laser treatment, and missing areas of laser treatment (skip areas).

A total of 64 ultra-widefield oral fundus fluorescein angiographic images were chosen for analysis of peripheral retinal vascular features and artefacts. The peripheral retinal features captured with oral fluorescein angiography included capillary non-perfusion and neovascularisation and leakage (Figure 3.4).

A summary of the image artefacts is provided in Table 3.4. Three hundred and forty five of 748 images had eyelid blocking the superior and/or inferior fundus (Figure 3.5A). One hundred and fifteen of 748 images had eyelashes obscuring the inferior fundus (Figure 3.5B). In 479 of 748 images, the nose obscured the temporal fundus (Figure 3.5C). Sixty of 748 images had an artefact from a nasal CPAP device obscuring the temporal fundus (Figure 3.5D).

Capturing of all fundus fluorescein angiographic images took a mean time of 5 minutes (range 3-7 minutes) per imaging session.

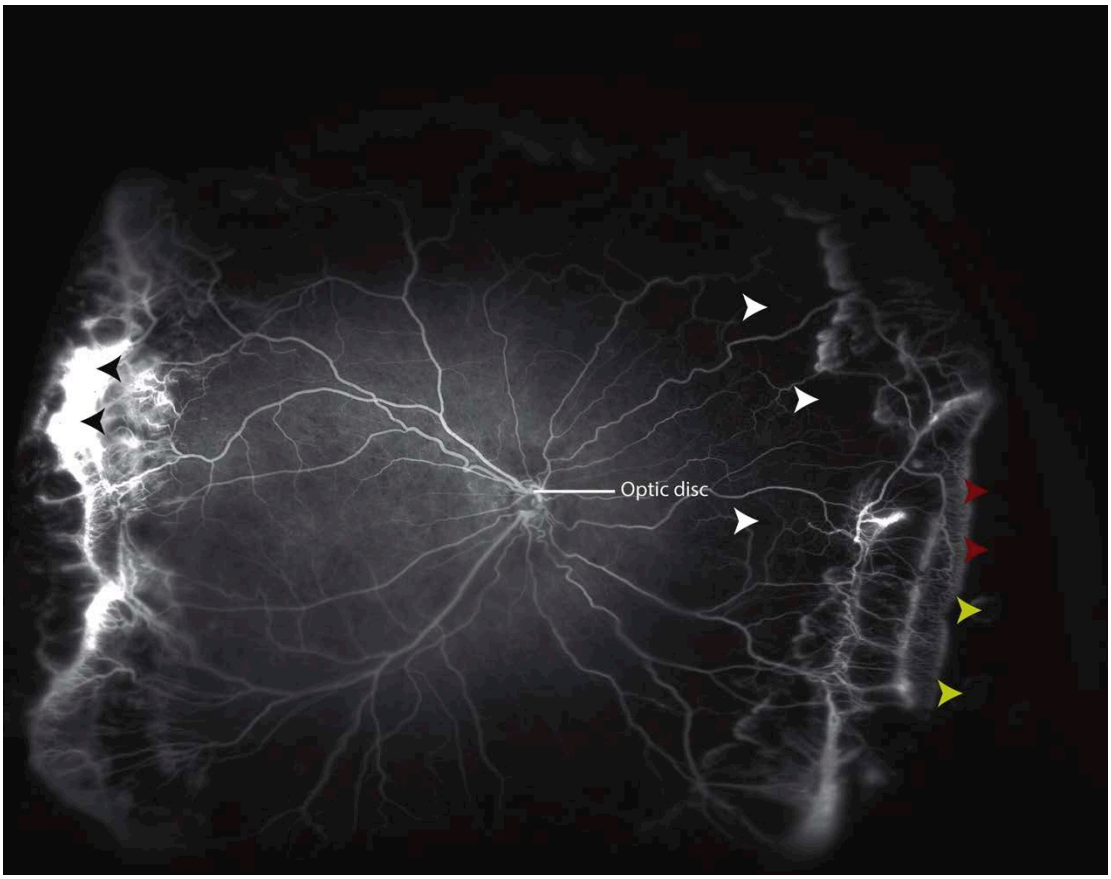

Figure 3.3: An example of peripheral retinal features captured with an Optos ultra-widefield intravenous fundus fluorescein angiographic image in an infant with retinopathy of prematurity

This is a late phase image of the right eye of an infant with stage 3 ROP in zone 2 with plus disease. Areas of neovascularisation and leakage (black arrowheads), regions of capillary non-perfusion (white arrowheads), staining from previous laser burns (yellow arrowhead), and areas of missed laser treatment (red arrowheads) are clearly visible in the peripheral retina.

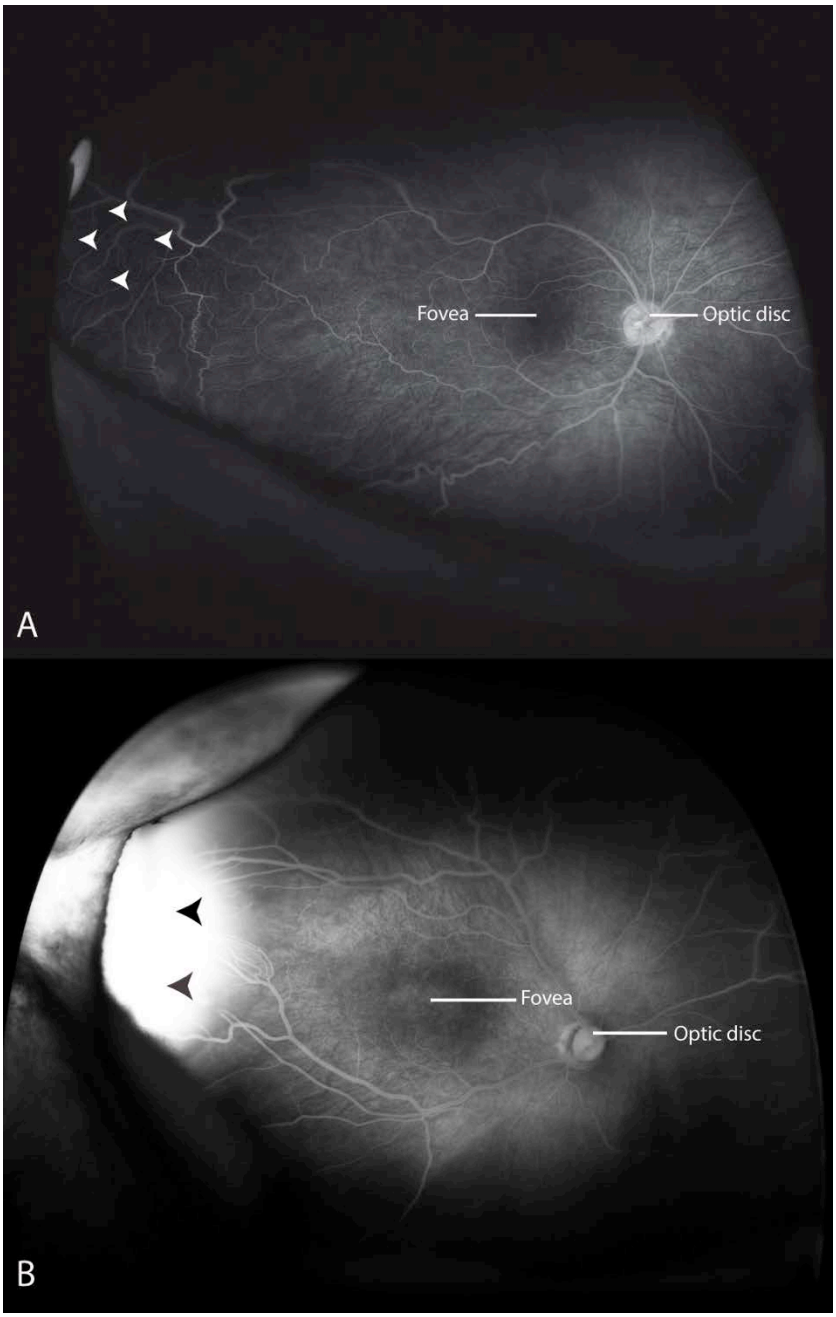

Figure 3.4: Examples of peripheral retinal features captured with Optos ultra-widefield oral fundus fluorescein angiography in infants with retinal diseases

(A) This late phase image of the right eye of an infant with IP (Patel, Fung, Muqit, Mordant and Geh, 2012, p310) demonstrates clearly areas of peripheral capillary non-perfusion (white arrowheads). (B) This late phase image of the right eye of an infant with stage 3 ROP in zone 2 demonstrates peripheral neovascularisation and leakage (black arrowheads).

Table 3.4: Artefacts from Optos ultra-widefield fundus fluorescein angiographic images acquired in infants with retinal diseases

Artefact	**Images (N = 748)**
Eyelid blocking	345 (46%)
Eyelashes	115 (15%)
Nose	479 (64%)
CPAP device	60 (8%)

N = number of images; CPAP = continuous positive airway pressure

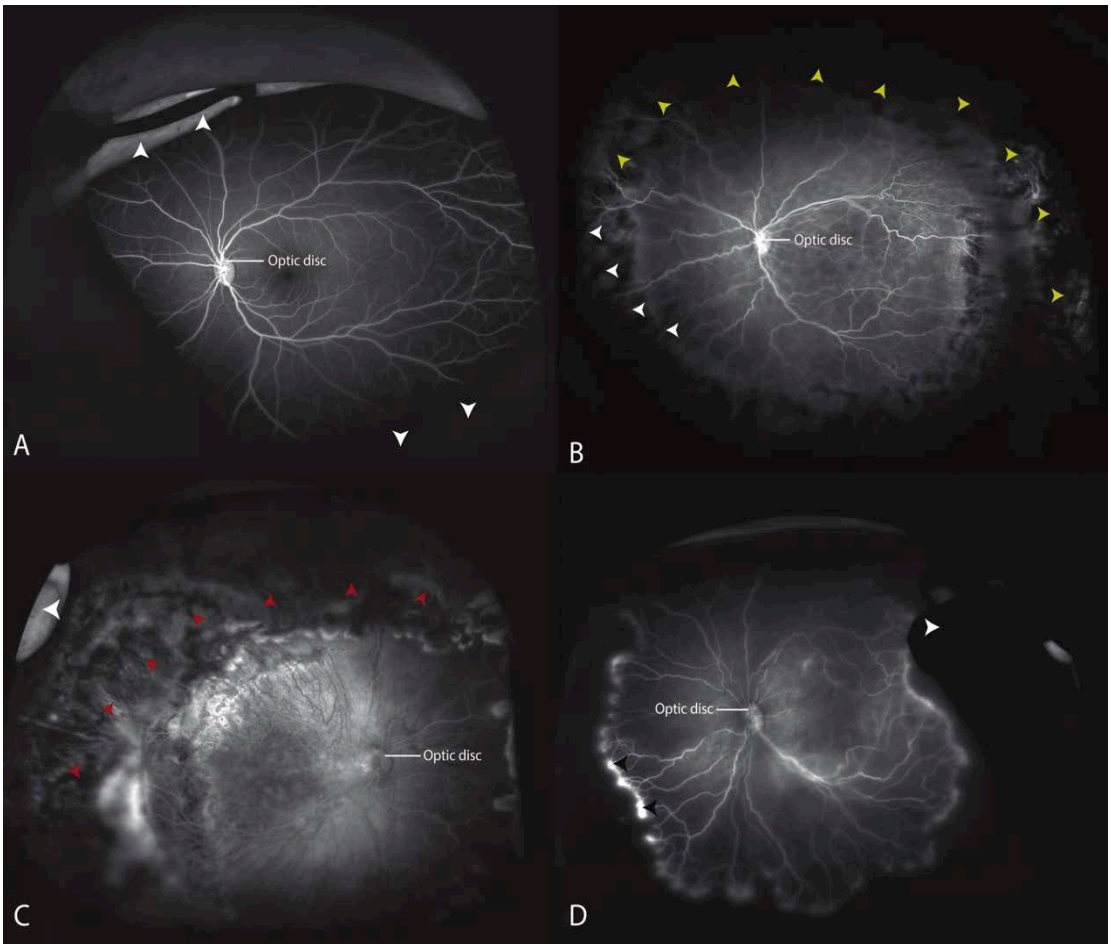

Figure 3.5: Examples of artefacts arising from Optos ultra-widefield fundus fluorescein angiography of infants with retinal diseases

(A) A venous phase image of a normal ultra-widefield fluorescein angiogram of the left eye of an infant with IP. The eyelids (white arrowheads) are seen blocking the superior and inferior view of the fundus. (B) An arteriovenous phase image of an ultra-widefield fluorescein angiogram of the left eye of an infant with previously treated ROP. Staining from previous laser burns is clearly seen in the peripheral retina (yellow arrowheads). Note how eyelashes (white arrowheads) obscure the view of part of the inferonasal fundus. (C) A late phase image of an ultra-widefield fluorescein angiogram the right eye of an infant with previously treated ROP. A nose artefact (white arrowhead) is seen in the temporal fundus. Extensive scarring from previous laser burns is seen in the peripheral retina (red arrowheads). (D) A venous

phase image of an ultra-widefield fluorescein angiogram of the left eye of an infant with stage 3 ROP in zone 1 with pre-plus disease. Neovascular tufts (black arrowheads) are seen in the peripheral retina. Note how an artefact from a nasal CPAP device (white arrowhead) is seen in the temporal fundus.

3.4. Discussion

To the best of our knowledge, we have evaluated for the first time non-contact ultra-widefield FFA with the Optos Panoramic 200MA in an ophthalmic outpatient setting in infants with a range of retinal diseases. The Optos Panoramic 200MA was capable of acquiring clinically useful, high-resolution, ultra-widefield fundus fluorescein angiographic images in infants with ROP, FEVR, and IP. The fundus fluorescein angiographic images acquired were able to document a range of peripheral retinal features. There were no adverse changes in physiological parameters in any infant that necessitated cessation of ultra-widefield fundus fluorescein angiographic imaging with the Optos Panoramic 200MA.

Ultra-widefield fundus fluorescein angiographic images were acquired with the Optos Panoramic 200MA in the majority of infants without the use of sedation. However, a 6-month-old term infant with excessive head movements required the use of oral sedation to help assist with the acquisition of fundus fluorescein angiographic images. The acquisition of fundus fluorescein angiographic images with the Optos Panoramic 200MA may be difficult or not possible without the use of sedation in infants who are 6 months or older.

The percentage of inadequate quality ultra-widefield fundus fluorescein angiographic images acquired in infants with the Optos Panoramic 200MA was 61% in this study. Excessive head and eye movements of an infant and poor positioning of the infant in front of the Optos Panoramic 200MA using the “flying baby” technique described in section 1.4.2.2 may be responsible for the high number of inadequate quality fluorescein angiographic images acquired. However, the ability of the Optos Panoramic 200MA to capture 200-degrees of retina in a single frame ensured that

only one adequate quality angiographic image of each phase was required per eye of an infant to adequately document retinal vascular pathologies in the posterior pole and the retinal periphery. The rapid image acquisition time (0.25 seconds) of the Optos Panoramic 200MA enabled a large amount of fundus fluorescein angiographic images to be captured over a short time period.

Due to difficulty with patient cooperation in the infant population, adequate evaluation of the peripheral retina using FFA often requires examination under anaesthesia (EUA) in the operating room. Although EUA is generally a safe procedure in infants, serious complications may occur, including cardiac arrest and respiratory failure [67]. Premature infants with a host of complications related to their underdeveloped organ systems may be unable to tolerate EUA in the operating room. The ability of the Optos Panoramic 200MA to capture the far peripheral retina in a simultaneous angiographic phase in infants in an outpatient setting may help ophthalmologists avoid performing fluorescein angiography in infants in the operating room and limit anaesthesia exposure to the infant patient.

In the outpatient setting, fundus fluorescein angiographic images were acquired with the Optos Panoramic 200MA in 6 infants following the oral administration of sodium fluorescein. As demonstrated in Figure 3.4, peripheral dye leakage and capillary non-perfusion were both extremely well visualised with Optos oral FFA. For infants with retinal vascular diseases who have inaccessible veins, oral FFA with the Optos Panoramic 200MA may be a useful tool for detecting and assessing capillary non-perfusion and dye leakage. The use of the Optos Panoramic 200MA for oral FFA in the outpatient setting may help improve the safety of fluorescein angiography in infants as the oral administration of sodium fluorescein is known to have a lower incidence of side-effects than intravenous administration [68].

There are several limitations to using the Optos Panoramic 200MA for acquiring fundus fluorescein angiographic images in infants. Firstly, the Optos Panoramic 200MA is not portable and is restricted to imaging infants in the outpatients setting. Secondly, the Optos Panoramic 200MA is not currently capable of imaging infants who are required to remain in a supine position. Thirdly, a large proportion of ultra-widefield fundus fluorescein angiographic images obtained in our series of infants have artefacts that decrease the field of view. The most common artefact in our study came from eyelids blocking the superior and inferior views of the fundus. In some infants, we managed to deal with this by ensuring the eyelids were held as wide open as possible with the paediatric lieberman adjustable speculum. Another common artefact in this study came from eyelashes obscuring the view of the inferior fundus. In a few infants, we managed to deal with this by taping down the eyelashes with steri-strips. Other methods have been described to reduce eyelash artefacts, such as placement of a specific disposable speculum [66].

In summary, the Optos Panoramic 200MA is capable of capturing clinically useful, high-resolution, ultra-widefield oral and IV fundus fluorescein angiographic images in infants with a range of retinal diseases in an ophthalmic outpatient setting.

Chapter 4

Evaluation of Heidelberg Spectralis Ultra-Widefield Fundus Fluorescein Angiography in Infants

4.1. Introduction

The RetCam (Clarity Medical Systems, Pleasanton, California, USA) is currently the only widely available imaging modality used to perform fundus fluorescein angiography (FFA) on a supine infant under general anaesthesia in the operating room. Peripheral sweeps and montage techniques are often necessary when information about the retinal periphery is required. These techniques are labour intensive, require highly skilled photographers, and do not permit the simultaneous capture of the posterior pole and periphery in a single frame, limiting the evaluation and comparison of the phases of the angiogram across different parts of the fundus.

As previously discussed in section 1.4.3.1, since July 2012 the Heidelberg Spectralis ultra-widefield imaging lens has been used in the operating room at the Oxford Eye Hospital (OEH) to perform ultra-widefield FFA in anaesthetised infants as part of the routine clinical care and management of their retinal diseases.

The purpose of this study was to evaluate non-contact ultra-widefield FFA with the Heidelberg Spectralis in infants with a variety of retinal diseases.

4.2. Methods

4.2.1. Infants

A retrospective review of all infants with retinal diseases who had non-contact ultra-widefield FFA under general anaesthesia in the operating room with the Heidelberg Spectralis at the OEH between July 2012 and July 2014 was performed. An infant was defined as any child from birth to the end of the first year of life. Medical records of all infants were reviewed with information collected on age, gender, diagnosis, and any respiratory or cardiovascular complications that occurred during the Heidelberg Spectralis FFA imaging process (see section 1.4.3.2). For infants who were born premature (defined as an infant born before a gestational age of 37 completed weeks), additional information on gestational age (GA) (measured from the first day of last menstrual period to the day of birth), postnatal age (PNA) (measured from the day of birth to the day of retinal imaging), and birth weight (BW) were collected. A term infant was defined as any infant born with a gestational age between 37 and 42 completed weeks.

4.2.2. Image analysis

Heidelberg Spectralis ultra-widefield fundus fluorescein angiographic images were reviewed with the Heidelberg Eye Explorer software version 1.9.10.0. The number of fluorescein angiographic imaging sessions and the number of fluorescein angiographic images acquired per imaging session were recorded for each infant. For each imaging session, all images were evaluated for the presence of angiographic phases (choroidal, arterial, arteriovenous, venous, late). The different phases of a fluorescein angiogram are explained in section 1.3.2.3.

The quality of each individual fluorescein angiographic image was determined as adequate or inadequate, based on field definition. An image was classed as adequate quality if the optic disc, the posterior pole (area of the retina located between the superior and inferior temporal arteries), and the peripheral retina (area of the retina that extends from the border of the posterior pole to the ora serrata) were all visible (Figure 4.1). An image was classed as inadequate quality if at least one of the optic disc, the posterior pole, or the peripheral retina were not visible (Figure 4.2).

All adequate quality fundus fluorescein angiographic images were used for analysis of captured peripheral retinal features and artefacts.

Image acquisition time was determined for each ultra-widefield fundus fluorescein angiographic imaging session by calculating the time difference between the first and last image captured. The time an image is captured with the Heidelberg Spectralis is automatically recorded and stored on the Heidelberg Eye Explorer software.

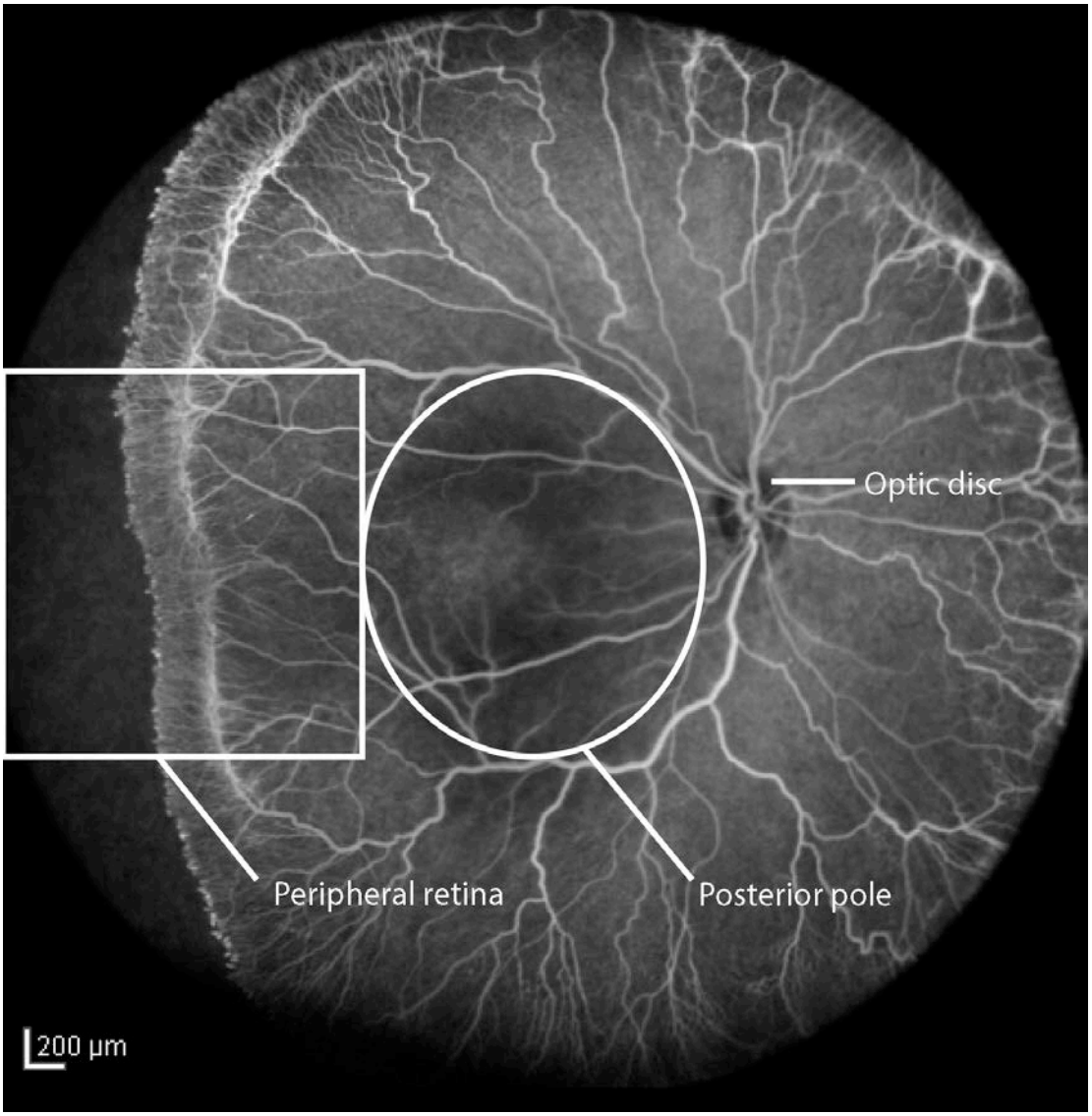

Figure 4.1: An example of an adequate quality Heidelberg Spectralis ultra-widefield fundus fluorescein angiographic image

In this late phase image of a fundus fluorescein angiogram of the right eye of an infant with regressed stage 3 ROP in zone 1, the optic disc, the posterior pole, and the peripheral retina are all visible.

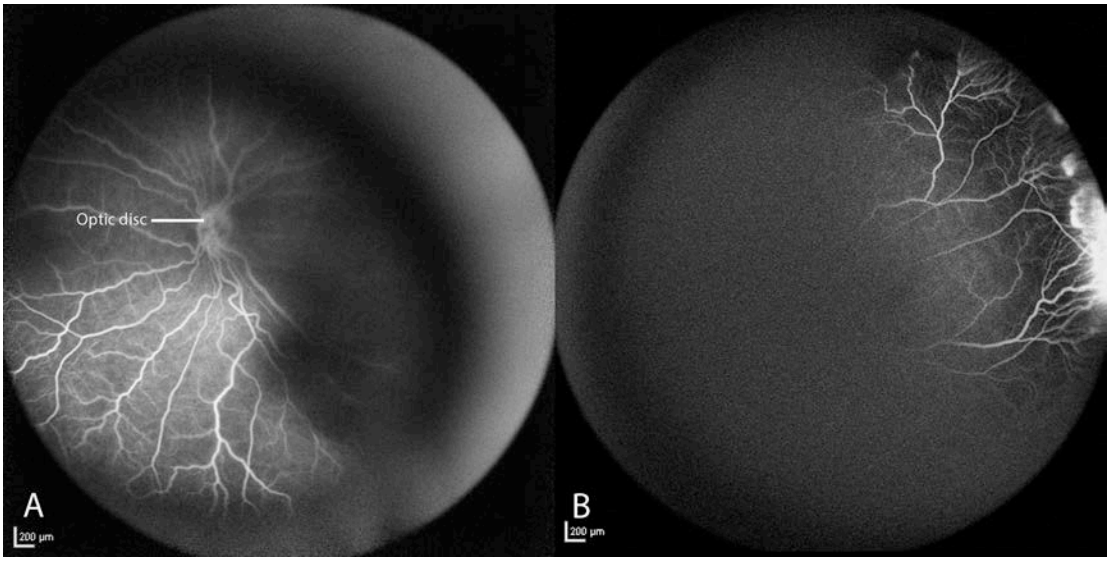

Figure 4.2: Examples of inadequate quality Heidelberg Spectralis ultra-widefield fundus fluorescein angiographic images

(A) In this late phase image of a fundus fluorescein angiogram of the left eye of an infant the macula is not visible. (B) In this venous phase image of a fluorescein angiogram of the left eye of an infant only the peripheral retina is visible.

4.3. Results

4.3.1. Infants

Over a 2-year period, a total of 11 infants with retinal diseases had non-contact ultra-widefield FFA under general anaesthesia in the operating room with the Heidelberg Spectralis. There were 6 male and 5 female infants. Of the 11 infants, 2 were term infants with incontinentia pigmenti (IP) and 1 was a term infant with a diagnosis of familial exudative vitreoretinopathy (FEVR). The characteristics of the 3 term infants are provided in Table 4.1. Eight of the infants were diagnosed with retinopathy of prematurity (ROP). The characteristics of the 8 infants with ROP are provided in Table 4.2. The mean GA was 24 weeks (range 23-26 weeks) and the mean BW was 744 grams (range 650-870 grams). The mean PNA at ultra-widefield FFA was 47 weeks (range 33-91 weeks). There were no adverse changes in physiological parameters in any infant that required cessation of ultra-widefield fundus fluorescein angiographic imaging with the Heidelberg Spectralis.

Table 4.1: Characteristics of 3 term infants who had non-contact ultra-widefield FFA with the Heidelberg Spectralis

Characteristic	**Infant 1**	**Infant 2**	**Infant 3**
Age (months)	3	6	2
Gender	Female	Female	Female
Diagnosis	IP	IP	FEVR

IP = incontinentia pigmenti; FEVR = familial exudative vitreoretinopathy

Table 4.2: Characteristics of 8 premature infants with ROP who had non-contact ultra-widefield FFA with the Heidelberg Spectralis

Characteristic	**NNU Infants (N = 8)**
Birth weight, grams	
Mean (SD)	744 (103.7)
Range	650-870
Gestational age, weeks	
Mean (SD)	24 (1.2)
Range	23-26
Postnatal age, weeks	
Mean (SD)	47 (18.3)
Range	33-91
Gender	
Male	N = 6
Female	N = 2

ROP = retinopathy of prematurity; FFA = fundus fluorescein angiography; NNU = neonatal unit; N = number of infants; SD = standard deviation

4.3.2. Image analysis

A total of 11 ultra-widefield fundus fluorescein angiographic imaging sessions with the Heidelberg Spectralis were conducted for 22 eyes, 11 right and 11 left, of 11 infants. The mean number of ultra-widefield fundus fluorescein angiographic images captured per imaging session was 113 (range 52-198). A total of 1251 individual ultra-widefield fundus fluorescein angiographic images were captured in 11 ultra-widefield fluorescein angiographic imaging sessions. Among these images, 1124 (89%) were classed as adequate quality and 127 (11%) were classed as inadequate quality. In all 11 imaging sessions, at least 1 adequate quality fluorescein angiographic image of all phases were captured in both eyes of an infant.

A total of 1124 ultra-widefield fundus fluorescein angiographic images were chosen for analysis of captured peripheral retinal features and artefacts. A range of peripheral retinal features was captured (Figure 4.3) including neovascularisation and leakage, retinal ischaemia, capillary non-perfusion, scars from previous laser treatment, and missing areas of laser treatment. In 43 of 1124 ultra-widefield fundus fluorescein angiographic images, an area of artefact arose from condensation that had developed across the ultra-widefield imaging lens during the image process (Figure 4.4). There were no other artefacts on any of the images obtained.

Capturing of all ultra-widefield fundus fluorescein angiographic images took a mean time of 7 minutes (range 5-9 minutes) per imaging session.

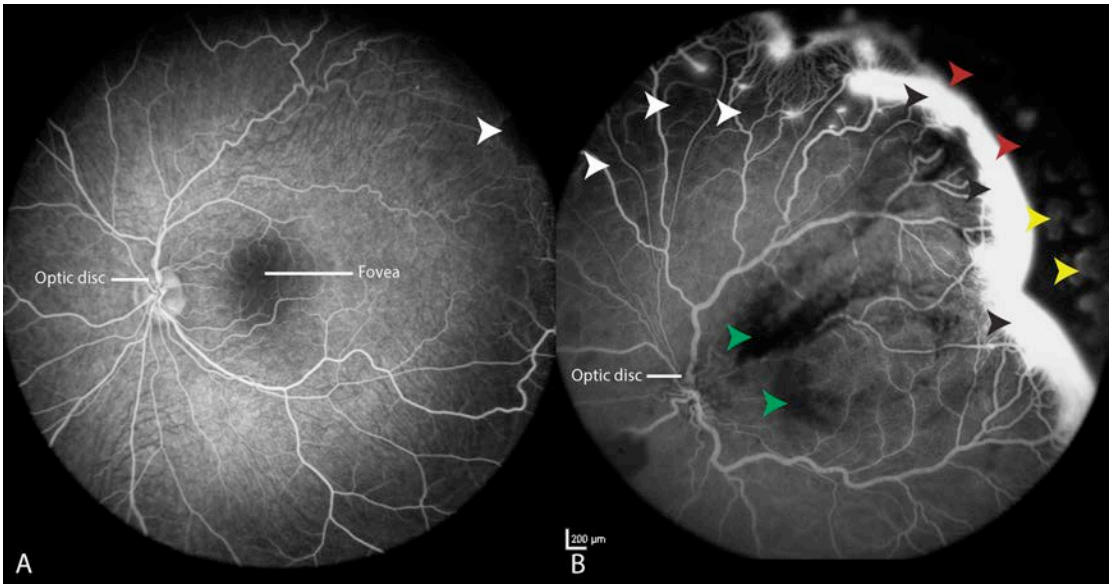

Figure 4.3: Examples of peripheral retinal features captured with Heidelberg Spectralis ultra-widefield fundus fluorescein angiography in infants with retinal diseases (Fung, Yusuf, Xue, Smith and Patel, 2015, p81-82)

(A) This late phase image of the left eye of an infant with IP demonstrates an area of retinal ischaemia in the far retinal periphery (white arrowhead). (B) This venous phase image of the left eye of an infant with stage 3 ROP in zone 2 with plus disease demonstrates areas of peripheral leakage (black arrowheads), capillary non-perfusion (white arrowheads), scars from previous laser burns (yellow arrowheads), and missing areas of laser treatment (red arrowheads). Note how retinal haemorrhages (green arrowheads) have obscured the view of the posterior pole.

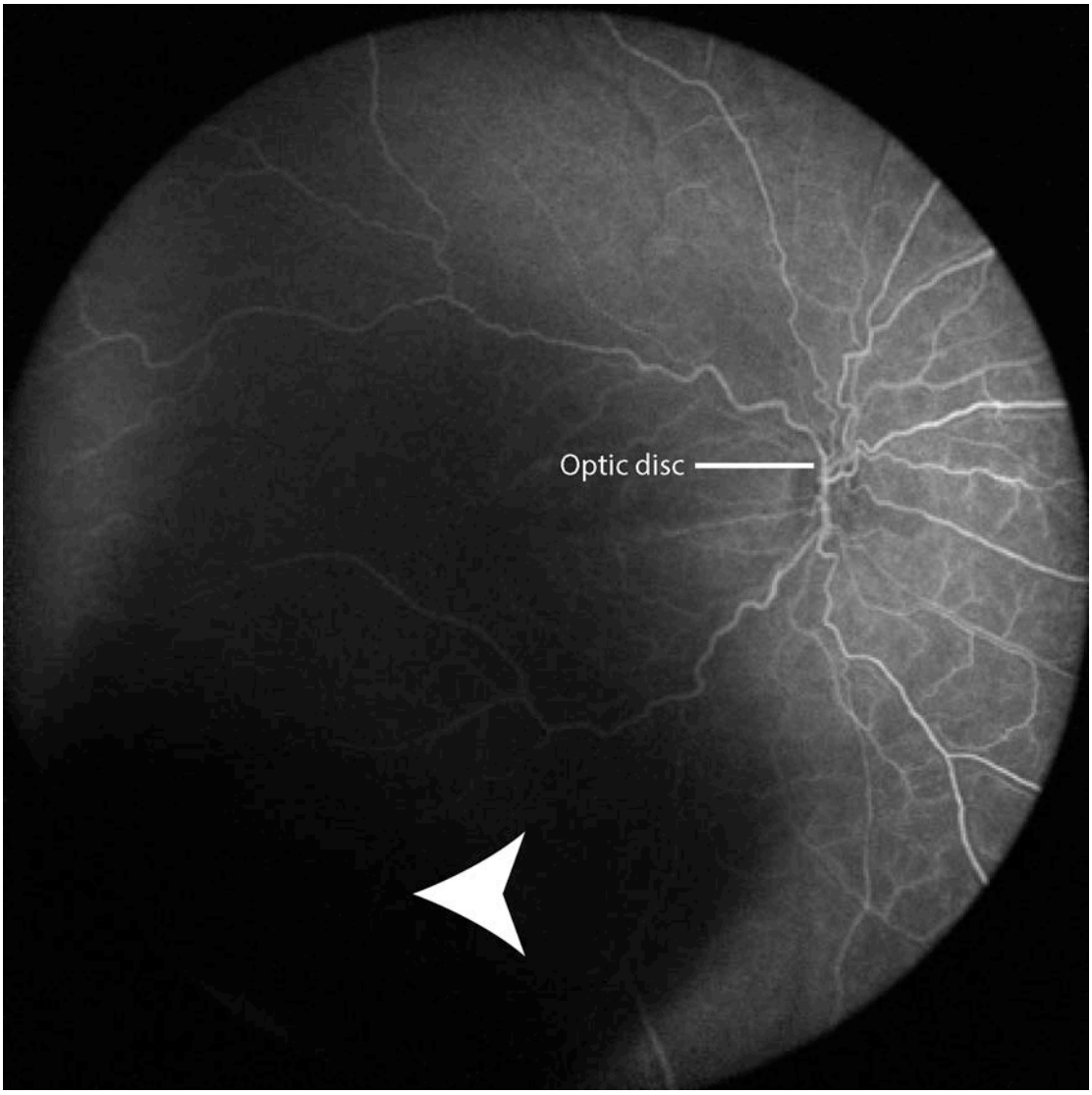

Figure 4.4: An example of an image artefact obtained with the Heidelberg Spectralis ultra-widefield imaging lens (Fung, Yusuf, Xue, Smith and Patel, 2015, p82)

This late phase image of a fluorescein angiogram of the right eye of an infant demonstrates a shadow artefact in the inferotemporal quadrant of the image (white arrowhead). The artifact arose from condensation of the ultra-widefield lens as a result of the close working distance of the ultra-widefield lens and the eye of an infant. Producing an air current across the ocular-device interface will eliminate this artifact.

4.4. Discussion

To the best of our knowledge, we have evaluated for the first time non-contact ultra-widefield FFA in anaesthetised infants with a range of retinal vascular diseases using a modified Heidelberg Spectralis in an operating room setting. There were no adverse changes in physiological parameters in any infant that necessitated cessation of ultra-widefield fundus fluorescein angiographic imaging with the modified Heidelberg Spectralis. In the operating room, the modified Heidelberg Spectralis was capable of acquiring clinically useful, high-resolution, ultra-widefield fundus fluorescein angiographic images in anaesthetised infants with ROP, FEVR, and IP. The fundus fluorescein angiographic images acquired were able to document a range of peripheral retinal features. A shadow artefact from the condensation of the ultra-widefield imaging lens was seen in 43 ultra-widefield fluorescein angiographic images. This may occur because of the necessary close working distance of the ultra-widefield imaging lens to the infant eye, but can be dealt with by creating an air current near the eye when the artefact is noted on the monitor. The percentage of inadequate quality fluorescein angiographic images acquired with the ultra-widefield imaging lens was 11% in this study. Poor alignment of the ultra-widefield imaging lens with the infant eye and the incorrect working distance of the ultra-widefield imaging lens to the infant eye may have contributed to the acquisition of inadequate quality fluorescein angiographic images.

There are several advantages of using the modified Heidelberg Spectralis for acquiring fundus fluorescein angiographic images in anaesthetised infants. Firstly, the confocal scanning laser ophthalmoscope of the Heidelberg Spectralis is capable of producing fluorescein angiographic images of superior quality at lower retinal

irradiances, allowing a greater sensitivity for detecting areas of capillary non-perfusion and vascular leakage [69]. Secondly, the ability of the Heidelberg Spectralis ultra-widefield imaging lens to capture the posterior pole and the periphery of the retina in a one shot image obviates photomontages, avoiding their potential limitations, which include skipped areas and local variations in magnification and contrast. Additionally, the large area of retina imaged may increase diagnostic yield since all retinal locations may be captured simultaneously at all time points in the study. Thirdly, there is no contact with the ocular surface with the ultra-widefield fluorescein angiographic system of the Heidelberg Spectralis and, as such, compression artefacts will not occur. Retinal imaging techniques that require ocular contact and depression of the globe may induce an oculocardiac response requiring cessation of the imaging study [44].

There are several disadvantages of using the modified Heidelberg Spectralis for acquiring fluorescein angiographic images in infants. Firstly, the modified Heidelberg Spectralis imaging system can only be used in infants who undergo a general anaesthetic. Secondly, the ultra-widefield imaging lens has to be positioned close to the infant eye to maximise the area of retina captured in an image. Due to the large size of the lens, one might find it difficult to use in an infant with a deep-set eye.

In summary, the modified Heidelberg Spectralis is capable of capturing clinically useful, high-resolution, ultra-widefield fundus fluorescein angiographic images in infants with a range of retinal diseases in an operating room setting.

Chapter 5

Summary and Future Work

5.1. Summary

This thesis evaluated non-contact ultra-widefield retinal imaging in infants with a range of retinal diseases.

In chapter 2, evaluation of non-contact ultra-widefield pseudocolour fundus imaging with the Optos Panoramic 200MA in the outpatient setting was performed for 42 non-sedated infants with a range of retinal diseases. A total of 517 ultra-widefield pseudocolour fundus images were analysed for peripheral retinal features captured and artefacts. It was found that the Optos Panoramic 200MA was capable of acquiring clinically useful, high-resolution, ultra-widefield pseudocolour fundus images in infants with retinopathy of prematurity (ROP), familial exudative vitreoretinopathy (FEVR), and incontinentia pigmenti (IP) without the use of sedation. The ultra-widefield pseudocolour fundus images acquired with the Optos Panoramic 200MA were able to document a wide range of peripheral retinal features including retinal haemorrhages, retinal exudates, retinal detachments, laser scars, and skip areas from previous laser treatment. A range of image artefacts was seen including artefacts from the nose, eyelids, and eyelashes.

In chapter 3, evaluation of non-contact ultra-widefield fundus fluorescein angiographic imaging with the Optos Panoramic 200MA in the outpatient setting was performed for 29 infants with a range of retinal diseases. One infant required the use of oral sedation to assist with the acquisition of fundus fluorescein angiographic images. A total of 684 intravenous fluorescein angiographic images and a total of 64

oral fluorescein angiographic images were analysed for peripheral retinal features captured and artefacts. It was found that the Optos Panoramic 200MA was capable of acquiring clinically useful, high-resolution, ultra-widefield fluorescein angiographic images in infants with ROP, FEVR and IP. A range of peripheral retinal features was captured with intravenous fluorescein angiography including neovascularisation and vascular leakage, capillary non-perfusion, staining of scars from previous laser treatment, and skip areas. The peripheral retinal features captured with oral fluorescein angiography included capillary non-perfusion and neovascularisation and leakage. For infants with retinal vascular diseases who have inaccessible veins, oral FFA with the Optos Panoramic 200MA may be a useful tool for detecting and assessing capillary non-perfusion and dye leakage.

In chapter 4, evaluation of non-contact ultra-widefield fundus fluorescein angiographic imaging with a modified Heidelberg Spectralis in the operating room setting was performed for 11 infants with a range of retinal diseases. A total of 1124 ultra-widefield fundus fluorescein angiographic images were chosen for analysis of captured peripheral retinal features and artefacts. It was found that the modified Heidelberg Spectralis was capable of acquiring clinically useful, high-resolution, ultra-widefield fluorescein angiographic images in infants with ROP, FEVR and IP. A range of peripheral retinal features was captured including neovascularisation and leakage, retinal ischaemia, capillary non-perfusion, scars from previous laser treatment, and missing areas of laser treatment. In 43 of 1124 ultra-widefield fundus fluorescein angiographic images, an area of artefact arose from condensation that had developed across the ultra-widefield imaging lens during the image process.

5.2. Future Work

1. The use of the Optos imaging device for telemedicine screening of retinopathy of prematurity should be explored.
2. It would be interesting to design a study to examine the feasibility of replacing RetCam imaging in infants with the Optos imaging modality, from the standpoint of both image quality and operator efficiency.
3. A study should be conducted to determine whether the significantly greater visualisation of the retinal periphery provided by the Optos imaging system would help to identify more pathology in infants with proliferative vasculopathies.
4. In chapter 3 of this thesis, high-resolution late phase ultra-widefield fluorescein angiographic images were successfully acquired in 6 infants with the Optos device following the oral administration of sodium fluorescein. A prospective study to determine the best dose of oral fluorescein to use in infants to achieve the best image quality using the Optos device would be worth performing.
5. A prospective study designed to determine the best time point for capturing images in infants after the oral administration of sodium fluorescein to achieve the best image quality using the Optos device would be useful.

References

1. Forrester, J.V., Dick, A.D., Mcmenamin, P.G. and Roberts, F. (2008) The eye: basic sciences in practice. 3rd ed., London: WB Saunders.

2. Justice, J.J. and Lehmann, R.P. (1976) Cilioretinal arteries. A study based on review of stereo fundus photographs and fluorescein angiographic findings. *Archives of Ophthalmology*, 94 (8): 1355-1358.

3. International committee for the classification of retinopathy of prematurity. (2005) The international classification of retinopathy of prematurity revisited. *Archives of Ophthalmology*, 123 (7): 991-999.

4. Wilson, C.M., Head, K.S., Fielder, A.R. and Wilkinson, A.R. (2008) What's new for ROP? An outline review of the revised guideline for the screening and treatment of retinopathy of prematurity. *Infant*, 4 (1): 20-24.

5. An international committee for the classification of retinopathy of prematurity. (2005) The international classification of retinopathy of prematurity revisited. *Archives of Ophthalmology*, 123 (7): 991-999.

6. Wilkinson, A.R., Haines, L., Head, K. and Fielder, A.R. (2008) UK retinopathy of prematurity guideline. *Early Human Development*, 84 (2): 71-74.

7. Good, W.V. (2004) Final results of the early treatment for retinopathy of prematurity (ETROP) randomised trial. *Transactions of the American Ophthalmological Society*, 102: 233-250.

8. Palmar, E.A., Hardy, R.J., Dobson, V., Phelps, D.L., Quinn, G.E., Summers, C.G., Krom, C.P. and Tung, B. (2004) 15-year outcomes following threshold retinopathy of prematurity: final results from the multicenter trial of cryotherapy for retinopathy of prematurity. *Archives of Ophthalmology*, 123 (3): 311-318.

9. Mintz-Hittner, H.A., Kennedy, K.A. and Chuang, A.Z. (2011) Efficacy of intravitreal bevacizumab for stage 3+ retinopathy of prematurity. *New England Journal of Medicine*, 364 (7): 603-615.

10. Jin, D.Y. and Jeang, K.T. (1999) Isolation of full-length cDNA and chromosomal localization of human NF-kB modulator NEMO to Xq28. *Journal of Biomedical Science*, 6 (2): 115-120.

11. Landy, S.J. and Donnai, D. (1993) Incontinentia pigmenti (bloch-sulzberger syndrome). *Journal of Medical Genetics*, 30 (1): 53-59.

12. Carney, R.G. (1976) Incontinentia pigmenti. A world statistical analysis. *Archives of Dermatology*, 112 (4): 535-542.

13. Watzke, R.C., Stevens, T.S. and Carney, R.G. (1976) Retinal vascular changes of incontinentia pigmenti. *Archives of Ophthalmology*, 94 (5): 743-746.

14. Rahi, J. and Hungerford, J. (1990) Early diagnosis of the retinopathy of incontinentia pigmenti: successful treatment by cryotherapy. *British Journal of Ophthalmology*, 74 (6): 377-379.

15. Catalano, R.A., Lopatynsky, M. and Tasman, W.S. (1990) Treatment of proliferative retinopathy associated with incontinentia pigmenti. *American Journal of Ophthalmology*, 110 (6): 701-702.

16. Gilmour, D.F. (2015) Familial exudative vitreoretinopathy and related retinopathies. *Eye (London, England)*, 29 (1): 1-14.

17. Warden, S.M., Andreoli, C.M. and Mukai, S. (2007) The Wnt signaling pathyway in familial exudative vitreoretinopathy and norrie disease. *Seminars in Ophthalmology*, 22 (4): 211-217.

18. Shukla, D., Singh, J., Sudheer, G., Soman, M., John, R.K., Ramasamy, K. and Perumalsamy, N. (2003) Familial exudative vitreoretinopathy (FEVR). Clinical profile and management. *Indian Journal of Ophthalmology*, 51 (4): 323-328.

19. Ikeda, T., Fujikado, T., Tano, Y., Tsujikawa, K., Koizumi, K., Sawa, H., Yasuhara, T., Maeda, M. and Kinoshita, S. (1999) Vitrectomy for rhegmatogenous or tractional retinal detachment with familial exudative vitreoretinopathy. *Ophthalmology*, 106 (6): 1081-1085.

20. Cavallerano, A.A. (1996) Ophthalmic fluorescein angiography. *Optometry clinics*, 5 (1): 1-23.

21. Brancato, R. and Trabeucchi, G. (1998) Fluorescein and indocyanine green angiography in vascular chorioretinal diseases. *Seminars in Ophthalmology*, 13 (4): 189-198.

22. Jennings, B.J. and Mathews, D.E. (1994) Adverse reactions during retinal fluorescein angiography. *Journal of the American Optometric Association*, 65 (7): 465-471.

23. Lipson, B.K. and Yannuzzi, L.A. (1989) Complications of intravenous fluorescein injections. *International Ophthalmology Clinics*, 29 (3): 200-205.

24. Kelley, J.S. (1977) Fluorescein angiography: techniques and toxicity. *International Ophthalmology Clinics*, 17 (2): 25-33.

25. Yannuzzi, L.A., Rohrer, K.T., Tindel, L.J., Sobel, R.S., Costanza, M.A., Shields, W., and Zang, E. (1986) Fluorescein angiography complication survey. *Ophthalmology*, 93 (5): 611-617.

26. Flynn, J.T., Cassady, J., Essner, D., Zeskind, J., Merritt, J., Flynn, R., and Williams, M.J. (1979) Fluorescein angiography in retrolental fibroplasia: experience from 1969-1977. *Ophthalmology*, 86 (10): 1700-1723.

27. Lepore, D., Molle, F., Pagliara, M.M., Baldascino, A., Angora, C., Sammartino, M., and Quinn, G.E. (2011) Atlas of fluorescein angiographic findings in eyes undergoing laser for retinopathy of prematurity. *Ophthalmology*, 118 (1): 168-175.

28. Ng, E.Y.J., Lanigan, B., O'Keefe, M. (2006) Fundus fluorescein angiography in the screening for and management of retinopathy of prematurity. *Journal of Pediatric Ophthalmology and Strabismus*, 43 (2): 85-90.

29. Azad, R., Chandra, P., Khan, M.A., and Darswal, A. (2008) Role of intravenous fluorescein angiography in early detection and regression of retinopathy of prematurity. *Journal of Pediatric Ophthalmology and Strabismus*, 45 (1): 36-39.

30. Goldberg, M.F (1994) The blinding mechanisms of incontinentia pigmenti. *Ophthalmic Genetics*, 15 (2): 69-76.

31. Shaikh, S., Trese, M.T. and Archer, S.M. (2004) Fluorescein angiographic findings in incontinentia pigmenti. *Retina*, 24 (4): 628-629.

32. DeVetten, G. and Ells, A. (2007) Fluorescein angiographic findings in a male infant with incontinentia pigmenti. *Journal of American Association for Pediatric Ophthalmology*, 11 (5): 511-512.

33. Tzu, J.H., Murdock, J., Parke, D.W., Warman, R., Hess, D.J. and Berrocal, A.M. (2013) Use of fluorescein angiography in incontinentia pigmenti: a case report. *Ophthalmic Surgery, Lasers, and Imaging Retina*, 44 (1): 91-93.

34. Canny, C.L.B. and Oliver, G.L. (1976) Fluorescein angiographic findings in familial exudative vitreoretinopathy. *Archives of Ophthalmology*, 94 (7): 1114-1120.

35. Ober, R.R., Bird, A.C., Hamilton, A.M. and Sehmi, K. (1980) Autosomal dominant exudative vitreoretinopathy. *British Journal of Ophthalmology*, 64 (2): 112-120.

36. Witmer, M.T. and Kiss, S. (2013) Wide-field imaging of the retina. *Survey of Ophthalmology*, 58 (2): 143-154.

37. Bulpitt, C.J. and Baum, J.D. (1969) Retinal photography in the newborn. *Archives of Disease in Childhood*, 44 (236): 499-503.

38. Fung, T.H.M., Smith, L.M. and Patel, C.K. (2014) Contemporary imaging of Retinopathy of Prematurity. *Infant*, 10 (5): 143-146.

39. Prakalapakorn, S.G., Freedman, S.F. and Wallace, D.K. (2014) Evaluation of an indirect ophthalmoscopy digital photographic system as a retinopathy of prematurity screening tool. *Journal of American Association for Pediatric Ophthalmology*, 18 (1): 36-41.

40. Johnson, K.S., Mills, M.D., Karp, K.A. and Grunwald, J.E. (2007) Semiautomated analysis of retinal vessel diameter in retinopathy of prematurity patients with and without plus disease. *American Journal of Ophthalmology*, 143 (4): 723-725.

41. Prakalapakorn S.G., Wallace, D.K. and Freedman, S.F. (2014) Retinal imaging in premature infants using the Pictor noncontact digital camera. *Journal of American Association for Pediatric Ophthalmology*, 18 (4): 321-326.

42. Shah, P.K., Narendran, V., Saravanan, V.R., Raghuram, A., Chattopadhyay, A. and Kashyap, M. (2006) Screening for retinopathy of prematurity – a comparison between binocular indirect ophthalmoscopy and RetCam 120. *Indian Journal of Ophthalmology*, 54 (1): 35-38.

43. Nakagawa, T.A. and Skrinska, R. (2001) Improved documentation of retinal hemorrhages using a wide-field digital ophthalmic camera in patients who experienced abusive head trauma. *Archives of Pediatric and Adolescent Medicine*, 155 (10): 1149-1152.

44. Adams, G.G., Clark, B.J., Fang, S. and Hill, M. (2004) Retinal haemorrhages in an infant following RetCam screening for retinopathy of prematurity. *Eye (London)*, 18 (6): 652-653.

45. Lim, Z., Tehrani, N.N. and Levin, A.V. (2006) Retinal haemorrhages in a preterm infant following screening examination for retinopathy of prematurity. *British Journal of Ophthalmology*, 90 (6): 799-800.

46. Kemper, A.R., Wallace, D.K. and Quinn, G.E. (2008) Systematic review of digital imaging screening strategies for retinopathy of prematurity. *Pediatrics*, 122 (4): 825-830.

47. Zepeda-Romero, L.C., Martinez-Perez, M.E., Ruiz-Velasco, S., Ramirez-Ortiz, M.A. and Gutierrez-Padilla, J.A. (2011) Temporary morphological changes in plus disease induced during contact digital imaging. *Eye (London)*, 25 (10): 1337-1340.

48. Mehta, M., Adams, G.G., Bunce, C., Xing, W. and Hill, M. (2005) Pilot study of the systemic effects of three different screening methods used for retinopathy of prematurity. *Early Human Development*, 81 (4): 355-360.

49. Webb, R.H. and Hughes, G.W. (1981) Scanning laser ophthalmoscope. *IEEE Transactions on Biomedical Engineering*, 28 (7): 488-492.

50. Webb, R.H., Hughes, G.W. and Delori, F.C. (1987) Confocal scanning laser ophthalmoscope. *Applied Optics*, 26 (8): 1492-1499.

51. Friberg, T.R., Pandya, A. and Eller, A.W. (2003) Non-mydriatic panoramic fundus imaging using a non-contact scanning laser-based system. *Ophthalmic Surgery, Lasers and Imaging Retina*, 34 (6): 488-497.

52. Wessel, M.M., Nair, N., Aaker, G.D., Ehrlich, J.R., D'Amico, D.J., Kiss, S. (2012) Peripheral retinal ischaemia, as evaluated by ultra-widefield fluorescein angiography, is associated with diabetic macular oedema. *British Journal of Ophthalmology*, 96 (5): 694-698.

53. Prasad, P.S., Oliver, S.C., Coffee, R.E., Hubschman, J.P. and Schwartz, S.D. (2010) Ultra-wide-field angiographic characteristics of branch retinal and hemicentral retinal vein occlusion. *Ophthalmology*, 117 (4): 780-784.

54. Mudvari, S.S., Virasch, V.V., Singa, R.M. and MacCumber, M.W. (2010) Ultra-wide-field imaging for cytomegalovirus retinitis. *Ophthalmic Surgery, Lasers and Imaging Retina*, 41 (3): 311-315.

55. Tsui, I., Franco-Cardenas, V., Hubschman, J.P. and Schwartz, S.D. (2013) Pediatric retinal conditions imaged by ultra wide field fluorescein angiography. *Ophthalmic Surgery, Lasers and Imaging Retina*, 44 (1): 59-67.

56. Kang, K.B., Wessel, M.M., Tong, J., D'Amico, D.J. and Chan, R.V. (2013) Ultra-widefield imaging for the management of pediatric retinal diseases. *Journal of Pediatric Ophthalmology and Strabismus*, 50 (5): 282-288.

57. Patel, C.K., Fung, T.H.M., Muqit, M.M.K., Mordant, D.J. and Geh, V. (2012) Non-contact ultra-widefield retinal imaging and fundus fluorescein angiography of an infant with incontinentia pigmenti without sedation in an ophthalmic office setting. *Journal of American Association for Pediatric Ophthalmology*, 17 (3): 309-311.

58. Patel, C.K., Fung, T.H.M., Muqit, M.M.K., Mordant, D.J., Brett, J., Smith, L. and Adams, E. (2013) Non-contact ultra-widefield imaging of retinopathy of prematurity using the Optos dual wavelength scanning laser ophthalmoscope. *Eye (London)*, 27 (5): 589-596.

59. Anand, R. (1989) Fluorescein angiography. Part 1. Technique and normal study. *Journal of Ophthalmic Nursing and Technology*, 8 (2): 48-52.

60. Fung, T.H.M., Yusuf, I.H., Smith, L.M., Brett, J., Weston, L. and Patel, C.K. (2014) Outpatient ultra-widefield intravenous fundus fluorescein angiography using the Optos P200MA scanning laser ophthalmoscope. *British Journal of Ophthalmology*, 98 (3): 302-304.

61. Hoyt, C.S. and Taylor, D. (2012) Pediatric ophthalmology and strabismus. 4th ed., London: WB Saunders.

62. Nayak, B.K. and Ghose, S. (1987) A method for fundus evaluation in children with oral fluorescein. *British Journal of Ophthalmology*, 71 (12): 907-909.

63. Witmer, M.T., Parlitsis, G., Patel, S. and Kiss, S. (2013) Comparison of ultra-widefield fluorescein angiography with the Heidelberg Spectralis noncontact ultra-widefield module versus the Optos Optomap. *Clinical Ophthalmology*, 7 (1): 389-394.

64. Vinekar, A., Sivakumar, M., Shetty, R., Mahendradas, P., Krishnan, N., Mallipatna, A. and Shetty, K.B. (2010) A novel technique using spectral-domain optical coherence tomography (Spectralis SD-OCT + HRA) to image non-anaesthetised infants: utility demonstrated in aggressive posterior retinopathy of prematurity. *Eye (London)*, 24 (2): 379-382.

65. Fung, T.H.M., Yusuf, I.H., Xue, K., Smith, L.M. and Patel, C.K. (2015) Heidelberg Spectralis ultra-widefield fundus fluorescein angiography in infants. *American Journal of Ophthalmology*, 159 (1): 78-84.

66. Inoue, M., Yanagawa, A., Yamane, S., Arakawa, A., Kawai, Y. and Kadonosono, K. (2013) Wide-field fundus imaging using the Optos Optomap and a disposable eyelid speculum. *JAMA Ophthalmology*, 131 (2): 226.

67. Tiret, L., Nivoche, Y., Hatton, F., Desmonts, J.M. and Vourc'h, G. (1988) Complications related to anaesthesia in infants and children. A prospective survey of 40240 anaesthetics. *British Journal of Anaesthesia*, 61 (3): 263-269.

68. Hara, T., Inami, M. and Hara, T. (1998) Efficacy and safety of fluorescein angiography with orally administered sodium fluorescein. *American Journal of Ophthalmology*, 126 (4): 560-564.

69. Nicholson, B.P., Nigam, Y., Miller, D., Agron, E., Dalal, M., Jacobs-EL, N., da Rocha Lima, B., Cunningham, D., Nussenblatt, R. and Sen, H.N. (2014) Comparison of wide-field fluorescein angiography and 9-field montage angiography in uveitis. *American Journal of Ophthalmology*, 157 (3): 673-677.

Publications

Fung, T.H.M., Yusuf, I.H., Xue, K., Smith, L.M. and Patel, C.K. (2015) Heidelberg Spectralis Ultra-Widefield Fundus Fluorescein Angiography in Infants. *American Journal of Ophthalmology*, 159 (1): 78-84.

Fung, T.H.M., Smith, L.M. and Patel, C.K. (2014) Contemporary imaging of Retinopathy of Prematurity. *Infant*, 10 (5): 143-146.

Fung, T.H.M., Yusuf, I.H., Smith, L.M., Brett, J., Weston, L. and Patel, C.K. (2014) Outpatient ultra-widefield intravenous fundus fluorescein angiography in infants using the Optos P200MA scanning laser ophthalmoscope. *British Journal of Ophthalmology*, 98 (3): 302-304.

Fung, T.H.M., Muqit, M.M.K., Mordant, D.J., Smith, L.M. and Patel, C.K. (2014) Non-contact ultra-wide-field oral fluorescein angiography in premature infants with retinopathy of prematurity. *JAMA Ophthalmology*, 132 (1): 108-110.

Patel, C.K., **Fung, T.H.M.**, Muqit, M.M.K., Mordant, D.J., Brett, J., Smith, L.M. and Adams, E. (2013) Ultra-wide field imaging of retinopathy of prematurity using the Optos dual wavelength scanning laser ophthalmoscope. *Eye (London)*, 27 (5): 589-596.

Patel, C.K., **Fung, T.H.M.**, Muqit, M.M.K., Mordant, D.J. and Geh, V. (2013) Non-contact ultra-wide field retinal imaging and fundus fluorescein angiography of a baby with incontinentia pigmenti without sedation in the outpatient setting. *Journal of American Association for Pediatric Ophthalmology*, 17 (3): 309-311.

Presentations

Fung, T.H.M., Yusuf, I.H., Smith, L.M. and Patel, C.K. Non-contact ultra-widefield fluorescein angiography in infants. *Investigative Ophthalmology & Visual Science April 2014, Vol.55, 205.*

Fung, T.H.M., Smith, L.M., Patel, C.K. Ultra-wide-field fluorescein angiography in premature infants with retinopathy of prematurity. *Oxford Ophthalmology Congress, July 2013.*

Fung, T.H.M., Muqit, M.M.K., Mordant, D., Smith, L.M. and Patel, C.K. Modification of Spectralis HRA + OCT for intraoperative multi-modality imaging in pediatric retinal diseases. *Investigative Ophthalmology & Visual Science June 2013, Vol.54, 1496.*